POLY(LACTIDE-CO-GLYCOLIDE) MICROSPHERES AND HYDROGEL DELIVERY SYSTEMS FOR
SOFT TISSUE AND CARTILAGE TISSUE ENGINEERING APPLICATIONS

by

Alicia J. DeFail

B.S. Chemical Engineering, Bucknell University, 2003

Submitted to the Graduate Faculty of

School of Engineering in partial fulfillment

of the requirements for the degree of

Doctor of Philosophy

University of Pittsburgh

2007

UNIVERSITY OF PITTSBURGH

SCHOOL OF ENGINEERING

This dissertation was presented

by

Alicia J. DeFail

It was defended on

November 26, 2007

and approved by

X. Tracy Cui, Assistant Professor, Department of Bioengineering

Constance R. Chu, Associate Professor, Department of Orthopaedic Surgery

Howard D. Edington, Associate Professor, Departments of Surgery and Dermatology

Dissertation Director: Kacey, G. Marra, Assistant Professor, Departments of Surgery and

Bioengineering

POLY(LACTIDE-CO-GLYCOLIDE) MICROSPHERES AND HYDROGEL DELIVERY SYSTEMS

FOR SOFT TISSUE AND CARTILAGE TISSUE ENGINEERING APPLICATIONS

Alicia J. DeFail, Ph.D.

University of Pittsburgh, 2007

Polymeric microspheres have been widely investigated as delivery systems and are clinically used today. We examined the use of poly(lactide-co-glycolide) (PLGA) microspheres in delivery systems for soft tissue engineering, chemotherapeutic delivery, and cartilage tissue engineering. Soft tissue defects due to trauma or tumor removal remain a clinical challenge. We examined the use of PLGA microspheres and adipose derived stem cells (ASCs) to fill in soft tissue defects. We first demonstrated the use of PLGA microspheres to increase ASC proliferation and survival by encapsulating fibroblast growth factor-2 (FGF-2). The released FGF-2 increased ASC proliferation and survival *in vitro*. Addition of the FGF-2 microspheres in an *in vivo* study resulted in an increase in angiogenesis. We then examined the ability of released adipogenic factors to induce the differentiation of ASCs into mature adipocytes. Oil red O staining and Western blots confirmed that adipogenesis was induced by the released factors. The second goal was to examine a delivery system to reduce the risk of local recurrence in breast cancer patients following a lumpectomy. Breast cancer lumps are commonly treated by tumor removal (lumpectomy) followed by radiation or chemotherapy, and both have adverse side effects. PLGA microspheres encapsulating doxorubicin were embedded with a natural scaffold, gelatin, to locally deliver chemotherapy and maintain the breast contour. Our results demonstrated a more controlled release from microspheres embedded within gelatin compared to microspheres alone. Released doxorubicin killed tumor cells *in vitro*. The implantation of the

scaffolds *in vivo* resulted in tumor ablation. Local and systemic toxicity were not observed even though a dose 60 times the normal dose was given. Our next objective was to analyze the release of TGF-beta1 (TGF-β1) from PLGA microspheres incorporated into a synthetic hydrogel, poly(ethylene glycol) (PEG)-genipin for cartilage repair. The release of TGF-β1 was dependent upon the genipin concentration of the hydrogel. The released TGF-β1 was bioactive, as demonstrated by the inhibition of mink lung cell proliferation. The final goal was to develop and characterize a hydrogel based on PEG-genipin to gel *in situ*. As such, we examined genipin and multi-branched aminated PEG. Gelation time was affected by pretreating genipin. Exposure of the genipin aqueous solution to air and oxygen decreased the gelation time. PEG structure also had an effect on gelation time. The gelation time was reduced by utilizing 4-arm PEG and increasing the temperature from 25°C to 37°C. The results of this thesis demonstrate the efficacy of PLGA microspheres embedded in hydrogels for use as delivery systems for soft tissue and cartilage tissue engineering. The delivery systems can be modified to tailor delivery rates, deliver multiple drugs/growth factors, tailor degradation, and promote tissue growth.

TABLE OF CONTENTS

LIST OF TABLES

LIST OF FIGURES

NOMENCLATURE

PLGA   Poly(lactide-co-glycolide)

PLA   Poly(lactide)

PGA   Poly(glycolide)

PEG   Poly(ethylene glycol)

PCL   Poly(caprolactone)

PVA   Poly(vinyl alcohol)

BSA   Bovine Serum Albumin

OPF   Oligo(poly(ethylene glycol) fumarate)

ASC   Adipose derived stem cell

FGF-2   Fibroblast growth factor-2

SIS   Small intestinal submucosa

Dex   Dexamethasone

PBS   Phosphate buffered solution

MS   Microspheres

Dox   Doxorubicin

MC   Methylene chloride

TGF-β1   Transforming growth factor-beta1

PREFACE

I would first like to thank and acknowledge my advisor, Dr. Kacey Marra. Thank you for the opportunity to work in your lab. I have truly enjoyed my years spent here and have learned so much. I appreciate all of the guidance and advice you have provided.

A big thank you to my committee, Dr. Tracy Cui, Dr. Constance Chu, and Dr. Howard Edingtion. Your advice has been so helpful. I appreciate all of the time, work, and guidance you have provided. You have each provided me with insight into your area of research.

Our collaborators have provided guidance and opportunities that I am so grateful to have experienced. Thank you Dr. J. Peter Rubin, Dr. Constance Chu, and Dr. Howard Edington. I have learned so much from all of you and have enjoyed working with you and your lab members.

I would like to thank the Department of Bioengineering with providing me the opportunity to become a graduate student and continue my education. Thank you to all of the members of the Plastic Surgery Research Lab. I enjoyed working in a lab where everyone is so willing to help each other out and my work would not have been possible without each and everyone of you. I would especially like to thank my fellow graduate students in the lab, Candace Brayfield, Lauren Kokai, and Christina Lee. Thank you for all of your help and advice throughout my time in the lab. I am grateful to have worked with people who have such an enthusiasm for research and are so generous with their time. Mostly I am grateful to have gotten to know each of you and become friends.

A special thank you to all of my friends who have supported me throughout my graduate studies, especially Joe Candiello and Dave Montag. I am so glad we met our first year of graduate school. You have been there since the beginning, and I am grateful we have remained friends. You have helped get through all the ups and downs.

It goes without saying that my parents have supported me and I would not have accomplished this without them. Thank you for all of your support and encouragement throughout my entire life. You have instilled in me the importance of education and have provided me with opportunities to continue my education. Thank you for always being there and helping me whenever needed, no questions asked. Thank you to my brother, Tony, you have always encouraged me to reach higher and accomplish more.

As well I am so thankful to have Andrew in my life during this time. Thank you for all of your help, understanding, and support. I am so lucky to have someone who supports me so much. I know things weren't always the easiest, and I owe you so much for putting up with me during this time.

1.0   INTRODUCTION

Delivery systems have been utilized for localization, prolonged release, and protection of drugs. The main reason to use delivery systems is to obtain and maintain a desired range of drug levels in the system. An ideal system is controlled release in which the levels are maintained within the desired range over long periods of time. The most basic form of a delivery system is an intravenous (IV) pump. However, due to the advances in materials science and in the area of biomaterials, controlled release can be maintained by polymer formulations. Controlled release can lead to improved drug performance, decreased side effects, ease of use, and lower costs than developing new drugs. Some of the critical factors in the design are the properties of the drug, the administration route, and the target tissue. Delivery systems can be diffusion, chemically, solvent, or external activation controlled. Bioerodible systems would not have to removed and are thus advantageous. We have designed biodegradable delivery systems utilizing polymer microspheres and hydrogel scaffolds for soft tissue and cartilage tissue engineering applications.

1.1   DELIVERY SYSTEMS AND TISSUE ENGINEERING

The advantages of delivery systems have led to their use clinically. Polymer delivery systems have been utilized for delivery of steroids, Norplant® (Wyeth Pharmaceuticals) and Progestasert®; human growth hormone, Nutropin Depot® (Genentech-Alkermes); and glaucoma

therapy, Ocusert®. Delivery systems are optimal due to the reduction of adverse reactions and side effects. Such is the case for chemotherapeutic drugs, which have numerous side effects.

1.1.1   Tissue engineering

Tissue engineering is a rapidly growing field. One approach to tissue engineering is combining the fields of cell therapy and biomaterials. The approach utilizes cells, scaffolds, and growth factors. Cell therapy has recently become a reality. Autologous cell sources can be utilized to create biological substitutes for injured or damaged tissues. However, a support system and favorable microenvironment must be supplied for cells to proliferate, differentiate, and produce the necessary factors to heal the surrounding area. In the natural environment, these are provided by the extracellular matrix (ECM). In tissue engineering, these criteria can be met by the combination of scaffold and growth factor delivery. The scaffold must support the cells, allow them to proliferate, and maintain their phenotype, or in some cases help induce their differentiation. It is also important that the scaffold can be degraded so that the ECM produced by the cells can be deposited and eventually replace the scaffold. ECM also contains growth factors that can be released. Injection of growth factors is insufficient since they diffuse away from the area and have short half lives. By incorporating growth factors into the scaffold, or separately, prolonged delivery can be obtained. In some cases, providing the scaffold and growth factor delivery is enough to regenerate or repair tissue without cells.

1.2   BIOMATERIALS

1.2.1   Polyesters

Poly(lactide-co-glycolide) (PLGA), a polyester, is an FDA approved polymer.   PLGA was first developed for use in absorbable sutures. PLGA has since been utilized for delivery devices and tissue engineering. PLGA (Figure 1-1) is a copolymer of poly(lactide) (Figure 1-2) and poly(glycolide) (Figure 1-3). Poly(L-lactide) (PLLA) is a crystalline polymer, poly(D,L-lactide) (PDLA) is an amorphous polymer, and poly(glycolide) (PGA) is a crystalline polymer. Polyesters are degraded by hydrolytic cleavage of ester linkages, resulting in bulk erosion. Homogenous degradation occurs throughout the polymer scaffold and the rate of water penetration is greater than the conversion of water soluble fragments. The molecular weight decreases due to continuous cleavage. The polymer scaffold will retain its shape and mass until significant degradation occurs. The PLGA chains are cleaved to monomeric acids that are then eliminated by the Kreb's cycle as CO_2 and in the urine as water.[5] PLGA polymers can be prepared in different ratios to tailor the *in vivo* degradation rates (Table 1-I).

Figure 1-1. Structure of PLGA.

Figure 1-2. Structure of PLA.

Figure 1-3. Structure of PGA.

3

Table 1-I. Degradation times of polyesters. [6]

Polymer	Approximate biodegradation time (months)
PLLA	18-24
PDLA	12-16
PGA	2-4
50:50 PLGA	2
85:15 PLGA	5

1.2.2   Hydrogels

Hydrogels are crosslinked networks that provide a three-dimensional environment to mimic the natural environment of tissues. The equilibrium swelling allows the diffusion of nutrients into the hydrogel and waste out. Hydrogels, which are typically water-insoluble swollen networks of water-soluble polymer chains, are useful for numerous tissue engineering applications[7-11].

Poly(ethylene glycol) (PEG) is a non-toxic, non-immunogenic polymer. PEG is one of the most widely studied polymers.[12-17] PEG hydrogels have been investigated as delivery systems. PEG-dimethacrylate (PEGDM) photo-crosslinkable hydrogels have been examined for the delivery of insulin like growth factor–I (IGF-I) and TGF-β1.[18] PEG-grafted chitosan and crosslinked PEG-polyacrylamide have been utilized as delivery systems.[19] Mikos' lab has examined degradable oligo(poly(ethylene glycol)fumarate) hydrogels (OPF).   The OPF hydrogels have been studied for delivery of TGF-β1[20, 21] and dual delivery of IGF-I and TGF-β1 from gelatin microspheres within the OPF gels.[22]

PEG hydrogels have been examined as cell scaffolds. Fibroblasts and chondrocytes adhere and proliferate on PEG hydrogels crosslinked by hydrolyzable polyrotaxane.[23, 24] Smooth muscle cells adhere to PEG crosslinked with genipin.[25] PEG-poly(caprolactone)

4

(PCL) scaffolds and PCL scaffolds were evaluated for human and rat bone marrow derived stromal cells. Cells adhered better to PEG-PCL copolymers than the PCL homopolymer.[26]

Furthermore, PEG hydrogels can be utilized as cell carriers. Quickly gelling hydrogels can encapsulate cells within their three-dimensional environment. PEGDM hydrogels have been utilized to encapsulate chondrocytes.[18, 27] PEG-LA-DM was reacted with poly(vinyl alcohol) (PVA) forming photo-crosslinkable hydrogels to encapsulate chondrocytes.[28]

1.3   MICROSPHERES AS DELIVERY SYSTEMS

1.3.1   Microsphere preparation

Microspheres can be prepared by different techniques, spray drying, single emulsion, double emulsion, and phase separation. The technique of encapsulation should meet the requirements set by the optimal protein/drug loading, stability of encapsulated protein/drug, low burst effects, high yield of particles, and manipulation of release properties.

Microspheres can be prepared utilizing a single, oil-in-water (o/w), emulsion/solvent extraction technique. The polymer is dissolved with the dissolved or suspended drug in an organic solvent (oil). This oil phase is then added to an aqueous solution (water). The organic solvent is removed by evaporation, resulting in an aqueous solution with hardened microspheres. This technique is best for more hydrophobic drugs. A water-soluble drug encapsulated using the single emulsion technique will probably result in a low encapsulation efficiency since the drug will most likely diffuse into the external aqueous phase.

The double emulsion, water in oil in water (w/o/w), solvent extraction technique is more favorable for water soluble drugs. The drug is first dissolved in an aqueous solution (water), which is emulsified with the polymer dissolved in an organic solvent (oil). This first emulsion is then added to a large aqueous solution (water), resulting in a second emulsion (w/o/w). As the solution is stirred, the solvent evaporates, and the polymer hardens forming microspheres (Figure 1-4).
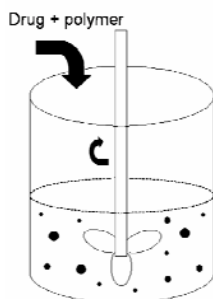
Figure 1-4. Preparation of polymer microspheres utilizing single or double emulsion technique.

1.3.2   Preparation parameters

The parameters used to prepare the microspheres can affect the microsphere size, encapsulation efficiency, and burst effect. The size of the microspheres is affected by polymer concentration, stirring rate, and emulsion time. The diameter of the microspheres increases linearly with increasing polymer concentration and decreases with an increase in vortexing time.[29] The number and size of pores is affected by the volume of internal aqueous phase in a double emulsion preparation.[29]

The encapsulation efficiency has been shown to be affected by polymer concentration, method of preparation, internal aqueous volume, stirring time for solvent evaporation, and stabilization of the primary emulsion. Increasing the polymer concentration, increases the

encapsulation efficiency.[29, 30] This is because the time for the microspheres to solidify is shorter, thus less time for the drug to transport into the external aqueous solution. The viscosity of the polymer drug dispersion in increased and thus it is more difficult for the drug to diffuse through the polymer solution to the external aqueous solution. An increase in internal aqueous volume decreases encapsulation efficiency.[31] An increase in internal aqueous phase may lead to aqueous drops present at the surface of emulsion and thus facilitate drug loss to the external water phase. The stirring time that allows solvent evaporation affects the encapsulation efficiency. Increasing the stirring time leads to a decrease in encapsulation efficiency due to drug loss to the external aqueous phase.[31] However, this can be overcome by the addition of salts to the external aqueous phase. When the primary emulsion is stable, a higher encapsulation efficiency follows. The primary emulsion can be stabilized by the addition of emulsifying agents such as bovine serum albumin (BSA), PVA, or Tween-80.

The release and burst effect of microspheres can also be affected by the preparation parameters. Smaller microspheres have a larger burst effect and a quicker release. The release rate increases with an increasing internal aqueous volume.[29] An increasing internal aqueous volume also results in more pores, which will lead to a quicker release. Low molecular weight polymers result in a high burst release, because the polymer is more soluble in the organic solvent and thus undergoes a slower solidification.[32] A lower molecular weight also results in more porous microspheres and smaller microspheres, both lead to a quicker release. The stabilizers affect the release kinetics as well as the encapsulation efficiency. By increasing the PVA concentration, the diameter is decreased; however, the initial burst is decreased.[32] The PVA may reduce the migration of the drug into the external aqueous phase.

1.3.3 Microspheres in scaffolds

Microspheres can be utilized as a delivery system alone. Studies have demonstrated that microspheres typically stay at the site of injection *in vivo* and are unlikely to cross biological barriers.[33] Phagocytosis of microparticles typically occurs in particles less than 10μm in diameter.[33] However, the desire to incorporate microspheres within scaffolds for tissue engineering or a more controlled release has been examined. Zhang et al. examined the incorporation of hydroxyl-functionalized glycerol poly(ε-caprolactone) (PGCL) microspheres in poly(N-isopropylacrylamide) (PNIPAAm) hydrogels.[34] Leach et al. examined the release of BSA from glycidyl methacrylate-hyaluronic acid (GMHA)-PEG hydrogels and BSA in PLGA microspheres in the GMHA-PEG hydrogels. The microspheres in the hydrogel extended the release of BSA compared to BSA in hydrogels alone.[35] Holland et al. has examined the release of growth factors from gelatin microspheres embedded within OPF hydrogels. The release of TGF-β1 from gelatin microspheres in OPF could be tailored by altering the OPF formulation and crosslinking time.[20, 21] Holland et al. further examined the delivery of both IGF-I and TGF-β1 from gelatin microspheres in OPF hydrogels.[22]

1.4   PROJECT OBJECTIVES

1.4.1   Objective #1: Delivery of FGF-2, insulin, and dexamethasone to induce adipogenesis of adipose derived stem cells for soft tissue engineering.

Objective #1:   Develop an injectable system for soft tissue reconstruction utilizing PLGA microspheres to promote adipose derived adult stem cells (ASCs) differentiation and survival. We will examine the effects of released FGF-2, insulin, and dexamethasone on ASCs.

Hypothesis: The released FGF-2 will promote ASC proliferation *in vitro* and angiogenesis *in vivo.* The released dexamethasone and insulin will promote the differentiation of the ASCs *in vitro.*

1.4.2   Objective #2: Controlled release of chemotherapy from PLGA microspheres/gelatin scaffolds as adjuvant therapy for breast cancer.

Objective #2: Develop a material that can be placed in the breast following a lumpectomy that will maintain controlled delivery of a chemotherapeutic agent locally to decrease the risk of local recurrence. The material will also temporarily maintain the volume and contour of the breast and promote tissue ingrowth and remodeling. We will encapsulate doxorubicin in PLGA microspheres and embed these in gelatin scaffolds. The effectiveness of the scaffolds to eradicate tumors will be assessed *in vitro* and *in vivo*.

Hypothesis: By embedding the microspheres in gelatin, the release of doxorubicin will be further controlled. The released doxorubicin will result in cell death *in vitro* and tumor eradication *in vivo*.

1.4.3   Objective #3: The controlled release of TGF-β1 from PEG-genipin biodegradable hydrogels for cartilage repair.

Objective #3: Develop a system to locally deliver TGF-β1 for cartilage regeneration. We will assess the release of TGF-β1 from PLGA microspheres and PLGA microspheres embedded within PEG-genipin hydrogels *in vitro*.

Hypothesis: The release of proteins from the PLGA microspheres within PEG-genipin hydrogels will differ depending on the degree of crosslinking. The dissolution rate *in vivo* can be tailored depending on the degree of crosslinking.

1.4.4   Objective #4: Modifications of PEG-genipin to increase gelation rate

Objective #4: Design and develop an injectable PEG-based biodegradable hydrogel. We will examine bi-functional, four-arm, and eight-arm amino-terminated PEG. We will characterize each of the hydrogels.

Hypothesis: By increasing the number of amine groups, the gelation time will decrease, thus the 8-arm PEG will gel faster than a 4-arm or diamine PEG. The gelation of PEG-genipin can be enhanced by varying parameters such as, temperature, exposure to air, and exposure to oxygen. The degradation of the 8-arm and 4-arm PEG hydrogels will be slower than the diamine PEG hydrogels.

2.0 DELIVERY OF FGF-2, INSULIN, AND DEXAMETHASONE TO INDUCE ADIPOGENESIS OF ADIPOSE DERIVED STEM CELLS FOR SOFT TISSUE ENGINEERING

2.1 INTRODUCTION

Soft tissue defects due to trauma or tumor resection often require reconstructive surgery. Autologous stem cell therapy has become a possibility for tissue reconstruction. In this study, we examined the use of adipose derived adult stem cells (ASCs) for soft tissue reconstruction. We designed an injectable system to deliver cells and growth factors. Fibroblast growth factor-2 (FGF-2) was encapsulated in PLGA microspheres. Released FGF-2 increased ASC proliferation and survival *in vitro*. ASCs were seeded on injectable small intestinal submucosa particles and injected subcutis along with FGF-2 microspheres in nude mice. FGF-2 microspheres increased angiogenesis *in vivo*; however, adipogenesis of the ASCs was not observed. Adipogenic factors, insulin and dexamethasone, were encapsulated in PLGA microspheres. The released factors induced adipogenesis of the ASCs *in vitro*. We have developed an injectable system to create a suitable environment for ASCs to proliferate and differentiate. Multiple injections at appropriate times could be performed to slowly fill soft tissue defects.

2.1.1   Soft tissue reconstruction

Tissue defects due to trauma, tumor resection, or congenital defects often require reconstruction. The current options for breast reconstruction include prosthetics (saline or silicone implants), moving adipose tissue with a vascular supply (such as TRAM), or autologous fat graft. Of these options, autologous fat grafting seems to be the most inviting. However, adipose tissue is not an effective filling material because of the insufficient vascularization once implanted and shrinkage/resorption over time. Grafted fat tissue becomes resorbed over time with 10% surviving after two years.[36] Microscopic examination demonstrates necrosis of adipocytes. Furthermore, mature adipocytes do not readily proliferate. Emerging research on autologous adult stem cells presents a potential innovative option for soft tissue reconstruction.

2.1.2   Adipose derived stem cells (ASCs)

Cell therapy is an integral area in regenerative medicine. One of the most promising candidates for cell therapy is the autologous stem cell. Investigators have found adult stem cells in various human tissues. The use of autologous stem cells is promising due to the lack of immunological risk as well as minimal ethical conflicts. Currently bone marrow has been the favored source of adult stem cells. Autologous and allogenic bone marrow stem cells have been studied extensively. Bone marrow consists of two populations of stem cells, hematopoietic (HSCs) and mesenchymal stem cells (MSCs)[37-39]. MSCs are multi-potent; they have the ability to differentiate into adipocytes, chondrocytes, myoblasts, and osteoblasts.[40, 41] However, bone marrow harvesting is painful and a potentially traumatic process. As well, bone marrow results in a low yield of mesenchymal stem cells, less than 0.01% of cells from bone

marrow aspirates are stem cells [41]. Multi-potent stem cells have been found in adipose tissue (ASCs) by Zuk et al.[1, 2] Adipose is a potentially abundant source of tissue that can easily be obtained. Nathan et al. found adipose derived stem cells to be superior with respect to minimal donor site morbidity, easy procurement, less risk of contamination during *ex vivo* expansion, rapid growth rate, and availability[42].

The differentiation of ASCs to all three germ layers has been examined. ASCs have the ability to differentiate into many different cell types. Figure 2-1 shows the different lineages ASCs have been differentiated into by various investigators (References in Appendix A). The differentiation of ASCs down the mesenchymal lineage is well accepted; however, transdifferentiation down the endodermal and ectodermal lineages remains controversial.
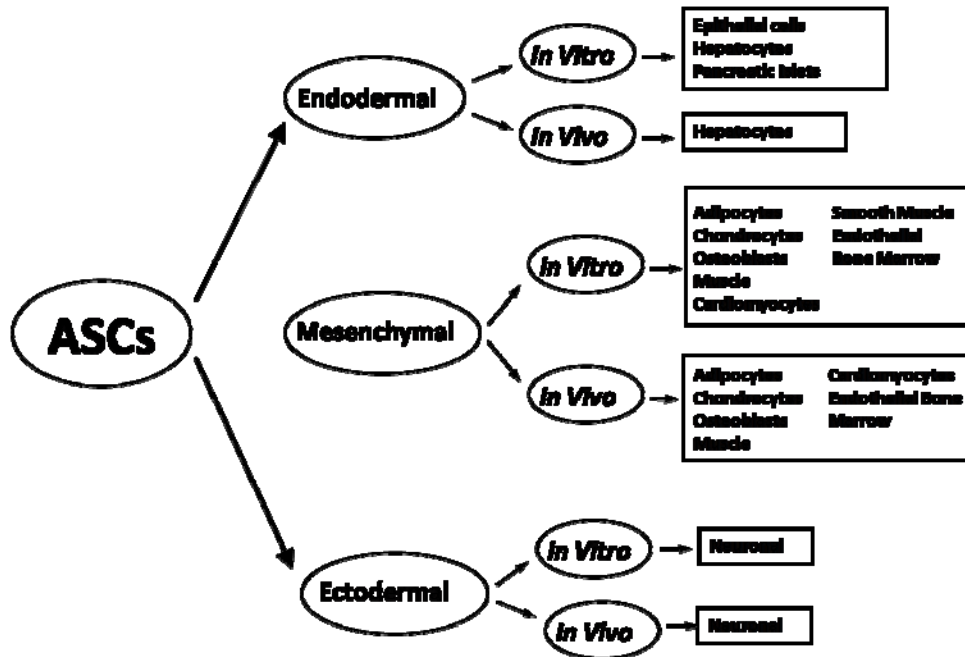
Figure 2-1. Plasticity of adipose derived stem cells.

ASCs may also induce vascularization of tissues *in vivo*. Hemmrich et al. have seen an increase in vascularization in scaffolds seeded with preadipocytes as compared to scaffolds

without cells[3, 43]. This may be due to the secretion of significant amounts of vascular endothelial growth factor (VEGF), hepatocyte growth factor (HGF), and transforming growth factor-beta (TGF-β), and small amounts of fibroblast growth factor (FGF-2) and granulocyte macrophage-colony stimulating factor (GM-CSF) from ASCs; furthermore, in hypoxic conditions VEGF release is increased[44].

2.1.3 Adipogenesis of ASCs

Adipose tissue is commonly found in subcutaneous loose tissue. Visceral adipose tissue surrounds internal organs. Adipose tissue is mainly composed of mature adipocytes. However, adipose tissue also contains fibroblasts, smooth muscle cells, pericytes, endothelial cells, and adipose derived stem cells. The structure of adipose tissue is important to understand adipocyte differentiation. Figure 2-2 is an overview of the stages in adipocyte differentiation, beginning with the stem cell and ending with a mature adipocyte.[45]
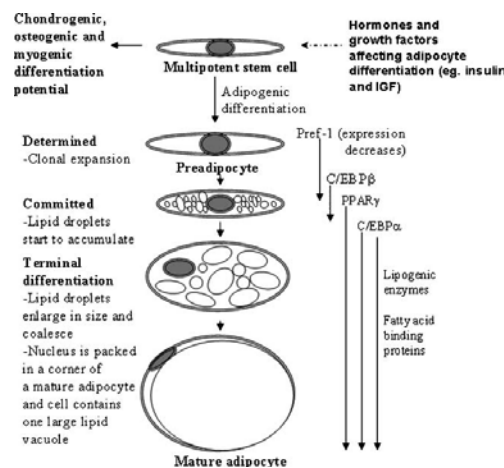
Figure 2-2. Adipocyte differentiation beginning with ASCs.[45]

14

Factors that induce adipocyte differentiation, adipogenic factors, include insulin, IGF-1, dexamethasone, cAMP, ciglitazone, and isobutyl-methylxanthine (IBMX).[46] Two important transcription factors, CCAAT/enhancer binding protein-α (C/EBP-α) and peroxisome proliferator-activated receptor-γ (PPAR-γ), have been shown to activate adipocyte genes that are required for adipocyte differentiation. PPAR-γ is the most specific to adipogenesis; it is induced before the transcriptional activation of most of the adipocyte genes. In cell culture, growth arrest due to cell density is necessary for differentiation, in which both C/EBP-α and PPAR-γ are involved.[47] Terminal differentiation is maintained by the expression of C/EBP-α and PPAR-γ, which act synergistically to activate transcription of genes.[46]

2.1.4 Fibroblast growth factor-2 (FGF-2)

A significant challenge in creating a large soft tissue mass is the limit of nutrients. A vascular supply is required for cells to survive. Controlled delivery of angiogenic factors at the site of implanted cells may promote survival and proliferation. Fibroblast growth factor-2 (FGF-2) is a growth factor known to induce angiogenesis and adipogenesis. FGF-2, or basic FGF (bFGF) is a 16-25 kDa growth factor that stimulates the proliferation of many cell types including fibroblasts, myoblasts, osteoblasts, endothelial cells, and chondrocytes [48]. The controlled release of FGF-2 has been extensively studied, and Table 2-I lists some of the delivery systems examined.

Table 2-I. FGF-2 Delivery Systems

Fibrin gel [49-51]	Gelatin [52-58]
Heparin gel [59]	Apatic substrates [60]
Hyaluronate-heparin [61]	Gelatin microspheres [62-66]
Glycosaminoglycan hydrogel [67]	PLGA microspheres [68-70]
Collagen hydrogel [71]	Heparin-alginate microcapsules [72]
Chitosan hydrogel [69, 73-75]	PLGA microspheres in alginate [76]
Dextran hydrogel [77]	Gelatin microspheres in collagen [78, 79]
Modified PEGDA [80]	Heparin modified PEG [81]

FGF-2 is also known for its angiogenic potential, due to its involvement by regulating the proliferation and migration of vascular endothelial cells[48]. The half life of FGF-2 has been reported as less than 50 minutes[82], 1.5 minutes, 4.5 minutes[83], and 3 minutes[84]. Even though these values differ, they are all relatively short. Due to its short half life, a delivery system is desired to maintain levels of FGF-2 *in vivo*. Sustained release of FGF-2 has been reported as three times more potent than a bolus of FGF-2 to increase vascular endothelial and smooth muscle cell proliferation.[85] FGF-2 increases capillary formation *in vivo* when compared to zero FGF-2.[63, 76, 86]

FGF-2 increases adipose tissue formation *in vivo*. Gelatin microspheres incorporating FGF-2 led to an increase in *de novo* induced adipogenesis and *in situ* adipogenesis of a rat fat pad versus free FGF-2.[63, 78, 79] Gelatin microspheres containing FGF-2 increased the formation of adipose tissue from preadipocytes seeded on collagen sponges.[65]

The effects of FGF-2 on adult stem cells have been examined. FGF-2 has been shown to increase mesenchymal stem cell (MSC) proliferation.[87-91] The treatment of MSCs with FGF-

2 induced adipogenesis with and without other differentiation components.[89, 92] FGF-2 has induced the proliferation of ASCs[93-95] and induced adipogenesis of preadipocytes.[65, 96] The addition of FGF-2 has resulted in larger adipose tissue formation *in vivo* compared to 0 FGF-2.[86] Released FGF-2 results in a significantly higher adipogenesis of preadipocytes *in vivo* than free FGF-2.[65, 78] In this study, we have chosen to focus on a controlled release of FGF-2 from polymer microspheres.

2.1.5 Small intestinal submucosa scaffolds

A critical element in tissue engineering is finding a suitable scaffold that promotes cell proliferation and differentiation. Naturally derived scaffolds may be advantageous due to properties such as biodegradability, biocompatibility, and the possibility to facilitate cell growth and proliferation. The response of ASCs to natural scaffolds such as decellularized human placenta[97], hyaluronic acid[97-99], CultiSphers[100], fibrin[101-103], collagen[99, 104], decellularized vein grafts[105], and gelatin[103, 106, 107] have been studied. Small intestinal submucosa (SIS) is a porcine derived extracellular matrix scaffold derived from the small intestinal submucosa. SIS contains several angiogenic growth factors, rendering the extracellular matrix (ECM) scaffold successful for tissue remodeling.[108] SIS has primarily been used in hernia repair[109], but has also shown promising results as a scaffold for cell adhesion.[110, 111] SIS has supported the attachment and proliferation of NIH Swiss mouse 3T3 fibroblasts, NIH 3T3/j2 fibroblasts, primary human fibroblasts, primary human keratinocytes, human microvascular endothelial cells (HMECs), and an established rat osteosarcoma cell line.[112, 113] The interaction of SIS and mesenchymal stem cells has been studied. Bone marrow stromal cells attach and proliferate on SIS without affecting their cellular activity and

function.[114, 115] The addition of SIS to MSCs *in vivo* has resulted in improvement of myocardial repair following infarction[116], bladder reconstruction *in vivo*[117], and osteogenesis *in vitro*.[114] SIS improved islet survival and function *in vitro,* leading to an increase in insulin secretion, and reduction of apoptosis.[118] Muscle derived stem cells migrate into and distribute within SIS scaffolds and form contracting myotubes.[119] Due to the promising results of these studies we have chosen to utilize SIS as our scaffold.

2.1.6   Dexamethasone and delivery systems

Dexamethasone (Dex) (Figure 2-3) is a synthetic corticosteroid with a radius of 6.5 Angstroms. Dex has most commonly been used to treat inflammation and auto-immune diseases.
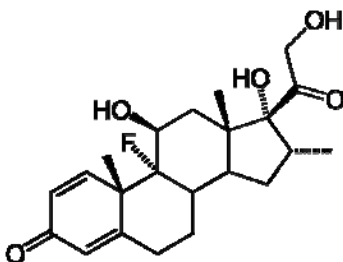
Figure 2-3. Structure of Dexamethasone

Dexamethasone is an important factor in adipogenesis. Dex has been shown to enhance adipogenesis by increasing the expression of C/EBP and PPAR-γ.[120, 121].   Dex is also responsible for preadipocyte recruitment.[120, 122, 123] Adipogenesis by Dex alone has also been demonstrated.[88, 124] However, an increase in adipocyte differentiation was seen with cells treated with both Dex and insulin, compared to either alone.[120] Dex is required to

establish a post-mitotic state of the ASCs, by distinguishing mitotic divisions of clonal expansion from those of logarithmic growth.[123] The addition of Dex increases cell differentiation compared to zero Dex.[124, 125]

Although the release of Dex for use in adipogenesis of ASCs has not been examined, to the best of our knowledge, Dex has been released to induce osteogenesis of mesenchymal stem cells.[126] However, due to the wide clinical applications of Dex, the controlled delivery of dex has been studied extensively. Table 2-II lists some of the delivery systems that have been characterized.

Table 2-II. Dexamethasone Delivery Systems

Polymer micro/nanospheres [127-133]	Poly(ortho ester) [134]
Starch microspheres [135]	Elastin-like polymer [136]
Ethylcellulose microspheres [137]	Si film [138]
PLA-PEG film [139]	Gelatin [140]
PEG hydrogels [126, 128]	Chitosan [131, 137]
Polypyrrole [141]	PLGA microspheres in PEG hydrogels [128]
PLGA [142]	PLGA microspheres in PVA hydrogels [143, 144]
Polyurethane [145]	PLGA microspheres in alginate[146]

2.1.7 Insulin and delivery systems

Insulin is a hormone that is secreted by the beta cells of the islets. Insulin has been well studied because it stimulates cells to absorb glucose and amino acids from blood. Patients with diabetes mellitus type I are treated with insulin, since their beta cells have been destroyed by their own bodies. Insulin is a peptide hormone composed of 51 amino acid residues with a molecular weight (MW) of ~6kDa. Insulin is another important adipogenic factor. Insulin stimulates lipogenesis by enhancing the rate of lipid filling and enhancing the fraction of cells that differentiate.[147]

The release of insulin has been extensively investigated, mostly for treatment of diabetes. Table 2-III lists some of the delivery devices utilized to maintain release of insulin.

Table 2-III. Insulin Delivery Systems

Polymer microspheres [148-157]	PEG hydrogels [158-161]
Chitosan microspheres [162-166]	Chitosan hydrogels [167, 168]
Gelatin microspheres [58, 169]	Acrylic hydrogels [170]
Hyaluronic acid microspheres [171]	PLGA microspheres in PVA [172]
Alginate-dextran nanospheres [173]	Solid-lipid microparticles [174]

More specifically, the release of insulin to induce adipogenesis has been demonstrated. Yuksel et al. showed that released insulin *in vivo* resulted in *de novo* adipose formation.[68] Similarly, insulin and IGF-1-loaded microspheres resulted in an increase in adipose flap weight at four weeks *in vivo* without adverse reactions to surrounding tissue.[175] We are focusing on insulin release to induce adipogenesis of ASCs.

In summary, our approach for soft tissue reconstruction focuses on the combination of injectable cells, scaffolds, and various growth factors. We have seeded our ASCs on SIS particulate scaffolds and delivered FGF-2 from polymer microspheres to induce cell survival and proliferation *in vivo*. We have also examined the induction of differentiation of ASCs due to released adipogenic factors, insulin and dexamethasone, *in vitro*.

2.2   METHODS

2.2.1   Isolation of ASCs

This study was conducted in accordance with the regulations of the Human Studies Committee of the University of Pittsburgh. Tissue collection was performed according to a protocol approved by the University of Pittsburgh Institutional Review Board.

The ASCs were isolated from fresh human abdominal adipose tissue harvested during elective surgery, as previously described.[176]   Adipose tissue was first treated with a collagenase (type II) solution and minced. The tissue in the collagenase solution was then gently agitated at 37°C, filtered to remove large debris, and centrifuged. The cellular pellet was resuspended in erythrocyte lysis buffer and centrifuged again. The resulting cellular pellet was plated and cultured on tissue culture treated flasks in ASC plating medium (DMEM/F12, 10% FBS, 1% pen/strep, Dexamethasone).

2.2.2   FGF-2 encapsulation and characterization

PLGA microspheres were prepared using a double emulsion technique as previously described.[70]   FGF-2 (R&D Systems, Inc, Minneapolis, MN) was reconstituted in a heparin (1:1), EDTA (1:1), sucrose (5mg/25μg FGF-2), 0.1% BSA solution. 200mg of PLGA (75:25) (Lactel Absorbable Polymers, Pelham, AL) was dissolved in 1.8 mL methylene chloride (MC). To form the first emulsion, 50 μL of the 25μg/mL FGF-2 solution and 1 mL of 1% PVA solution were added to the dissolved PLGA and vortexed. The first emulsion was then added to a stirring 0.1% PVA solution and stirred at 900 rpm. After five minutes, 100 mL of 2% isopropanol was

added dropwise and then stirred for 2 hours. The microspheres were collected by centrifugation, frozen at -20°C, and freeze-dried. Empty microspheres were also prepared using the same protocol, omitting the addition of FGF-2.

Morphological characterization of the microspheres was examined using scanning electron microscopy (SEM). The microspheres were gold coated using a Cressington 108 Auto (Cressington, Watford UK). Microspheres were then viewed using a JSM-6330F scanning electron microscope (JEOL, Peabody, MA) operated at 10 kV accelerating.

The release of FGF-2 from the microspheres was analyzed utilizing a commercially available Enzyme Linked Immunosorbent Assay (ELISA) kit (R&D). Microspheres (10mg) were placed in a microcentrifuge tube containing 1 mL of Phosphate Buffered Solution (PBS) (n=5). At various time points, the tubes were centrifuged and the supernatant collected, and then frozen at -80°C until analysis. The samples were then refreshed with 1 mL PBS and vortexed for 5 seconds.

2.2.3   FGF-2 *in vitro* effects on ASCs

The effects of FGF-2 concentration on ASC proliferation was investigated to determine the optimal concentration of FGF-2 to use in subsequent studies. ASCs (30-35 year old female, abdominal deep, passage 2) were seeded at a density of 10,000 cells/mL per well of a tissue treated 24-well plate in ASC plating medium. The cells were allowed to attach and proliferate for 24 hours. The ASCs were then washed with PBS and treated with one of the experimental groups. The experimental medium contained 0.5% FBS, 1% pen/strep, and Dexamethasone, except for the control that contained 10% FBS (ASC plating medium). The groups are as follows: 1) 10% FBS medium, 2) 0ng FGF-2, 3) 1ng FGF-2, or 4) 10ng FGF-2 (n=5 for each

group). After 72 hours, the plates were washed with PBS, frozen, and analyzed utilizing CyQuant® (Molecular Probes, Eugene, Oregon)[177]. CyQUANT® is a fluorescence-based cell proliferation assay that utilizes a green fluorescent dye that binds to cellular nucleic acids. Viable cell number was calculated utilizing a standard curve.

An *in vitro* study was performed to examine the effects of the FGF-2 microspheres on ASC proliferation. ASCs (30-35 year old female, abdominal deep, passage 2) were seeded at a density of $3x10^5$/mL into each well of a 24-well tissue culture plate in ASC plating medium. Cells were allowed to attach and proliferate for 24 hours. The ASCs were then washed with PBS and treated with one of the following groups for 48 hours: 1) 0ng/mL FGF-2, 2) 1ng/mL free FGF-2, 3) FGF-2 microspheres releasing 1ng of FGF-2 over 48 hours, or 4) empty microspheres (n=5 for each group). FGF-2 microspheres were suspended in Transwell® inserts above the attached ASCs. The amount of microspheres added to each well was determined by calculating the microspheres necessary to release a total of 1ng of FGF-2 over 48 hours, thus a final concentration of 1ng FGF-2 per milliliter of media was obtained. The wells were washed with PBS, frozen, and then the viable cell number was quantified utilizing CyQuant®.

A longer *in vitro* study was performed to simulate a similar environment the cells would experience *in vivo*. ASCs from three different patients, age range 30-45 years old and three different depots were utilized in this study. The experiment was performed with ASCs from each of the following depots: 1) super abdominal, 2) deep abdominal, and 3) back. ASCs were seeded at a density of $15x10^3$ cells/mL into wells of a 24-well plate in plating medium and allowed to attach and proliferate for 48 hours. All groups were then placed in experimental medium, containing no serum (DMEM/F12, 1% pen/strep, dexamethasone) for 24 hours. After 24 hours, cells were treated with one of the following groups, 1) 0ng/mL FGF-2 (control group),

2) 1ng/mL free FGF-2, 3) FGF-2 microspheres releasing a total of 1ng FGF-2 over 14 days, or 4) empty microspheres (n=5 for each group, repeated for each cell type). The amount of FGF-2 microspheres was the same amount that was used for the *in vivo* studies (21mg). The medium was changed every other day for all groups. The medium containing 1ng free FGF-2 was prepared on day 1, thus for the duration of the experiment the cells in the free FGF-2 group were treated every other day with 1ng FGF-2. After 14 days, the plates were washed with PBS, frozen, and then the viable cell number was quantified utilizing CyQuant®.

2.2.4   FGF-2 *in vivo* effects

ASCs (30-35 year old female, abdominal deep, passage 5) were seeded on SIS particles (13 million cells on 0.16g SIS) utilizing a spinner flask (Bellco Glass, Vineyard, NJ) and incubated at 37ºC with 5% CO_2 on a stir plate set to rotate at 15 rpm. The ASCs were cultured in the spinner flask for 14 days before being utilized for the *in vivo* study. The medium was changed in the spinner flask three times a week by allowing the SIS particles to settle and removing half of the medium and replacing it with fresh medium. At various times points, SIS seeded particles were removed, fixed, and stained with DAPI, a fluorescent nuclear stain. At the time of the procedure, syringes (1cc and 22G needles) for injection were prepared with 0.2mL of SIS and medium (DMEM/F12, 10% FBS). Male athymic nude mice n=5 (for each group) (8 weeks, 25 grams, Harlan, IN, USA) were anesthetized with isoflurane. The mice were injected with ASCs seeded on SIS as a control group. The experimental groups included ASCs seeded on SIS and either 1) 1ng free FGF-2, or 2) FGF-2 microspheres (a total of 1 ng FGF-2 to be released over the 14 days, 21mg of microspheres). The free FGF-2 and FGF-2 microspheres were injected subcutaneously (100 µL of DMEM/F12 as a carrier) along with the ASCs seeded on SIS

into the same site. The injected areas were sutured with Vicryl 4-0, to ensure identification at the time of sacrifice. On day 14, the animals were sacrificed. Samples from the injected area, determined as the area enclosed by the sutures, were excised and divided in half. One half was fixed in 10% buffered formalin and embedded in paraffin and the other half was frozen utilizing Optimal Cutting Temperature (OCT) compound.

2.2.5   Histological analysis

Samples embedded in paraffin were stained with hematoxylin and eosin (H&E) and adjacent sections for Factor VIII. The number of blood vessels within the injected area was quantified from H&E slides by three blind observers. Each image was presented to an observer, and the number of evident blood vessels in the cross-section was manually counted. Factor VIII staining was performed to verify the blood vessels present.

The frozen sections were imaged for fluorescent analysis. The cells implanted *in vivo* were pre-labeled with Red Fluorescent Cell Linker, PKH26, (Sigma-Aldrich, Mo, USA). PKH Fluorescent Cell Linker Kits provide fluorescent labeling of live cells over an extended period of time, with no apparent toxic effects.[178, 179] PKH linker exhibits no significant leaking or transfer from cell to cell. PKH26, a red fluorochrome, has excitation (551 nm) and emission (567 nm) characteristics compatible with rhodamine or phycoerythrin detection systems. The linkers are physiologically stable and show little to no toxic side effects on cell systems. Labeled cells retain both biological and proliferative activity, and are ideal for cell tracking studies.

2.2.6 Dexamethasone encapsulation and characterization

Dexamethasone-sodium phosphate (Sigma Aldrich) PLGA microspheres (Dex MS) were prepared using a single emulsion/solvent extraction technique as previously described. PLGA (75:25), 100mg, was dissolved in 4.5 mL MC. Dex (20mg) was dissolved in 0.5mL methanol which was then added to the polymer solution. This solution was then added to a stirring 0.2% PVA solution (600mL) and stirred at 1200 rpm for two hours. The microspheres were collected by centrifugation, frozen at -20$^\mathrm{o}$C, and freeze-dried. Empty microspheres were also prepared using the same protocol, omitting the addition of Dex. Morphological characterization of the microspheres was examined using SEM as previously described.

The release of Dex from the microspheres was analyzed spectrophotometrically at 242nm. Microspheres (10mg) were placed in a microcentrifuge tube containing 1 mL of PBS (n=5). At various time points, the tubes were centrifuged, the supernatant collected, and then frozen at -80$^\mathrm{o}$C until analysis. The samples were refreshed with 1 mL PBS and vortexed. The amount of Dex released was determined by comparison to a standard curve.

The following equations were used to characterize the microspheres:

$$LC = \frac{D_E}{S_w} \qquad \textbf{Equation 2-1}$$

$$Yield = \frac{M_{Pi}}{M_{Pf}} \times 100\% \quad \textbf{Equation 2-2}$$

In equation 2-1, LC is the loading capacity, which determines the amount of drug per weight of microspheres. Where, D_E is the amount of drug encapsulated and S_w is the mass of the microspheres. The yield is calculated by equation 2-2, where M_{Pi} is the initial mass of polymer used to fabricate the microspheres and M_{Pf} is the final mass of the microspheres.

The encapsulation efficiency was determined by a method previously described by Sah et al.[180] Briefly, 20mg of microspheres were dissolved in 2mL DMSO for 1 hour. Then 10mL of 0.05N NaOH containing 0.05w/v% SDS solution was added for 1 hour. The amount of Dex in the resulting solution was assessed as mentioned above, spectrophotometrically.

2.2.7   Insulin encapsulation and characterization

Insulin loaded PLGA microspheres (Insulin MS) were prepared using a double emulsion/solvent extraction technique as previously described. 400mg of PLGA (75:25) was dissolved in 2.0 mL methylene chloride (MC). To form the first emulsion, 15mg of insulin (Sigma) was dissolved in 0.2mL of PBS, which was then added to the dissolved PLGA and vortexed. The first emulsion was added to a stirring 100mL of 2.0% PVA solution and stirred at 500 rpm. After 2 min, 400 mL of water was added and then stirred for 3 hours at 500rpm. The microspheres were collected by centrifugation, frozen at -20°C, and freeze-dried. Empty microspheres were also prepared using the same protocol, omitting the addition of insulin. The microspheres were morphologically characterized using SEM as previously described.

The released insulin was analyzed utilizing FluoroProfile Protein Quantification Kit (Sigma Aldrich, St Louis, MO). Microspheres (10mg) were placed in a microcentrifuge tube containing 1 mL of PBS (n=5). At various time points, the tubes were centrifuged, the supernatant collected, and then frozen at -80°C until analysis. The samples were refreshed with 1 mL PBS and vortexed.   For analysis, 50μL of the sample and 50μL of the working reagent were added to a black 96 well plate and the fluorescence was measured at 485nm excitation and 635nm emission.

The yield and loading capacity were calculated as mentioned above (section 2.2.6). The encapsulation efficiency was determined as mentioned above (section 2.2.6). The amount of insulin in the resulting solution was assessed utilizing a BCA kit (Pierce, Rockford, USA).

2.2.8 *In vitro* effects of released dexamethasone and insulin on ASC differentiation

The optimal weight of microspheres to induce ASC adipogenesis was determined for subsequent studies. According to the release study, 4mg of dexamethasone and 5mg of insulin microspheres would achieve the desired released adipogenic factors. To further assess this, three different amounts of each microsphere type was assessed, x, 2x, and 5x.

ASCs (female, super abdominal, 35-40 years old, passage 2) were seeded into tissue culture treated 12-well plates at a density of 50,000 cells/mL. The cells were allowed to adhere and proliferate for seven days in ASC plating medium. The cells were then treated for fourteen days in various treatment groups. The negative control group was treatment with DMEM/F12 medium containing 1%pen/strep (n=6). The positive control group was treatment with differentiation medium, DMEM/F12 with 1% pen/strep containing differentiation components (22µM biotin, 17µM D-pantothenic acid; 1.0µM ciglitazone, 0.2nM T3, 10mg/L transferin, and 540µM IBMX (IBMX for first 48 hours only)), and 0.5µM insulin, and 0.2nM dexamethasone (Diff medium)(n=6).

The combined effects of Dex and insulin MS were assessed. Cells were treated with Diff medium containing 0 insulin and 0 dexamethasone (Diff components + 0 insulin + 0 dexamethasone) (Diff-Dex-Ins medium). The treatment group was treated with the same medium (Diff-Dex-Ins medium) plus 4mg, 8mg, or 20mg Dex MS plus 5mg, 10mg, or 25mg

insulin MS. ASCs in the negative control medium were also treated with 4mg, 8mg, or 16mg Dex MS plus 5mg, 10mg, or 25mg insulin MS.

2.2.9   Differentiation of ASCs utilizing dexamethasone and insulin microspheres

To further assess the ability of Dex and insulin MS to replace Dex and insulin in medium, the optimal amount of microspheres previously demonstrated were used for all subsequent studies. A similar study as described above was performed. ASCs (female, back, 40-45 yo, passage 1) were seeded into tissue culture treated 6-well plates at a density of 200,000 cells/mL. The cells were allowed to adhere and proliferate for seven days in ASC plating medium. The cells were then treated for fourteen days in various treatment groups.

The effects of the dexamethasone microspheres on ASC differentiation were examined by comparing treatment of cells with Diff medium containing 0 dexamethasone (Diff components + 0.5μM insulin + 0 dexamethasone) (Diff-Dex medium) with cells in the same medium (Diff-Dex medium) plus 8mg of Dex MS.

To determine the effects of insulin microspheres on ASC adipogenesis, cells were treated with Diff medium containing 0 insulin (Diff components + 0 insulin + 0.2nM dexamethasone) (Diff-insulin medium). The adipogenesis was compared to cells treated in the same medium (Diff-insulin medium) plus 10mg insulin MS.

The combined effects of Dex and insulin MS were assessed in a similar manner. Cells were treated with Diff medium containing 0 insulin and 0 dexamethasone (Diff components + 0 insulin + 0 dexamethasone) (Diff-Dex-Ins medium). The treatment group was treated with the same medium (Diff-Dex-Ins medium) plus 8mg Dex MS plus 10mg insulin MS. ASCs in the negative control medium were also treated with 8mg Dex MS plus 10mg insulin MS. As a

further control, empty MS were added to cells treated in the negative control medium. The

treatment groups were as summarized in the following table.

Table 2-IV. Treatment Groups with Dexamethasone and Insulin Microspheres

Treatment Group	DMEM/F12	Diff Components	Dex	Insulin	Dex MS	Insulin MS
Negative Control	X					
Positive Control	X	X	X	X		
Diff - Dex	X	X		X		
Diff – Dex + Dex MS	X	X		X	X	
Diff - Insulin	X	X	X			
Diff - Insulin + Insulin MS	X	X	X			X
Diff - Dex – Insulin	X	X				
Diff – Dex – Insulin + Dex MS + Insulin MS	X	X			X	X
+ Dex MS + Insulin MS	X				X	X
Empty MS	X					

2.2.10 Oil red O staining

After 14 days of treatment, the ASCs were washed with PBS, fixed in a 10% buffered

formalin solution for 10 minutes, washed with DI water (two times), and stained with Oil red O

for 30 minutes, then washed with water. The ASCs were then imaged under light microscopy.

Four fields of view per well were imaged to determine the number of cells with lipid inclusions

per field of view. All values were normalized to the positive control.

2.2.11 Western blot analysis

Cell lysates were collected following fourteen days of treatment. Cells were first washed

with PBS and then 100µL of lysis buffer (m-PER, Pierce, Rockford, IL) and proteinase inhibitor

(1:100 dilution, Sigma Aldrich, St. Louis, MO) were added to each well. The protein solutions

were frozen at -80°C until analysis. Total protein was measured using the BCA Protein Assay

Kit. Equal amounts of protein from each sample were loaded into a 10% SDS-PAGE gel for gel electrophoresis. The separated proteins were then transferred to a nitrocellulose membrane. The membrane was blocked in 5%milk/PBS/Tween-20 for 2 hours and then the primary antibody (PPAR-γ, Santa Cruz, Santa Cruz, CA) in 1%milk/PBS/Tween-20 was applied overnight at 4°C. The secondary antibody (Jackson ImmunoResearch Laboratories, West Grove, PA) in 1%milk/PBS/Tween-20 was applied for 1 hour. The proteins present on the membrane were detected using the ECL Plus detection system (Amersham, Piscataway, NJ). Expression of GAPDH was used as an internal control.

2.2.12 Statistical analysis

All values are reported as means ± standard deviations. ANOVA was used for comparisons between groups. In vitro experiments with two groups were compared using t-test analysis. Differences were significant when $p < 0.05$.

2.3   RESULTS

2.3.1   FGF-2 characterization

We have encapsulated FGF-2 into PLGA microspheres. Figure 2-4 depicts the FGF-2 microspheres using scanning electron microscopy (SEM). SEM was also utilized to determine the morphology and diameter of the microspheres. The microspheres exhibit a smooth round

morphology.   The diameter of the microspheres ranged from 1μm to 65μm (Figure 2-5), the

average diameter of the microspheres was 9.19 ± 9.51 μm.
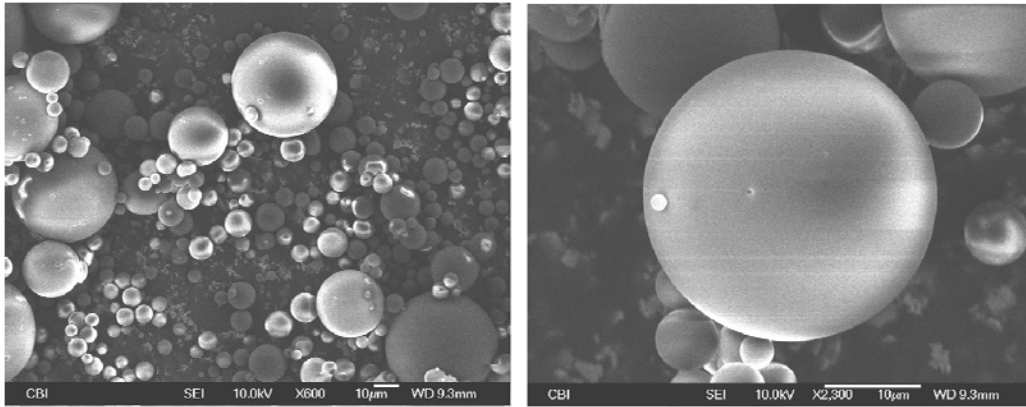
Figure 2-4. SEM of FGF-2 microspheres.[181]
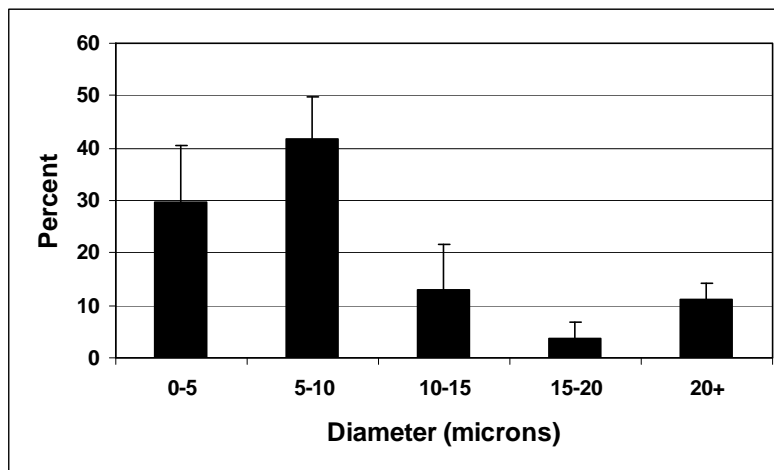
Figure 2-5. Diameter distribution of FGF-2 microspheres.[181]

The release of FGF-2 from the microspheres was determined using an ELISA kit. FGF-2

was released over 14 days (Figure 2-6). The majority of the FGF-2 was released within the first

day; 96% was released in the first 24 hours. The remaining 4% was released over the following

13 days.
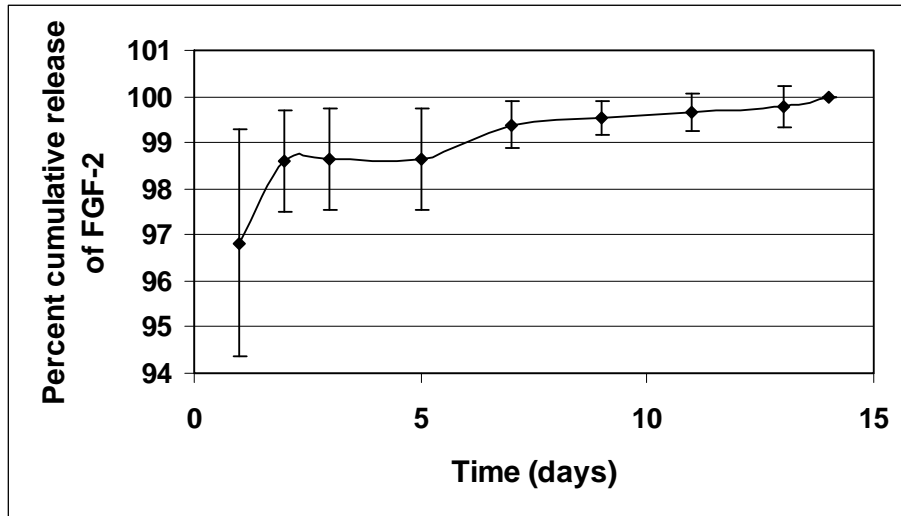
Figure 2-6. Percent cumulative release of FGF-2 from PLGA microspheres.

2.3.2   Effects of FGF-2 on ASCs *in vitro*

The optimal concentration of FGF-2 to induce ASC proliferation was determined. FGF-2 at a concentration of 0, 1, and 10ng/mL was examined.   A significant increase in cell proliferation was seen in all groups compared to 0ng FGF-2 (Figure 2-7).   There were no significant differences between the 1ng/mL and the 10ng/mL group.   Since increasing the amount of FGF-2 to 10ng did not result in a significant increase, and the trend showed more proliferation in the 1ng/mL group, 1ng/mL FGF-2 was used for all subsequent studies.
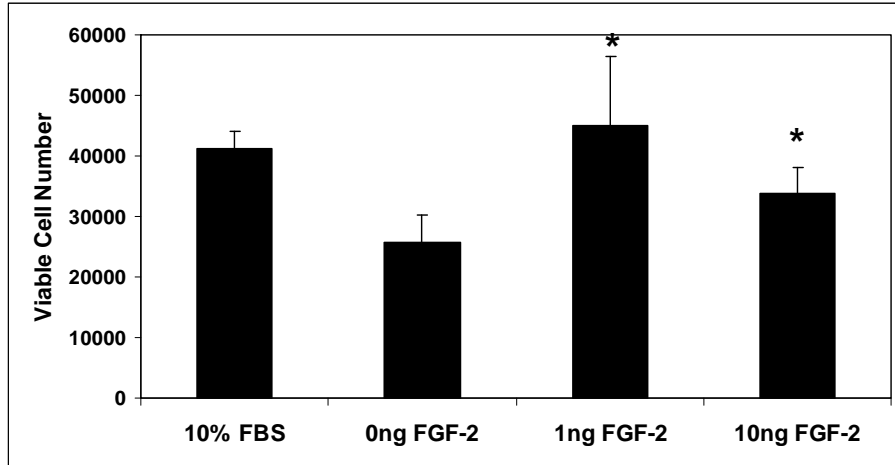
Figure 2-7. Viable ASCs after treatment for 72 hours.
(n=5) *p<0.05 compared to 0ng FGF-2.

Transwell® inserts and CyQuant® were utilized to determine the effects of FGF-2 on ASC proliferation. The ASCs were treated with 1 ng free FGF-2, FGF-2 microspheres (releasing a total of 1 ng FGF-2 over 48 hours), or empty microspheres. A significant increase in cell proliferation was seen with the addition of 1 ng of free FGF-2 (p=0.031). A slight increase in cell proliferation was seen in the group treated with FGF-2 microspheres, when compared to media alone (p=0.056) (Figure 2-8).
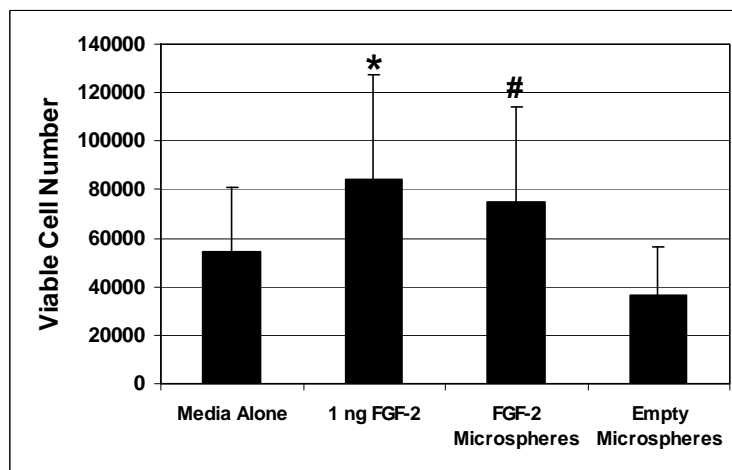
Figure 2-8. Viable ASCs after treatment for 48 hours.
*p<0.05, #p<0.10[181]

34

A longer *in vitro* study was performed over 14 days to determine the effect of the FGF-2 microspheres and free FGF-2 on the ASCs (Figure 2-9). All groups were treated with medium containing no serum. Cell survival was significantly increased in the group treated with the FGF-2 microspheres compared to all groups (Figure 2-9). The cells treated with 1ng/mL free FGF-2 at each feeding were not significantly different from cells in the control group. There was also no significant difference between cells treated with empty microspheres when compared to those in the control group (0ng FGF-2). The FGF-2 microspheres resulted in an increase in ASC survival and proliferation in the absence of serum. These results were consistent among the three types of ASCs.
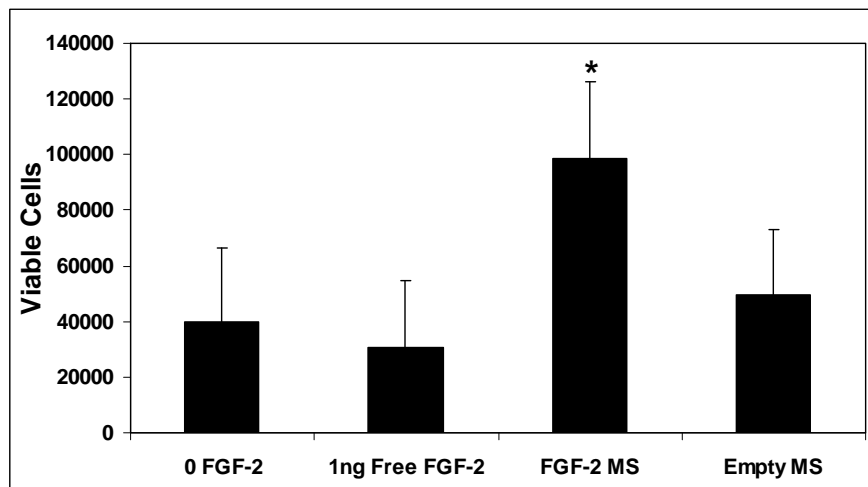
Figure 2-9. Viable ASCs after 14 days *in vitro*.
***p<0.05[181]**

2.3.3 Effects of released FGF-2 on ASCs *in vivo*

ASCs were labeled with PKH26 and seeded onto SIS particles and injected subcutaneously into nude mice (Figure 2-10). Two groups of mice were then given an additional injection of either 1 ng of free FGF-2 or FGF-2 microspheres, releasing a total of 1 ng

FGF-2 over the 14 days. The third group was not treated with any further injections (n=5 for each group).
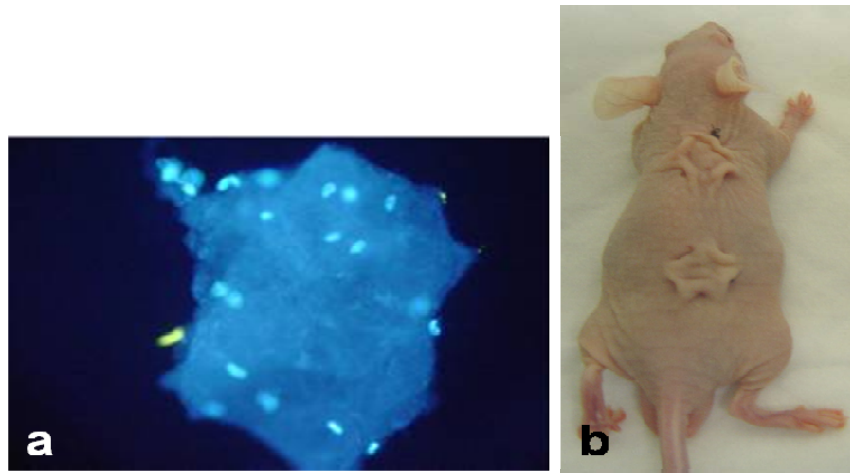
Figure 2-10. ASCs seeded on SIS particle (a). Injection sites on the back of mouse (b).[181]

The mice were sacrificed after 14 days; sections were embedded in paraffin and stained with H&E and Factor VIII. Cell survival was determined by locating the PKH26 labeled cells. Figure 2-11b depicts the PKH26 labeled cells and the corresponding H&E staining (Figure 2-11a) from a mouse treated with FGF-2 microspheres. Cells survived in all three groups. Factor VIII staining was performed to confirm the presence of blood vessels. Representative images of H&E and the corresponding Factor VIII staining for each group are shown in Figure 2-12. The arrows in the H&E images denote the injection site of ASC seeded SIS particles (a,c,e). The arrows denote staining of blood vessels (b,d,f). A vascular network surrounding the injected area could be seen in mice treated with FGF-2 microspheres (Figure2-13a). The number of blood vessels in the injection area was quantified from H&E images (Figure 2-13b). The mice that received the injection of FGF-2 microspheres had a significant increase in the number of blood vessels present.
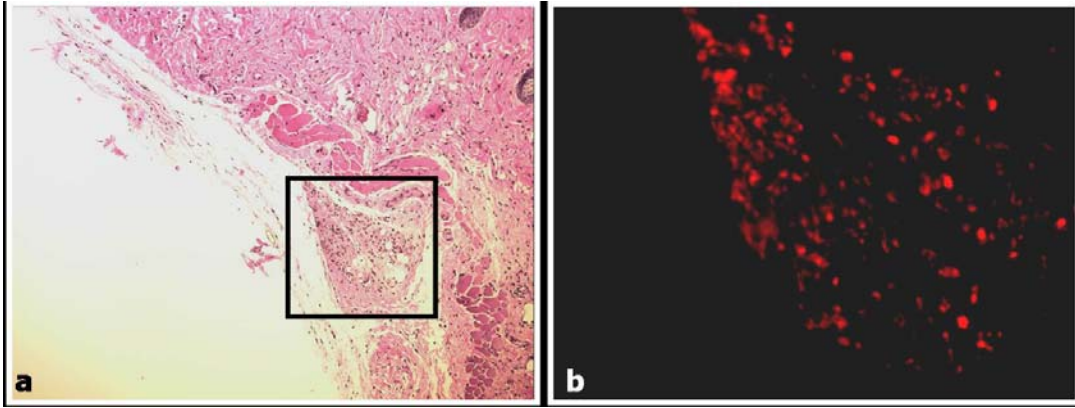
Figure 2-11. ASCs present after 14 days *in vivo*.
H&E staining of ASC and SIS injection area (100x) (a) PKH26 labeled ASCs 14 days after injection (400x)
(b). [181]
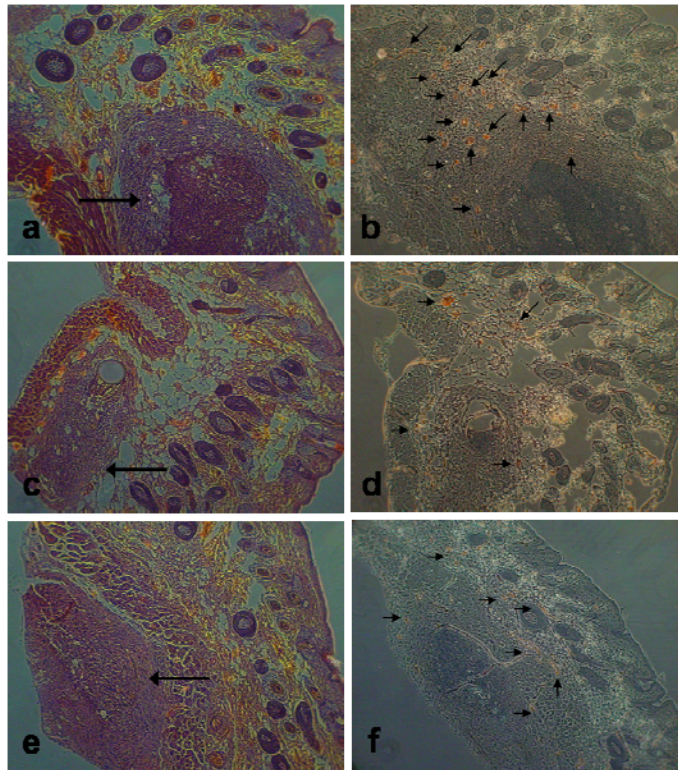
Figure 2-12. H&E and corresponding Factor VIII images 100x.
FGF-2 microsphere injection (a and b), free FGF-2 injection (c and d), and control (0 FGF-2) (e and f).
Arrows in H&E images denote site of injection. Arrows in Factor VIII images denote blood vessels.[181]
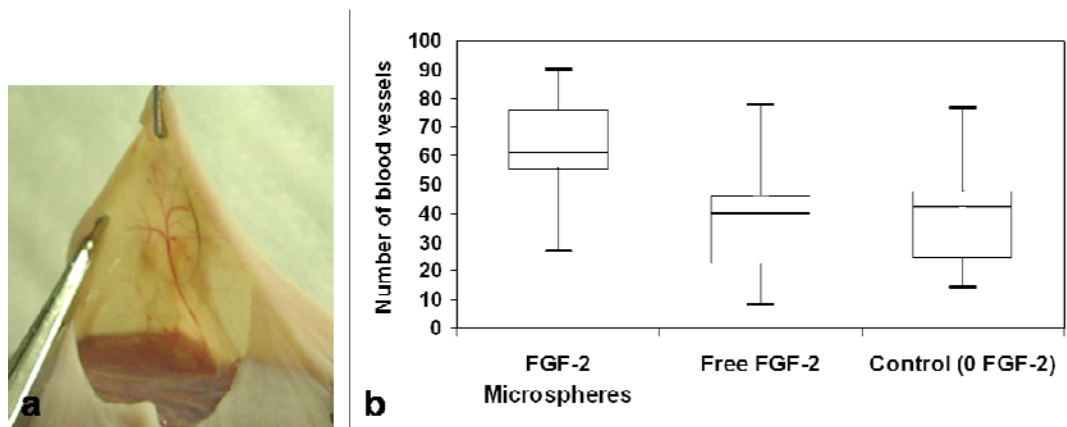
Figure 2-13. Image depicting vascularization in mouse treated with FGF-2 microspheres (a). Boxplot of number of blood vessels surrounding injection area (b).[181]

2.3.4 Dexamethasone microsphere characterization

Dex microspheres were examined by SEM (Figure 2-14). The microspheres had an average diameter of 10 μm. The diameter distribution of the Dex MS is shown in Figure 2-15. The release of dexamethasone occurred over 52 days (Figure 2-16). A controlled release was maintained. After one day $28.4 \pm 5.3\%$ of total dexamethasone released was released. A large burst effect was not observed, which is most likely due the hydrophobic nature of dexamethasone. After 48 days, $96.0 \pm 1.3\%$ was released. The yield was $70.3 \pm 12.6\%$. The loading capacity was 7.24 ± 1.48μg Dex per mg of microspheres.
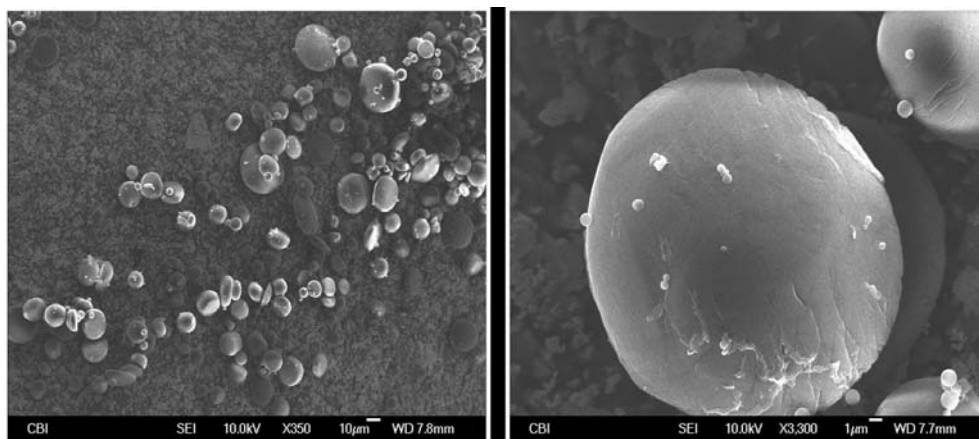
Figure 2-14. SEM of dexamethasone microspheres.
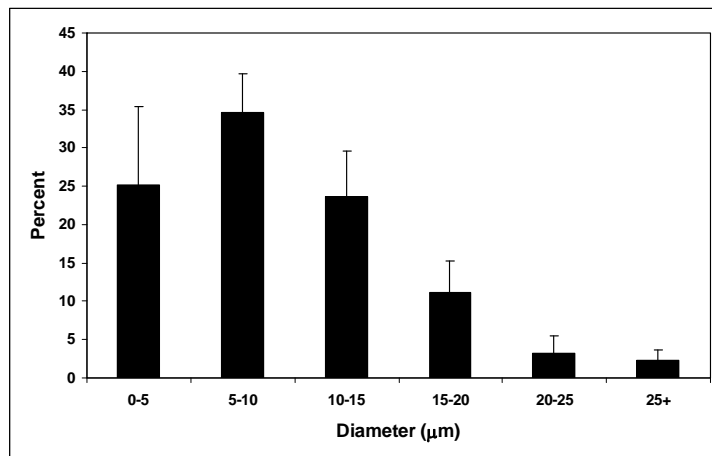
Figure 2-15. Diameter distribution of dexamethasone microspheres. Results expressed as means ± standard deviations.
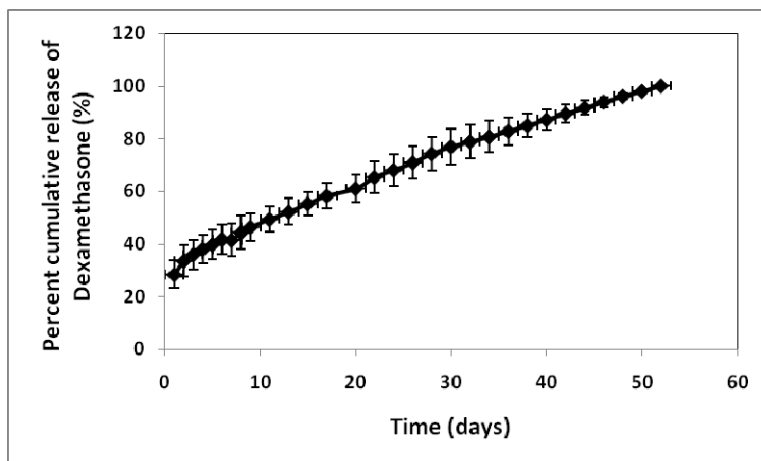
Figure 2-16. Cumulative release of dexamethasone per milligram of microspheres. Results expressed as means ± standard deviations (n=8).

2.3.5 Insulin microsphere characterization

Insulin microspheres were examined utilizing SEM (Figure 2-17). The average diameter of the insulin microspheres was 272 µm (Figure 2-18). The release of insulin was maintained over 52 days (Figure 2-19). The insulin microspheres yield was 35.6±10.8%. The loading capacity was 11.6 ± 2.3 µg insulin per mg of microspheres.
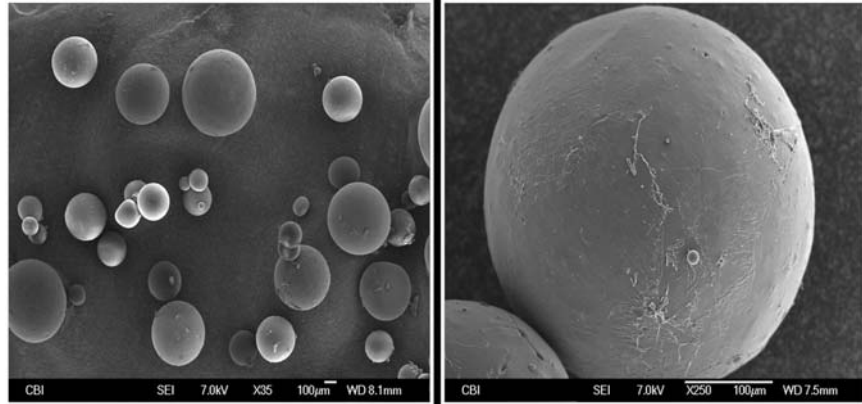
Figure 2-17. SEM of insulin microspheres.
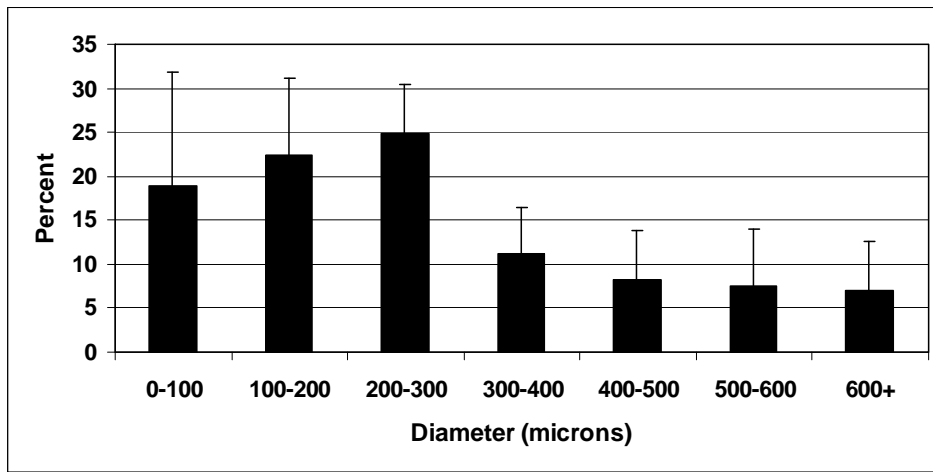
Figure 2-18. Diameter distribution of insulin microspheres.
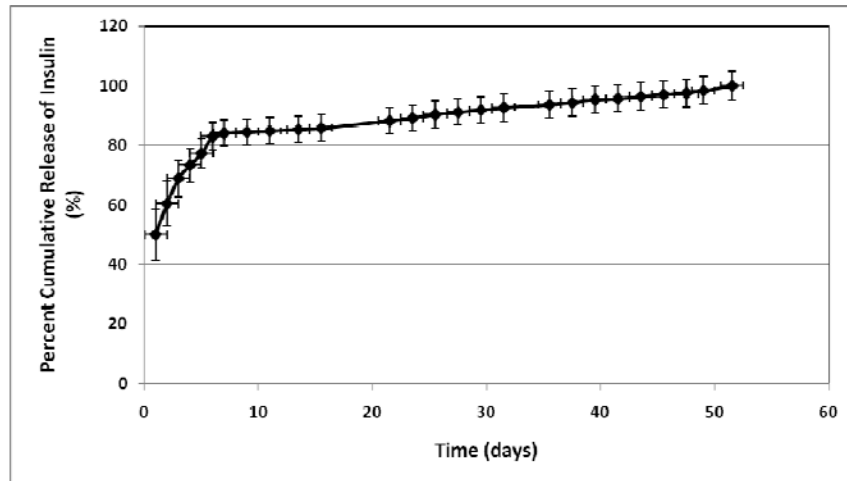
Figure 2-19. Percent cumulative release of insulin.
All points are reported as means ± standard deviations (n=8).

2.3.6 Effects of dexamethasone and insulin microspheres on ASC differentiation

To determine the optimal amount of microspheres required to induce differentiation, three different weights of each type of microsphere was examined. The combination of the microspheres in negative control medium showed the most differentiation with 8mg dexamethasone and 10mg insulin, as noted by Oil red O staining (Figure 2-20c). The group treated with 4mg and 5mg of dexamethasone and insulin microspheres resulted in some differentiation, but more was seen in the 8 and 10mg group (Figure 2-20b). The ASCs in the group treated with 20mg dexamethasone and 25mg insulin microspheres appear to have died (Figure 2-20d). This is most likely due to such a large dose of the adipogenic factors.
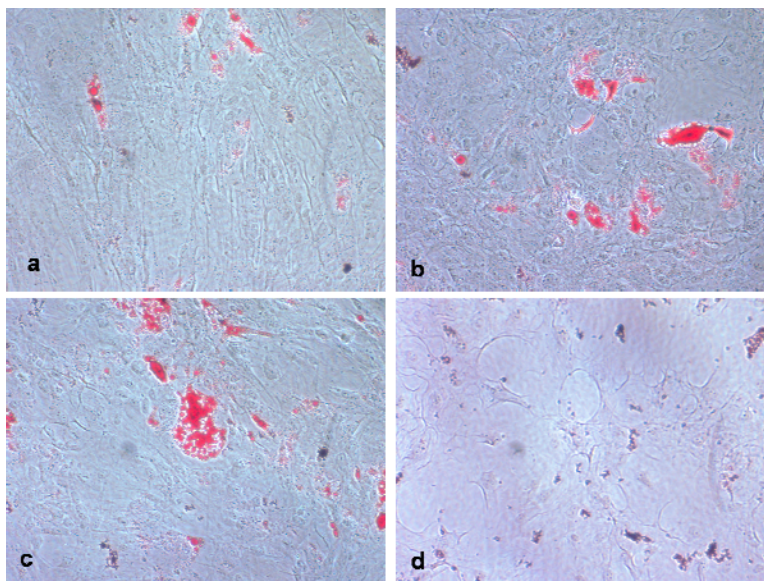
Figure 2-20. Oil Red O staining of ASCs.
ASCs treated with negative control medium (a), negative control medium + 4mg dexamethasone MS + 5mg insulin MS (b), negative control medium + 8mg dexamethasone MS + 10mg insulin MS (c), negative control medium + 20mg dexamethasone + 25mg insulin MS (d).

These effects are even more apparent under light microscopy in the groups treated with Diff-Dex-Insulin medium. With the addition of 4mg Dex and 5mg insulin MS, some differentiation has occurred (Figure 2-21b). Again, it appears as though the ASCs were dying in

the group treated with the largest amount of microspheres (Figure 2-21d).   The best

differentiation occurred in the group treated with the 8mg Dex and 10mg insulin MS (Figure 2-

21c).
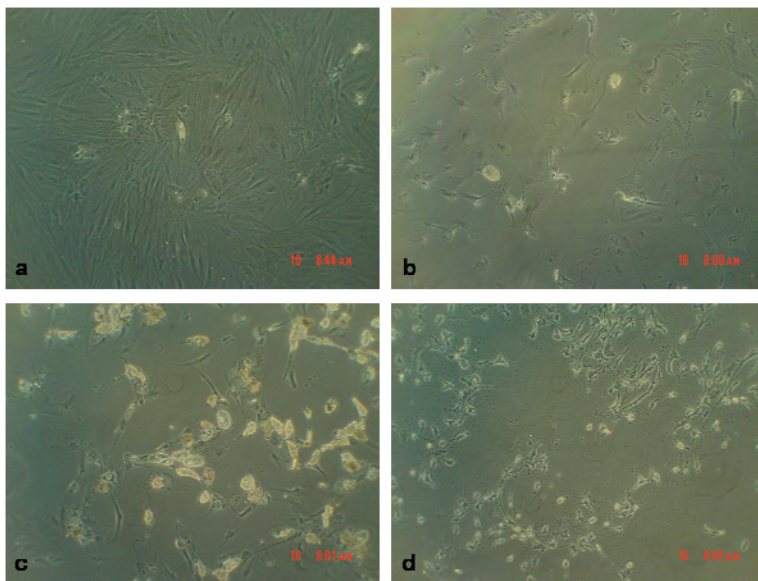
Figure 2-21. Light microscopy of ASCs.
ASCs treated with Diff-Dex-Ins medium (a), Diff-Dex-Ins medium + 4mg Dex MS + 5mg insulin MS (b), Diff-Dex-Ins + 8mg Dex MS + 10mg insulin MS (c), and Diff-Dex-Ins medium + 20mg Dex MS + 25mg insulin MS (d).

2.3.7   Effects of released dexamethasone *in vitro*

To assess the ability of Dex MS to replace dexamethasone in media we examined the

differentiation of ASCs following treatment with 8mg of dexamethasone microspheres. Little to

no differentiation could be detected by Oil red O staining in the groups treated with the negative

control (DMEM/F12 medium) or the ASCs treated with Diff-Dex medium (Figure 2-22a and c).

However, differentiation of the ASCs did occur in the group treated with Dex MS (Figure 2-

22d). The same results were seen by the quantification of cells with lipid inclusions per field of

view (Figure 2-23). However, the results demonstrated no difference in PPAR-γ expression

between cells treated with Diff-Dex medium and Diff-Dex medium + Dex MS (Figure 2-24).

42
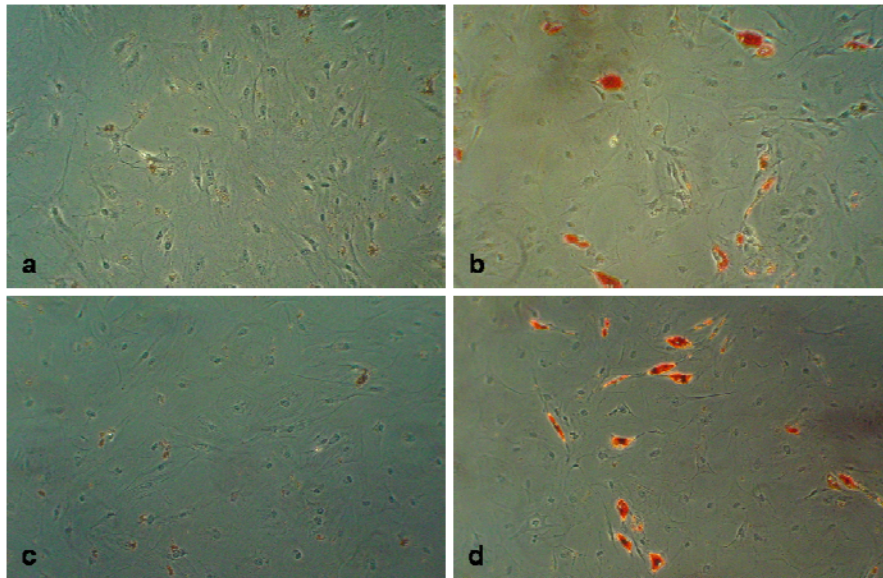
Figure 2-22. Oil Red O Staining after treatment with Dex groups.
Oil Red O staining of ASCs treated with negative control medium (a), positive control medium (Diff medium) (b), Diff-Dex medium (c), Diff-Dex medium + Dex MS (d).
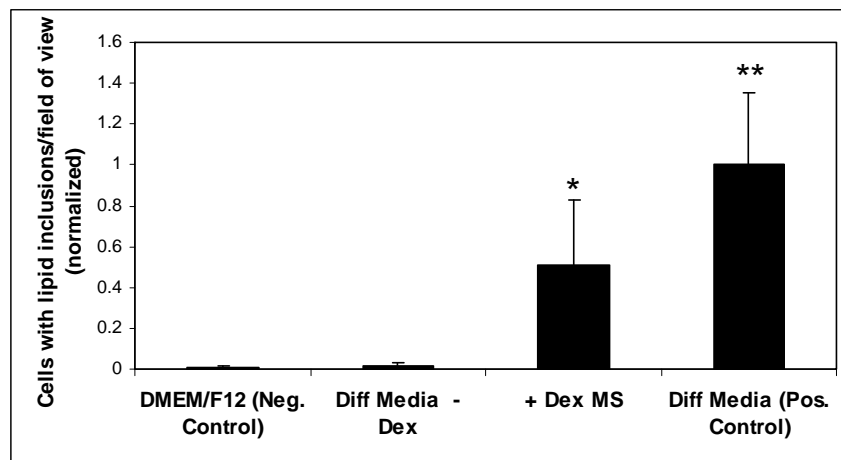
Figure 2-23. Quantification of ASCs with lipid inclusions per field of view after treatment with Dex groups.
*$p<0.05$ compared to negative control and Diff Media-Dex, **$p<0.05$ compared to all groups (n=6 or 5).
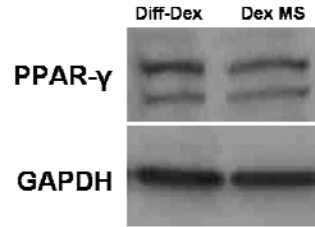
Figure 2-24. PPAR-γ expression in ASCs treated with Diff-Dex medium and Diff-Dex medium + Dex MS. GAPDH shown as a loading control.

2.3.8 Effects of released insulin *in vitro*

The effectiveness of insulin microspheres to replace insulin media was also examined. The group treated with the Diff-Insulin media resulted in some adipogenesis of the cells; however, with the addition of insulin microspheres many more cells differentiated (Figure 2-25 c and d). With the addition of the insulin microspheres, there was no statistical difference compared to the positive control group (Figure 2-26). Expression of PPAR-γ was increased in the group treated with insulin microspheres, compared to no insulin (Figure 2-27).
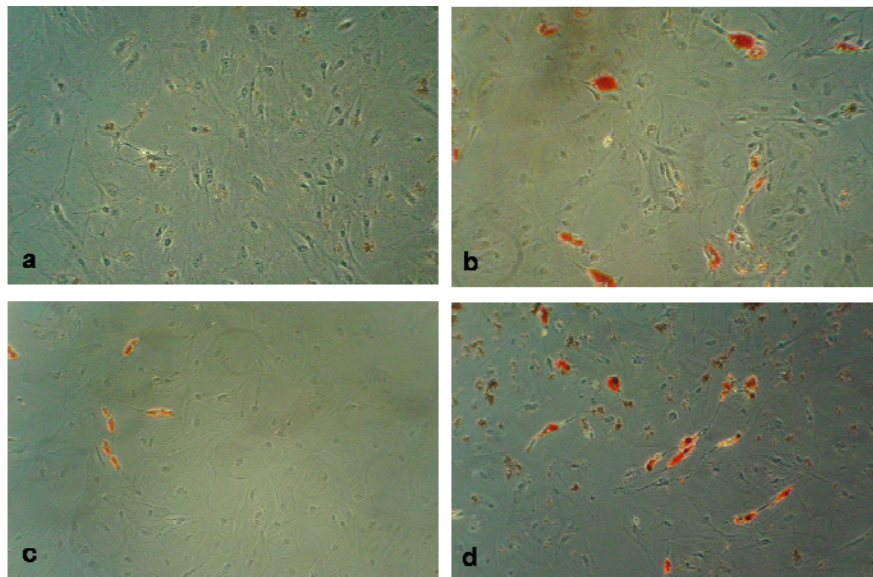
Figure 2-25. Oil Red O staining of ASCs treated with Insulin groups.
Negative control medium (a), positive control medium (b), Diff-Insulin medium (c), Diff-Insulin medium + insulin MS (d).
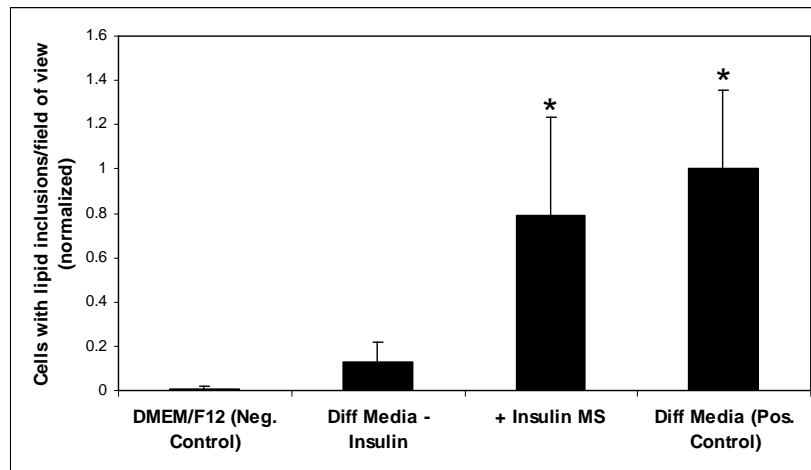
Figure 2-26. Number of ASCs with lipid inclusions per field of view in insulin groups.
***p<0.05 compared to negative control and Diff Media-Insulin (n=5 or 6).**
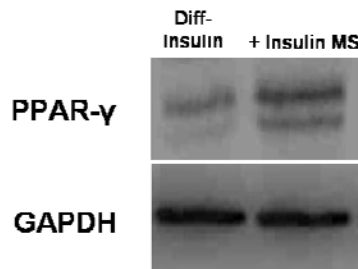
Figure 2-27. PPAR-γ expression in ASCs treated with Diff-Insulin medium and Diff-Insulin medium + insulin MS.
GAPDH used as a loading control.

2.3.9 Combined effects of released dexamethasone and insulin *in vitro*

The effects of both the released dex and insulin were examined in combination with medium containing differentiation components and without. Cells treated in medium containing the differentiation components but 0 insulin and 0 dex resulted in almost no differentiation. With the addition of dex and insulin MS, many more cells stained positive for Oil red O (Figure 2-28 c and d). Again the number of cells with lipid inclusions per field of view were quantified (Figure

2-29). The positive control had significantly more cells with lipid inclusions than any of the other groups. The group treated with the dex and insulin microspheres also had a significant increase in cells with lipid inclusions compared to no microspheres and the negative control group. The western blots demonstrated a slight increase in PPAR-γ expression in the group treated with both the dex and insulin MS (Figure 2-30).
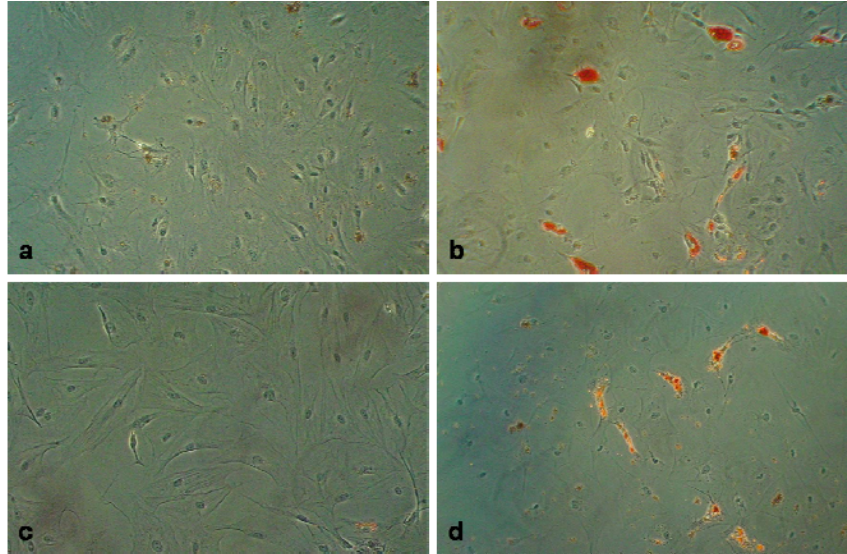
Figure 2-28. Oil Red O staining of ASC of ASCs treated with Dex and Insulin groups.
Negative control medium (a), positive control medium (b), Diff-Dex-Insulin medium (c), Diff-Dex-Insulin medium + Dex MS + insulin MS (d).
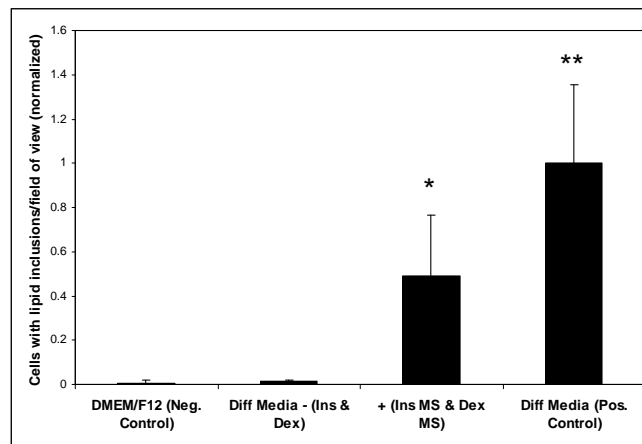
Figure 2-29. Number of ASCs with lipid inclusions per field of view in Dex and Insulin groups.
*p<0.05 compared to negative control and Diff Media-Dex-Insulin, **p<0.05 compared to all other groups (n=5 or 6).

46
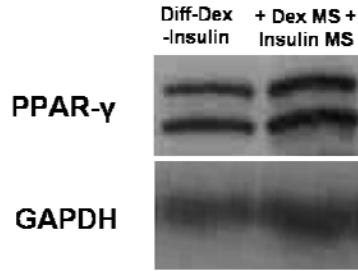
Figure 2-30. PPAR-γ expression in ASCs from Diff-Dex-Insulin medium and Diff-Dex-Insulin medium + Dex MS + insulin MS.
GAPDH used as an internal loading control.

Dex and insulin microspheres were added to cells treated in the negative control medium. Adipogenic differentiation did occur, with cells staining positive for Oil red O (Figure 2-31d). Even though this group had significantly more cells with lipid inclusions over the negative control, it also had significantly less than the positive control (Figure 2-32). A control of empty microspheres from both microsphere protocols was added to cells treated with the negative control medium. The empty microspheres did not have an effect on ASC differentiation, as very little differentiation was observed (Figure 2-31c).
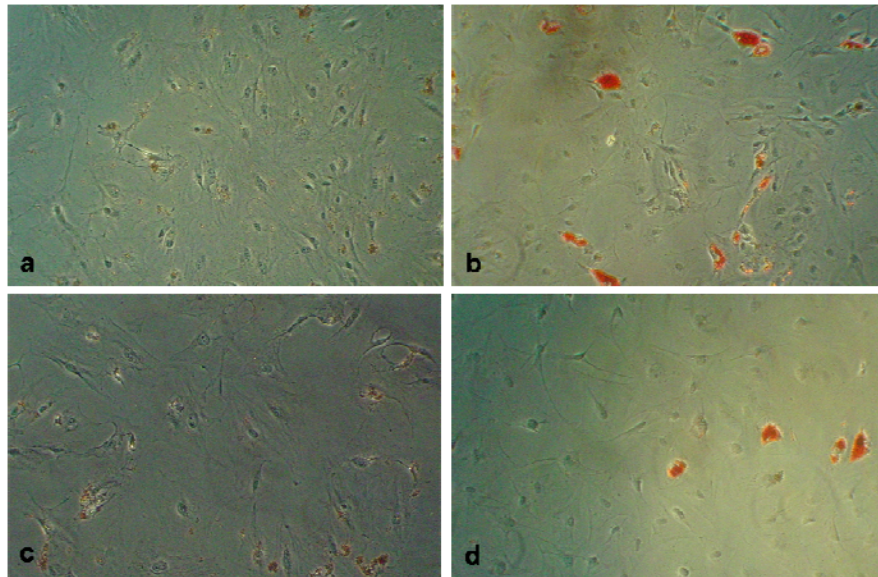
Figure 2-31. Oil Red O staining of ASCs treated with empty microspheres and Dex and Insulin.
Negative control medium (a), positive control medium (b), Empty MS(c), negative control medium + Dex MS + insulin MS (d).
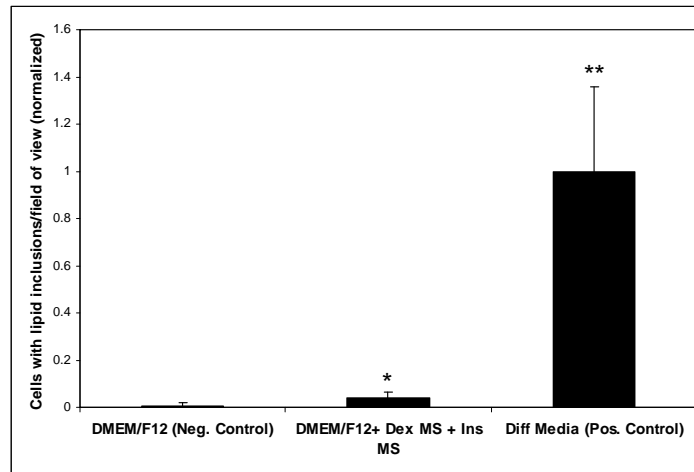
Figure 2-32. Number of ASCs with lipid inclusions per field of view with Dex and Insulin microspheres alone. *p<0.05 compared to negative control, **p<0.05 compared to all other groups (n=5 or 6).

2.4   DISCUSSION

The current therapeutic options for soft tissue reconstruction have inherent problems. These options include autologous tissue flaps, which are highly invasive and may lead to donor site morbidity; prosthetic implants, which pose problems of capsular contracture and device failure over time; and materials derived from mammalian tissue, such as acellular human dermis, which are subject to resorption. Autologous cell-based therapies have potential for soft tissue reconstruction. One such cell source can be derived from liposuctioned or whole fat and readily expanded in culture, termed preadipocytes, or adipose-derived stem cells. These cells can tolerate the mechanical trauma of the harvest techniques better than mature adipocytes.[182] Moreover, these cells can be easily differentiated into mature fat cells *in vitro* using a defined inductive medium.

In this study, we examined the effects of FGF-2 microspheres on ASC survival and proliferation *in vitro*. The FGF-2 microspheres resulted in an increase in cell survival and proliferation over groups treated with free FGF-2 (p<0.01) and no FGF-2 (p<0.01) over 14 days *in vitro*. The effects of FGF-2 on mesenchymal stem cells have been well studied. Solchaga et al. examined the mitotic effects of FGF-2 on bone-marrow MSCs and found similar results to ours.[90] As well, Hankemeier et al. found that a lower dose of 3ng/mL FGF-2 resulted in increased proliferation in bone marrow MSCs over 30ng/mL FGF-2.[91] Kakudo et al. examined the effects of FGF-2 on ASCs during different phases. They found by adding FGF-2 to medium during the proliferation phase, adipogenesis was increased.[183] This is most likely due to the increase in cell proliferation and thus resulting in cell arrest, which as mentioned before, is important in adipogenesis.

Based on our *in vitro* results, we chose to examine the effect of FGF-2 microspheres *in vivo*. We examined the effect of released FGF-2 on vascularization of the ASC/SIS construct. FGF-2 is a known powerful angiogenic growth factor. Our results demonstrate that vascularization is indeed increased due to the controlled release of FGF-2 from the biodegradable PLGA microspheres (p<0.05). Others have examined the role of FGF-2 in angiogenesis, as well as the release of FGF-2 from microspheres. Perets et al. examined *in vivo* angiogenesis after implantation of PLGA FGF-2 loaded microspheres in alginate composite scaffolds and saw an increase in capillary density as well as the size of vessels over empty scaffolds.[76] Similarly, Sakakibara et al. showed the release of FGF-2 from gelatin microspheres resulted in an increase in neovessels surrounding the injection area.[66] Masuda et al. examined the effects of varying amounts of FGF-2 (0.01, 0.1, 1, and 10μg) in Wistar rats subcutaneously. After two weeks, neovascularization was increased in all FGF-2 groups

49

compared to rats treated with no FGF-2.[58] At four weeks, no difference in capillary density could be seen between the groups, except the lowest dose of FGF-2 (0.01μg) was greater than the control (0μg FGF-2).[58] These results are consistent with our lower dose of FGF-2 (1ng/mL).

The effects of FGF-2 on vascularization in areas of adipogenesis have also been studied. Recently, Vashi et al. studied the controlled release of FGF-2 from collagen matrices as related to adipose formation in a mouse tissue engineering model.[79] Tabata et al. showed similar results to our study. *De novo* adipose tissue formation and capillary formation were examined after implanting matrigel with FGF-2 loaded gelatin microspheres subcutis in BALB/c mice. After six weeks, capillary formation was significantly greater in mice treated with FGF-2 gelatin microspheres over free FGF-2 or empty microspheres.[63] Some discussion has been invoked about whether or not the vascularization is due to a foreign body response to the microspheres. However, this has been examined by many other researchers. No inflammatory response to PLGA/PEG microspheres was seen in a study by Yuksel et al.[175] Kang et al. observed an initial inflammatory response after injection of PLGA microspheres, but no long term effects were seen.[150] The inflammation is believed to be due to trauma of injection, which is present with or without microspheres. These results further validate that the neovascularization seen in our study was due to released FGF-2 and not a foreign body response.

Many have examined the potential of preadipocytes or ASCs to form adipose tissue *in vivo*. In our study, our cells did survive; however, we did not see a large adipose tissue mass after two weeks *in vivo*. Others have seen similar results. For example, Choi et al. recently evaluated adipogenesis *in vivo* utilizing MSCs attached to PLGA microspheres.[184] Their results demonstrated that if the MSCs were pre-treated with adipogenic media prior to injection,

there was substantially more adipose tissue formation. The group that was not pretreated resulted in little to no lipid containing cells after two weeks *in vivo*.[184] Similar results were seen by Lee et al. with ASCs. The adipogenesis of ASCs seeded on poly(glycolic acid) (PGA) scaffolds implanted overlying the skull of Lewis rats was examined. ASCs received treatment with either control or adipogenic medium for 7 days prior to implantation. After four and eight weeks, adipose tissue was present in the adipogenic induced scaffolds and absent in the ASC group.[185] Hemmrich et al. seeded preadipocytes on hyaluronic sponges which resulted in no fat formation at three, eight, or twelve weeks *in vivo* in nude mice.[43] While these groups did not examine the delivery of growth factors to induce differentiation, others have examined the delivery of FGF-2. Kimura et al. reported after six weeks in vivo, collagen sponges seeded with preadipocytes and FGF-2 gelatin microspheres resulted in adipogenesis; significantly less adipogenesis was seen with the addition of free FGF-2.[65] Hiraoka et al. implanted preadipocyte-seeded collagen scaffolds with FGF-2 incorporated gelatin microspheres in mice within the fat pad. At two weeks, cells were present, but no mature adipocytes were present. However, lipid accumulation was seen at 4 and 6 weeks.[78] These results indicate that had our *in vivo* study gone on longer we might have seen adipose tissue formation. It may also indicate that other adipogenic factors may be necessary to induce adipogenesis.

We continued to assess the ability of ASCs for soft tissue reconstruction by examining the release of adipogenic factors, insulin and dexamethasone, to induce differentiation. We successfully encapsulated dex and insulin in PLGA microspheres. We did not see a burst release from the dex microspheres and maintained the release for over 50 days. These results were in accordance with Yoon et al. They also did not see a burst effect from PLGA scaffolds and maintained a release over 30 days.[142] We saw an initial burst release

51

from the insulin microspheres, an average of 50% of the total insulin released over 52 days was released on the first day. Similarly, Ibrahim et al. saw an initial burst of 71% from insulin loaded PLGA microspheres.[149]

Researchers have examined the effects of released insulin on adipose tissue formation. Masuda et al. examined the *de novo* adipogenesis in rats injected with combinations of gelatin microspheres containing FGF-2, insulin, and insulin-like growth factor-1 (IGF-1) subcutaneously. Their results showed that the largest amount of adipogenesis occurred with the combination of insulin, IGF-1, and FGF-2 as well as with the combination of insulin and IGF-1.[58] Yuksel et al. reported the release of IGF-1 as well as insulin from PLGA microspheres (combined with polyethylene glycol) enhanced *de novo* adipose tissue formation.[186] Their study demonstrated the potential of long-term local insulin and IGF-1 delivery to induce adipogenic differentiation to mature lipid-containing adipocytes from non-adipocyte cell pools that were administered directly to the deep muscular fascia of the rat abdominal wall. However, to the best of our knowledge no one has examined the release of dex and insulin from PLGA microspheres to induce adipogenesis of ASCs. In this study, we demonstrated that ASC differentiation could be induced by released dex and insulin. The insulin loaded microspheres successfully replaced insulin in media. There were no significant differences in the number of cells that had differentiated compared to the positive control. PPAR-γ expression was markedly increased compared to treatment without insulin. However, the results for the dexamethasone loaded microspheres were not as successful. Although there was a statistical difference compared to zero dexamethasone, the number of cells with lipid inclusions was significantly decreased compared to the positive control. The expression of PPAR-γ did not seem to increase or decrease compared to treatment without dexamethasone. More studies should be performed to

optimize the amount of microspheres necessary to better induce differentiation. Preliminary studies were performed at three different amounts of dex microspheres, 4, 8, and 20mg, which resulted in 8mg being optimal. However, there may be a more optimal amount between 8 and 20mg of dex microspheres.

2.5   CONCLUSIONS

In our study, we aimed to enhance ASC survival and adipogenesis. We improved vascularization of the implanted ASC/SIS constructs by injecting PLGA microspheres encapsulating FGF-2. Our results demonstrated that the number of blood vessels surrounding the implant after two weeks was significantly higher when compared to both implants without FGF-2 (control) and also simple injection of free FGF-2. We did not see a difference in cell survival or adipogenesis at this point.

We induced differentiation of ASCs *in vitro,* by replacing dex and insulin in media with released adipogenic factors from PLGA microspheres. The number of cells with lipid inclusions was significantly increased compared to the negative control and to controls lacking the adipogenic factors.

This finding has implications for new clinical therapies in soft tissue reconstruction. An injectable engineered soft tissue replacement can be used to reconstruct a defect, but would have to be administered in serial treatments and will depend on successful vascularization of the cell/scaffold construct before more material can be added. Including FGF-2 microspheres with the cells and scaffold mixture would not only enhance survival of the implanted cells, but could decrease the time required for successful vascularization and accelerate the treatment process.

These injections could be followed by dex and insulin microspheres to enhance adipogenesis of the cells.

2.6   FUTURE EXPERIMENTS

We have successfully completed our aim to encapsulate factors to enhance and induce differentiation of ASCs. Future studies must be performed to demonstrate their potential for soft tissue reconstruction.   Longer studies *in vivo* must be done to determine if the FGF-2 microspheres will have an effect on cell survival and adipogenesis. Since we did not achieve differentiation at a desired level from the dexamethasone microspheres, more *in vitro* studies should be performed to optimize the amount of microspheres necessary. Furthermore, induction of differentiation with insulin and dexamethasone microspheres alone resulted in minimal adipogenesis *in vitro*.   Other adipogenic factors may be necessary to obtain optimal differentiation. From studies within our lab, ciglitazone, a PPAR-γ agonist, has been shown to be an important adipogenic factor. Another important factor may be IBMX, a cAMP enhancer. Finally, *in vivo* studies including all of the adipogenic microspheres, with possible multiple injections of microspheres and cell-seeded particles should be performed.

3.0 CONTROLLED RELEASE OF CHEMOTHERAPY FROM PLGA MICROSPHERES/GELATIN SCAFFOLDS AS ADJUVANT THERAPY FOR BREAST CANCER

3.1 INTRODUCTION

The American Cancer Society estimates 178,480 people will be diagnosed with breast cancer in 2007 and 40,460 people will die from breast cancer.[187] Breast cancer is the second leading cancer cause of death among women (lung cancer is first).[188] Most patients are treated by surgery followed by an adjuvant therapy such as radiation, chemotherapy, or biological therapy. An alternative solution to systemic chemotherapy would have a high impact clinically. The current study was designed to examine the efficacy of a scaffold to release chemotherapy locally and act as a temporary filler to support the contour of the breast following lumpectomy. This approach could serve as an alternative to adjuvant breast irradiation. We have examined the release of factors from microspheres alone (Chapter 2), in this chapter we examine the use of PLGA microspheres in an FDA-approved, natural hydrogel, gelatin. As such, doxorubicin encapsulated microspheres were fabricated and incorporated into gelatin scaffolds during gelation. *In vitro* release kinetics and efficacy was demonstrated utilizing a murine mammary tumor cell line, 4T1. The ability of the scaffold to eradicate tumor *in vivo* was also assessed. A lumpectomy model was used by inoculating Balb/c mice with 4T1 cells in the

mammary fat pad. A scaffold was then implanted adjacent to the fat pad. Mice were sacrificed and tumor eradication was analyzed. The biocompatibility and radiotransparency of the scaffold *in vivo* was also analyzed. Incorporating the microspheres in the gelatin scaffolds further controlled the release of doxorubicin. The scaffolds effectively eradicated tumor *in vitro* and *in vivo,* and the scaffold is radiotransparent. The drug-polymer scaffold can be used as a controlled delivery system to potentially eradicate tumors and preserve soft tissue contour.

3.1.1 Breast cancer and current treatments

Breast cancer originates from the lining of the milk duct either from duct cells or lobules at the ends of the ducts.[189] Breast cancers are thus categorized as ductal or lobular carcinoma or mixed (a combination of both). Breast cancer can be treated with local treatments to prevent cancer from recurring or systemically to destroy cells that have metastasized. Early breast cancers may be appropriately treated with a combination of breast conserving surgery along with adjuvant breast irradiation.[190] The surgery removes the tumor, which means that some cancer cells may remain in the breast. The role of adjuvant breast irradiation is to reduce the local recurrence rate associated with breast conserving surgery alone.[191] Radiation therapy however is expensive, time consuming, and increases the cosmetic deformity of surgery.[192] The cosmetic deformity resulting from surgery and radiotherapy is synergistic and consists of both a volume loss and contour deformity, which is individually variable and can be pronounced (Figure 3-1).[193, 194] Surgical correction of the deformed, treated breast is technically difficult and involves the transfer of tissue from the surrounding breast or adjacent chest wall using plastic surgery techniques.[195, 196] In the absence of surgical repair, the lumpectomy defect

56

fills with fluid and there is a gradual ingrowth of fibrous (scar) tissue and the area contracts. There is a limited capacity for the surrounding adipose tissue to regenerate in the defect.

Figure 3-1. Deformation following surgery and radiation therapy.

3.1.2 Delivery systems to treat cancer

Some patients may be treated with systemic chemotherapy either as adjuvant therapy (at the time of diagnosis) or to treat cancer that has metastasized to other areas of the body. Seven drugs are commonly used as systemic adjuvant chemotherapy for breast cancer cyclophophamide, methotrexate, 5-fluorouracil, doxorubicin, epirubicin, and paclitaxel or docetaxel.[189] Many side effects occur due to systemic treatment, including nausea, vomiting, loss of appetite, and hair loss. Due to these systemic side effects or hard to target tumors, polymer/chemotherapy conjugates have been developed for regional therapy. The treatment of brain metastases has been treated in this manner and presumably a similar approach could serve as an effective adjuvant treatment for patients undergoing breast conservation surgery for breast cancer. Polymeric delivery devices can be utilized to safely delivery chemotherapy locally. Figure 3-2 demonstrates the compartmental representation of the transport of drugs from locally injected microspheres, demonstrating the pathway of the drug to the blood and healthy tissue.
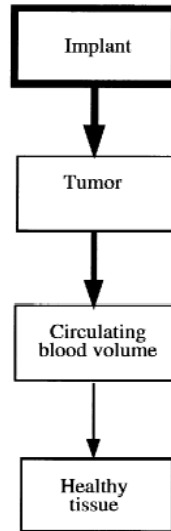
Figure 3-2 Compartmental representation of the transport of released drugs from polymeric microspheres injected intratumorally.[197]

Polymeric delivery devices have been clinically utilized to treat patients. Polymeric chemotherapy devices currently available include Zoladex® (AstraZeneca) and Lupron Depot® (TAP Pharmaceutical Products Inc.)[198] to treat prostate cancer, Gliadel® (MGI Pharma) to treat brain cancer, Sandostatin LAR® Depot (Novartis) to treat acromegaly, carcinoid syndrome or VIPoma. One case has been examined for the treatment of breast cancer utilizing regional chemotherapy from doxorubicin-loaded albumin microspheres.[199] A Phase II clinical trial examined the efficacy of treating metastatic breast cancer with albumin-paclitaxel nanoparticles.[200] By utilizing the nanoparticles a higher dose could be given ($300mg/m^2$) than normal (135-$200mg/m^2$) which resulted in a significant anti-tumor effect.   Delivery of chemotherapy from polymer microspheres injected along solid tumors results in eradication of the tumor compared to little effect when treated with a bolus injection or systemic chemotherapy.[201]   Experiments with PLA microspheres *in vivo* demonstrated that locally released doxorubicin could not be detected in systemic serum levels.[202]

A slow release biodegradable polymer scaffold could be placed in the breast defect at the time of a lumpectomy and would serve two purposes. First, the controlled delivery of a therapeutic agent (chemotherapy or biotherapy) to the breast could theoretically control local tumor recurrence. Second, the implant would act as a temporary filler, supporting the contour of the breast and eventually encouraging tissue ingrowth. The clinical need to both deliver drugs locally and support tissue growth into the surgical defect with differing time kinetics suggest the design of a biphasic construct. The ideal device should be transparent to the conventional imaging modalities used to follow breast cancer patients. This approach could hypothetically serve as an alternate to adjuvant breast irradiation resulting in an improved cosmetic result, and cost reduction as well as the potential to individualized therapy and improve current outcomes.

3.1.3   Doxorubicin

Doxorubicin (Figure 3-3), an anthracycline antibiotic with an antitumor effect, interacts with DNA to inhibit cellular functions.[203, 204] Doxorubicin, also known as adriamycin, has a molecular weight of 280g/mol. Doxorubicin has been used to treat cancer for almost four decades. Treatment with doxorubicin is restricted due to its cumulative-dose limit to prevent cardiotoxicity.[205-207] Doxorubicin is limited to a lifetime dose of 450-550mg/m^2 because of cardiotoxicity.[207] However using a controlled, biodegradable delivery system may reduce the distribution of drug in the heart[207] and thus a higher dose may be delivered. In addition, doxorubicin is unstable in an aqueous environment at 37°C and pH=7.4. Fan et al. observed a 30-40% degradation of doxorubicin over 48 hours; however, when placed in a gelatin implant the drug was stable for up to 5 months at these conditions.[208] Due to these limitations, various drug delivery systems have been studied, including microspheres,[202, 209-211]

59

pegylation,[212-216] and liposomes[217-219] to deliver doxorubicin. The fabrication technique and construct material should be chosen based on the hydrophobicity of the drug, the duration of its therapy, and the intended use/implantation site. The delivery of doxorubicin from controlled delivery systems has been examined (Table 3-I).
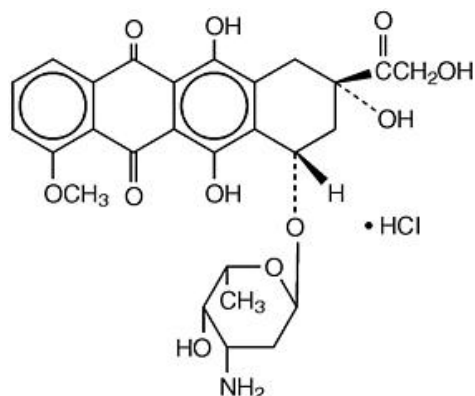
Figure 3-3. Structure of doxorubicin.

Table 3-I. Delivery systems of doxorubicin.

Polymer Microspheres [201, 202, 209, 211, 220]	Pegylated Liposomes [212-216]
Dextran Microspheres [221]	PVA Micelles [222]
Chitosan Microspheres [223]	HPMA hydrogel [224, 225]
Ion Exchange Microspheres [226, 227]	Gelatin [208, 228]
Albumin Microspheres [229]	Silica gel [230]
Polyisohexylcyanocarylate Nanoparticles [231, 232]	Starch [233]
Liposomes [217-219, 234]	PCL-Chitosan-PEG [235]

In vivo experiments have demonstrated the anti-tumor efficacy of dextran microspheres[221, 236] and PLGA microspheres[201] for the treatment of breast cancers. Minimal systemic toxicity as well as prolonged animal survival was seen in groups treated by the microspheres. Similarly, Konishi et al. demonstrated the advantages of controlled delivery of doxorubicin from gelatin scaffolds.[228] Their results showed a significant decrease in tumor

60

(fibrosarcoma) size as well as an increase in prolonged survival without toxic effects. By incorporating doxorubicin into gelatin hydrogels, sufficient intratumor levels were maintained over 14 days. Yoo et al. demonstrated the advantage of a single injection of doxorubicin-loaded PLGA nanoparticles over daily injections of free doxorubicin to treat tumors *in vivo*.[220] Similarly, Lin et al. saw an increase in cytotoxicity of doxorubicin delivered from PLGA microspheres compared to the free drug.[209]

3.1.4 Gelatin

Gelatin is commonly used in both the pharmaceutical and biomedical field. It is nontoxic, biodegradable, inexpensive, nonimmunogenic, and FDA approved. Gelatin was first approved by the FDA as a food ingredient and was approved the status of Generally Regarded as Safe (GRAS). In 1993, the FDA reapproved the GRAS status of gelation. Gelatin is a macromolecular protein derived from collagen. Gelfoam, a commercially available sterile gelatin is commonly used clinically. Gelatin has been widely studied for drug and protein delivery, as gelatin microspheres[20, 62, 63, 65] or gelatin hydrogels.[55, 140, 208, 228] Gelatin has also been examined for use as scaffolds for tissue engineering.[237-239] In this study we encapsulated doxorubicin in PLGA microspheres embedded within gelatin scaffolds to obtain local controlled delivery to treat breast cancer.

3.2   METHODS

3.2.1   Doxorubicin encapsulation and characterization

Doxorubicin (Dox) was encapsulated in PLGA microspheres using a protocol previously described by Mallery et al.[210] Dox microspheres were prepared using a double emulsion/solvent evaporation method. 250mg of PLGA (75:25) was dissolved in 0.80 mL of a mixture of 1:6 methanol to MC. 6mL of 2mg/mL doxorubicin-HCL solution (Bedford Laboratories, Bedford OH) was added to the PLGA solution. The combined solution was emulsified by adding 1.0 ml of 1% PVA solution and vortexed for one minute. This emulsion was poured into 50 mL of 0.30% PVA and stirred for 2 hours at 550 rpm. The microspheres were collected by centrifugation, washed with DI water, frozen, and freeze-dried. Empty PLGA microspheres were prepared by the same procedure, without the addition of the drug. The yield, loading capacity, and encapsulation efficiency of the microspheres were determined. The microspheres were examined morphologically by SEM. The images were also used to determine the diameter distribution of the Dox microspheres.

3.2.2   Doxorubicin gelatin constructs

Gelatin was crosslinked with glutaraldehyde following protocols by Ulubayram et al.[240] and Kang et al.[237] Briefly, to prepare crosslinked gelatin scaffolds, 25 mL of 3% gelatin solution (Sigma Aldrich) was prepared. 0.4mL of 0.5% glutaraldehyde solution was added and the solution was stirred for an additional 5 minutes. The solution was then poured into a mold and allowed to stand for 12 hours. The gelatin was treated with 0.1M glycine

followed by a water wash to react with any remaining glutaraldehyde. The gelatin was frozen at –20°C. Scaffolds to be examined by SEM were freeze-dried. To incorporate PLGA microspheres into the gelatin, the gelatin was prepared as previously mentioned and the desired amount of microspheres were added to the gelatin in the mold and sufficiently mixed. The scaffold was frozen, and samples prepared for SEM were freeze-dried.

3.2.3   Release of Doxorubicin from microspheres and gelatin constructs

The release profile of Dox from PLGA microspheres was determined by incubating 16.5mg of microspheres in 1 mL of PBS (pH 7.4) at 37 °C (n=5). At appropriate intervals, the samples were centrifuged and refreshed with 1 mL of PBS. The amount of Dox released into the PBS was detected by measuring the absorbance of the supernatant at 483 nm using a Genesys10 Spectrophotometer (Thermo Fisher Scientific, Waltham, MA). Gelatin cylinders were punched out using a 6 mm dermal biopsy punch. The gelatin cylinder was placed in 1 mL of PBS at 37°C (n=5). The amount of Dox released was also determined spectrophotometrically as described above.

3.2.4   Effects of Doxorubicin on cancer cells *in vitro*

The effects of Dox on 4T1 tumor cells (ATCC, murine mammary tumor cell line) were determined quantitatively by the addition of various concentrations of Dox to the media. The 4T1 mouse mammary tumor cells were maintained in 4T1 media (RPMI 1640, 10% FBS, 1% p/s, 2mM L-glutamine, 10mM MEM essential amino acids, 1mM sodium pyruvate) and passaged two times a week. 4T1 mouse mammary tumor cells were seeded in a 96-well tissue

culture plate at a concentration of 7500 cells per well (n=5). Cells were incubated at 37°C for 24 hours. Media was replaced with 0.017mg/mL Dox serially diluted 1:1 to 1:16 in media and incubated for 24 hours. Utilizing MTT, the number of viable cells was determined, measuring the absorbance at 570 nm (Tecan SpectraFluor).

The induction of 4T1 cell death due to Dox was assessed qualitatively using propidium iodide to stain the dead cells. Propidium iodide is a simple qualitative cell viability assay that stains non-viable cells red; it cannot cross the membrane of viable cells. Adherent cells were prepared by seeding 4T1 cells on circular 18mm sterile glass coverslips in 12-well polystyrene tissue culture plates and cultured until confluent. Non-adherent cells were removed by washing with PBS. The remaining cells were treated with various concentrations of Dox (1mg/mL, 0.17mg/mL, 0.017mg/mL, 0.0017mg/mL) for 4 hours, 6 hours, and 24 hours. At the end of each time point, the medium was removed, followed by a gentle PBS wash. 1mL of PBS with 5μL of the 1mg/mL propidium iodide (Sigma) stock solution was added to each well. The cells were imaged live with a fluorescent microscope after incubation for 15 minutes at room temperature.

The activity of the released Dox was examined by determining the induction of cell death of the 4T1 tumor cells. The cells were seeded in a 24-well tissue culture plate with 4T1 media. One mL of 10,000 cells/mL media was added to each well and then incubated at 37°C for 12 hours. Five treatment groups were examined: 1) 4T1 media, 2) Dox-loaded microspheres, 3) Dox-loaded microspheres in gelatin, 4) Empty microspheres and 5) Empty microspheres in gelatin (n=5 for each). The microspheres and gelatin constructs were placed in Transwell® baskets. The amount of microspheres alone and microspheres embedded within the gelatin construct were equivalent (34.2mg). The cells were incubated at 37°C for 48 hours. The cells were then washed with PBS and frozen at –80°C.

3.2.5 Scaffold preparation and characterization for *in vivo* experiments

The gelatin constructs were prepared as previously described (Section 3.2.2). For the *in vivo* scaffolds, 129.3mg microspheres per scaffold were added to the gelatin solutions and thoroughly mixed. The gelatin constructs were punched out using a 6mm dermal biopsy punch (Figure 3-4). Constructs that were to be examined by a scanning electron microscope (SEM) were freeze-dried. The constructs were examined morphologically by scanning electron microscopy (SEM).
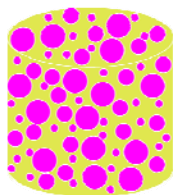
Figure 3-4. Representation of Dox scaffold used for *in vivo* studies.

3.2.6 Inoculation of tumor

An animal model of a lumpectomy was created by inoculating the mice with tumor and treating them at the same time point. 4T1 tumor cells were maintained in 4T1 media and passaged 2 times a week. 4T1 cells were labeled with CFDA-SE (carboxy-fluorescein diacetate, succinimidyl ester) (Molecular Probes) as described by the manufacturer's protocol. The viability of the cells was examined utilizing trypan blue after labeling and before implantation. Cells were then suspended in 4T1 media to a final concentration of 10^6 cells/mL. Female BALB/c mice were inoculated in the lower left mammary fat pad with 10^5 4T1 cells in 100 μL of 4T1 medium at day 0.

3.2.7 Implantation of scaffold

The mice were anesthetized with ketamine and xylazine. A skin incision was made next to the inoculated mammary fat pad. The constructs were inserted under the skin over the mammary fat pad (Figure 3-5). The incision was closed with sutures followed by VETBOND™ tissue adhesive (3M).
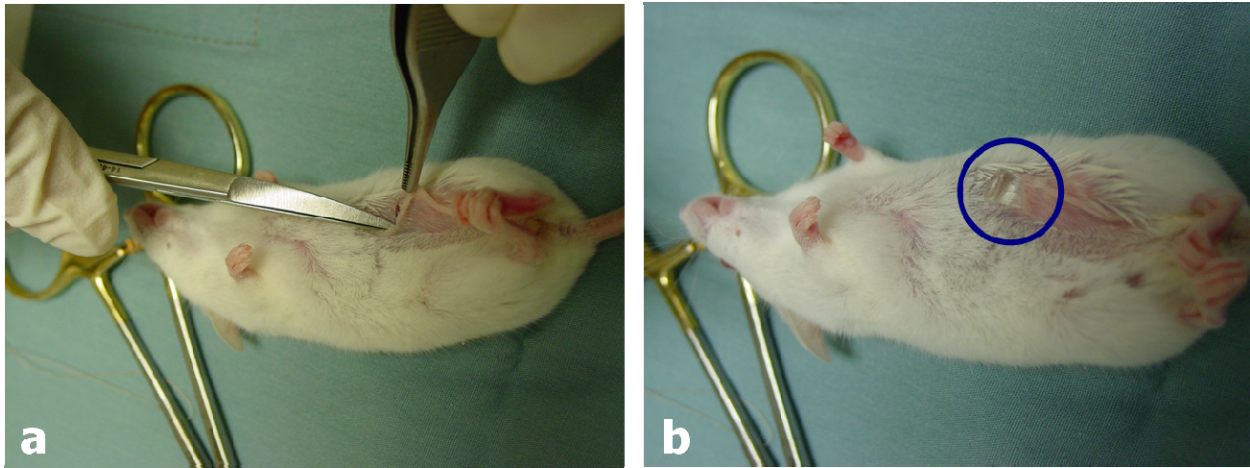
Figure 3-5. Implantation of gelatin scaffold.
Incision made above mammary fat pad (a) gelatin scaffold slid into place over the mammary fat pad (b).

3.2.8 Radiography analysis

The radiotransparency of the constructs was determined by examining X-rays of the mice after implantation of the constructs. Mice were treated (as described above) with one of the following: 1) implantation of empty construct and no tumor, or 2) implantation of empty construct plus tumor. After 14 days, the mice were sacrificed and immediately x-rayed.

3.2.9 Tumor eradication and side effects

Directly following inoculation with tumor, the mice were treated with one of the following groups: 1) two dox MS gelatin constructs (2Dox) (n=10), 2) one dox MS construct (n=5), 3) one empty MS construct (n=10), or 4) nothing (n=10). The constructs were implanted as described above. The mice were initially weighed and then throughout the course of the experiment. Their weight was expressed as a percentage to initial body weight. The mice were sacrificed at day 23. The tumors were excised and the tumor diameters were measured using calipers. The volume was then calculated using the formula $v=ab^2$, where a and b are perpendicular diameters and a > b.[241]

3.2.10 Optimization of delivery system

Gelatin solutions, either 3% or 5%, were crosslinked utilizing a glutaraldehyde solution. Gelatin scaffolds were punched out using a 6mm dermal biopsy punch. Scaffolds were placed in 1mL PBS at 37°C. PBS was replaced every other day for 150 days, and then the PBS was replaced weekly until the end of the study. Once scaffolds became viscous, instead of solid, they were considered degraded.

A relatively large amount of Dox microspheres was required to successfully treat the mice, 2Dox scaffolds. By encapsulating Dox in the powder form, the encapsulation efficiency may increase. Doxorubicin microspheres were encapsulated as previously described (Section 3.2.1), except 6mg of powder Dox (Fisher Scientific) was added instead of 6mL of Dox-HCL. Doxorubicin powder microspheres (~15mg) were placed in PBS (n=3). The released doxorubicin was measured as previously mentioned (Section 3.2.3)

3.2.11 Statistical analysis

The results are expressed as means ± standard deviations.   Unpaired, two-tailed t-tests were performed at each time point. Comparisons of means representing multiple measurements over time were analyzed using repeated-measures analysis of variance (ANOVA) and least squares deviation. The threshold for statistical significance was set at $p \leq 0.05$.

3.3   RESULTS

3.3.1   Effects of doxorubicin on cancer cells

The induction of cell death due to Dox was determined using the MTT assay. As expected, the 4T1 cells responded in a dose-dependent manner to the Dox. As the concentration of Dox was increased, the number of viable cells was reduced (Figure 3-6). A significant decrease in viable cells at each concentration of Dox was observed when compared to the control (0mg/mL). After 24 hours, 62,015 ± 3,717 viable cells were present in the control (0mg/mL Dox) compared to the lowest concentration of Dox, 37,910 ± 2,902 cells remained viable ($p<0.0001$).   The highest concentration of Dox resulted in 14,935 ± 1,855 viable cells ($p<0.000001$, compared to control).
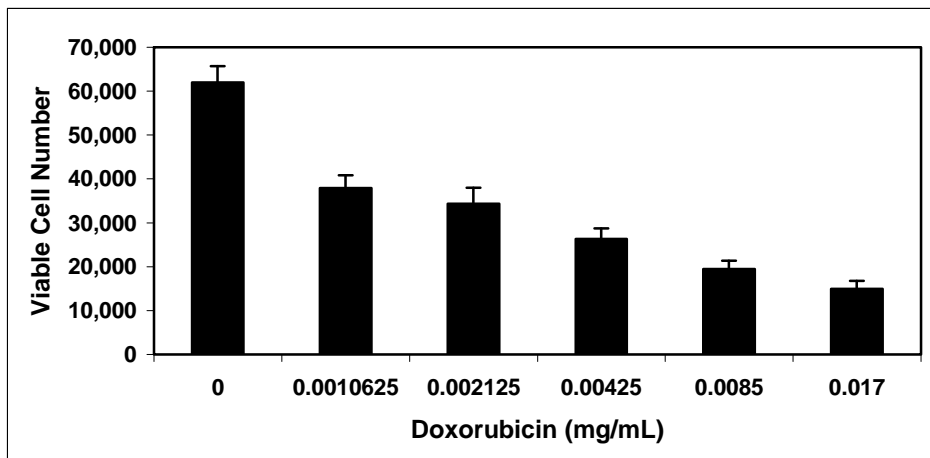
Figure 3-6. Viable cell number following treatment of 4T1 cells with doxorubicin.
All values are reported as means ± standard deviations (n=5). A significant difference (p<0.05) was observed between each groups except between 0.0010625 and 0.002125mg/mL dox.[242]

Propidium iodide was used to qualitatively assess the effect of Dox on 4T1 cells. Dead cells stained red with propidium iodide. As seen in Figure 6, as the concentration of Dox increased, the number of cells stained red. This trend corresponds to that of the MTT assay. (Figure 3-7)
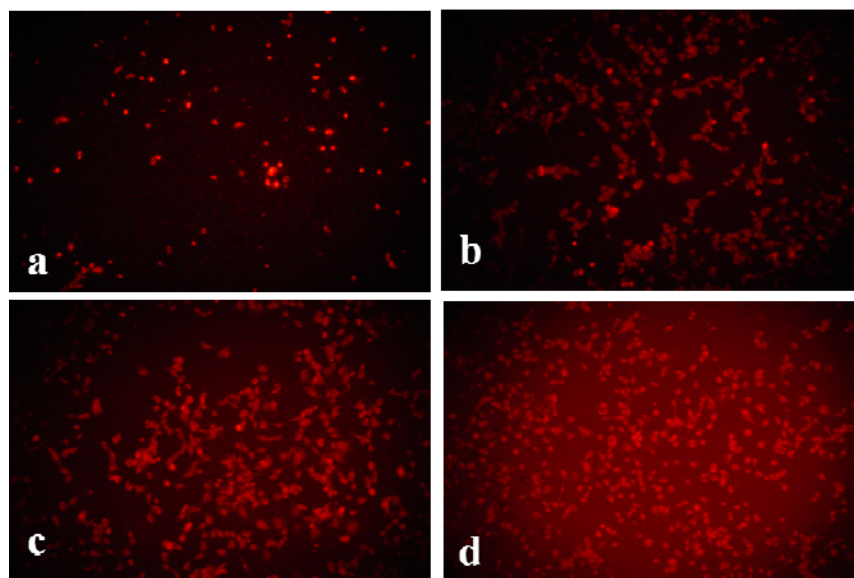
Figure 3-7. Stained dead 4T1 cells, using propidium iodide.
4T1 cells treated with 0.0017mg/mL Dox(a), 0.017mg/mL Dox(b), 0.17mg/mL Dox(c), and 1mg/mL Dox(d) for 6 hours (200x).[242]

3.3.2 Doxorubicin microsphere and gelatin construct characterization

The Dox PLGA microspheres were characterized using SEM. The microspheres exhibited a smooth round morphology (Figure 3-8). The diameter of the Dox microspheres was determined from SEM images. The average diameter was 73.55 ± 75.32 μm. The diameter distribution of the microspheres is shown in Figure 3-9. The yield for the Dox-loaded microspheres was $61.44 \pm 6.81\%$. The loading capacity of the dox microspheres was 0.66 ± 0.41 μg per mg of microspheres. The encapsulation efficiency was $1.03 \pm 0.65\%$.
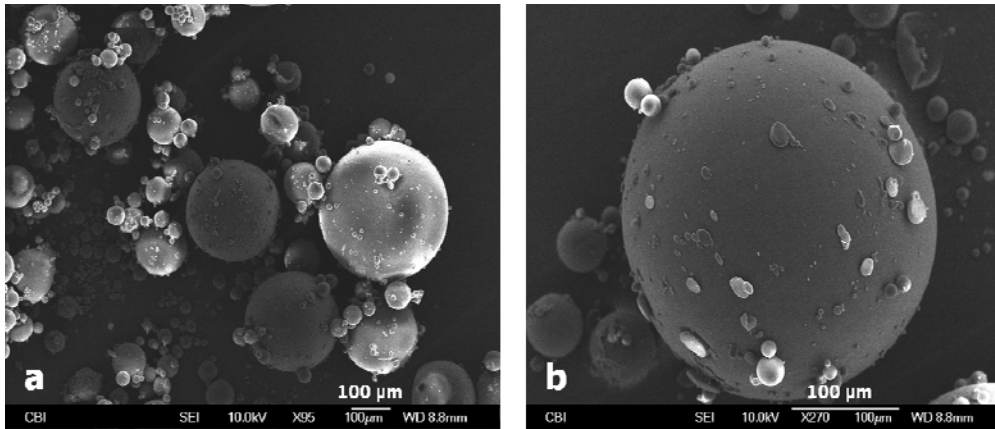
Figure 3-8. SEM of doxorubicin PLGA microspheres.
Under low magnification (a) and high magnification (b).[242]
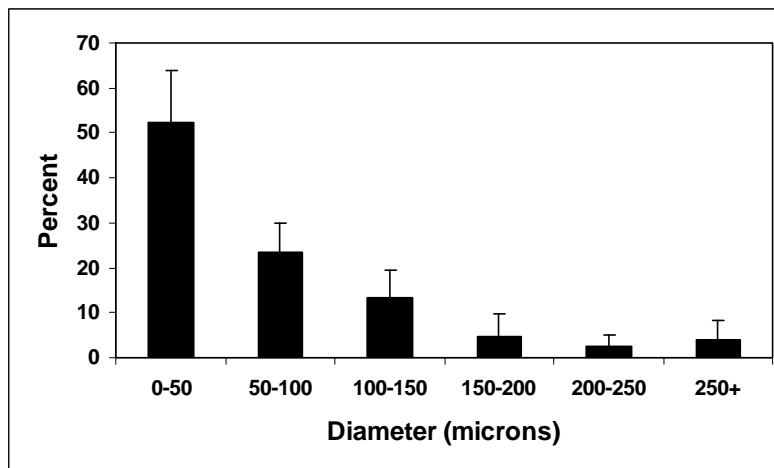
Figure 3-9. Diameter distribution of doxorubicin microspheres.[242]

The gelatin constructs were characterized using SEM. As seen in Figure 3-10, the microspheres were embedded within the gelatin pores and appear to be distributed homogenously. The gelatin scaffolds were porous with an average porosity of 46.1 ± 11.1%.
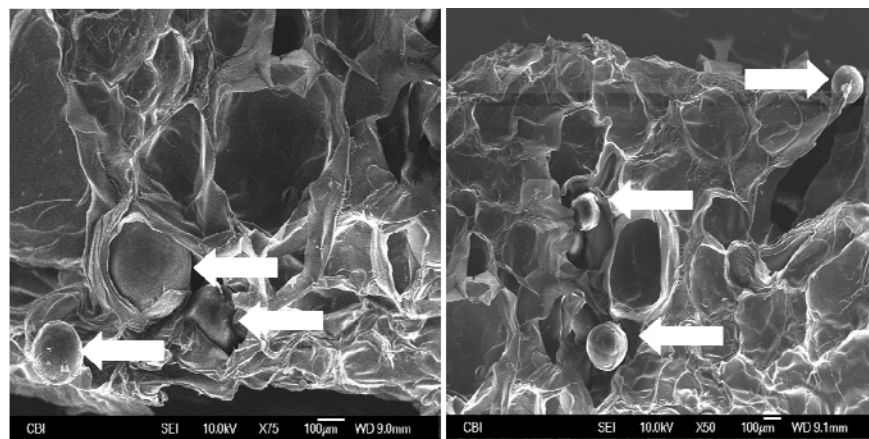
Figure 3-10. SEM of doxorubicin microspheres embedded in gelatin scaffolds. The white arrows point to microspheres.[242]

The release of Dox from the PLGA microspheres and gelatin constructs was examined by placing the microspheres or gelatin in a centrifuge tube and measuring the absorbance of the supernatant at various time points. The release of Dox from the microspheres was controlled and maintained over 30 days, as shown in Figure 3-11. The release profile of the Dox microspheres was compared to the release from the Dox microspheres embedded within the gelatin construct. The release from the gelatin was delayed when compared to the Dox microspheres alone. Comparing the percent of total Dox released from the microspheres alone to the gelatin constructs, the difference between the release rates can be determined. On Day 1 the Dox microspheres released 10.8 ± 6.0% of their total amount of drug released and the gelatin constructs released 7.6 ± 0.5%. About 50% of the total Dox released was released by the microspheres on day 8 (49.0 ± 11.0%) and by day 11 for the gelatin constructs (51.5 ± 2.7%).

The microspheres released about 90% ot the total released doxorubicin, 90.3 ± 2.0%, by day 20 and the gelatin constructs released 91.0 ± 3. 8% by day 26. Over days 5 through 16, the cumulative release was statistically significantly higher from the Dox microspheres alone (p<0.05).
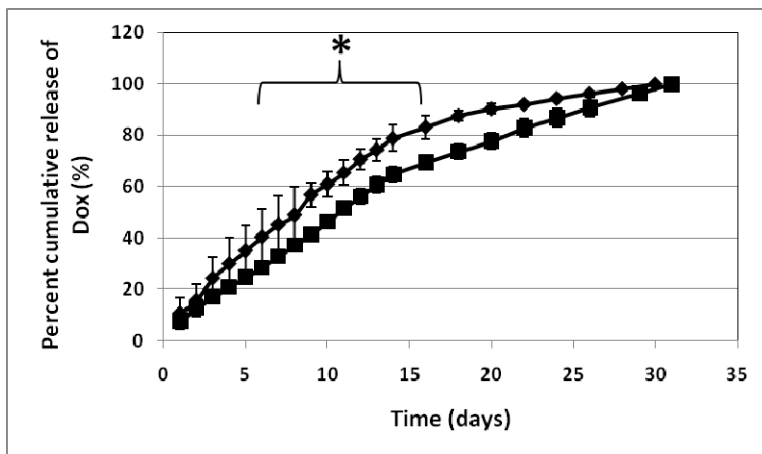
Figure 3-11. Percent cumulative release of doxorubicin.
Release from doxorubicin microspheres (-♦-) and doxorubicin microspheres embedded in gelatin scaffolds (-■-). *p<0.05, between PLGA microspheres and PLGA microspheres embedded within gelatin at each time point (days 5-16). All values reported as means ± standard deviations (n=5).

3.3.3 *In vitro* effects of microspheres and gelatin constructs on 4T1 cells

The bioactivity of the released Dox was determined by the effectiveness of Dox to induce 4T1 cell death. Four treatments were examined and compared to 4T1 cells cultured in 4T1 media. Figure 3-12 depicts the percent viable cells (normalized to 4T1 cells in 4T1 media). The Dox released from both the Dox microspheres and Dox gelatin significantly reduced the number of viable cells (p<0.001). The 4T1 tumor cells treated with the microspheres alone were exposed to 0.0051mg/mL of Dox over 48 hours. There was not a significant difference between the released Dox groups. The effect of empty microspheres was also examined; induction of cell death did not occur due to the empty microspheres alone. Residual glutaraldehyde from

crosslinking the gelatin constructs was a concern, thus empty microspheres embedded within gelatin was also assessed. However, no significant induction of death was seen in the glutaraldehyde crosslinked gelatin group.
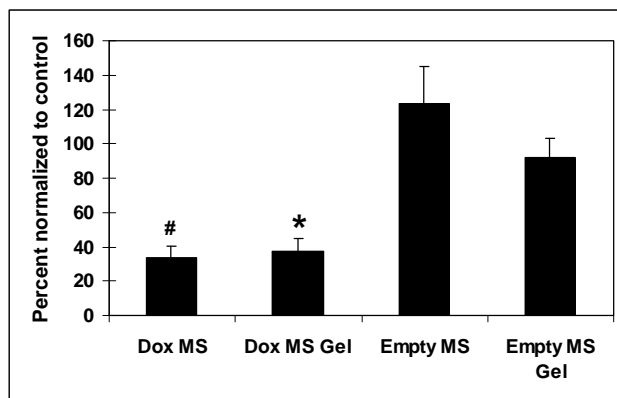
Figure 3-12. Viable cell number normalized to cells in 4T1 media after treatment for 48 hours. All values are reported as means ± standard deviations (n=5). *$p<0.05$ when comparing dox MS to empty MS, empty MS/gelatin, and 0mg/mL dox in media. #$p<0.05$ when comparing dox MS/gelatin to empty MS, empty MS/gelatin, and 0mg/mL dox in media.[242]

3.3.4 *In vivo* scaffold characterization

The constructs were examined by SEM. The microspheres are distributed homogenously through the porous gelatin constructs (See Figure 3-13).
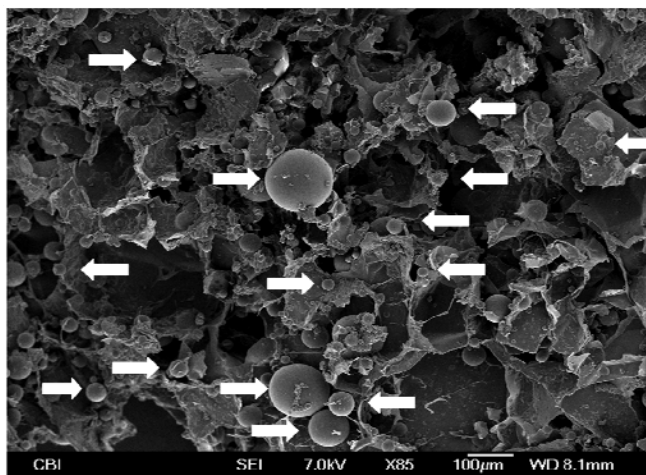
Figure 3-13. SEM of microspheres in gelatin scaffolds for *in vivo* studies. Arrows point to doxorubicin microspheres embedded within the scaffold.

3.3.5 X-ray/mammography

Mice with and without tumor were implanted with empty MS constructs. X-rays were performed to determine the radiotransparency of the constructs. Figure 3-14a, is the x-ray of a mouse with a tumor and an empty MS construct. The circle and arrow denote the area of the tumor and the construct. Figure 3-14b, depicts a mouse with only an empty MS construct, no tumor. The arrow denotes the site of the empty MS construct, which cannot be detected/observed on this x-ray. As the tumor can be seen in Figure 3-14a and no construct is seen in Figure 3-14b, we conclude that our scaffold is radiotransparent.
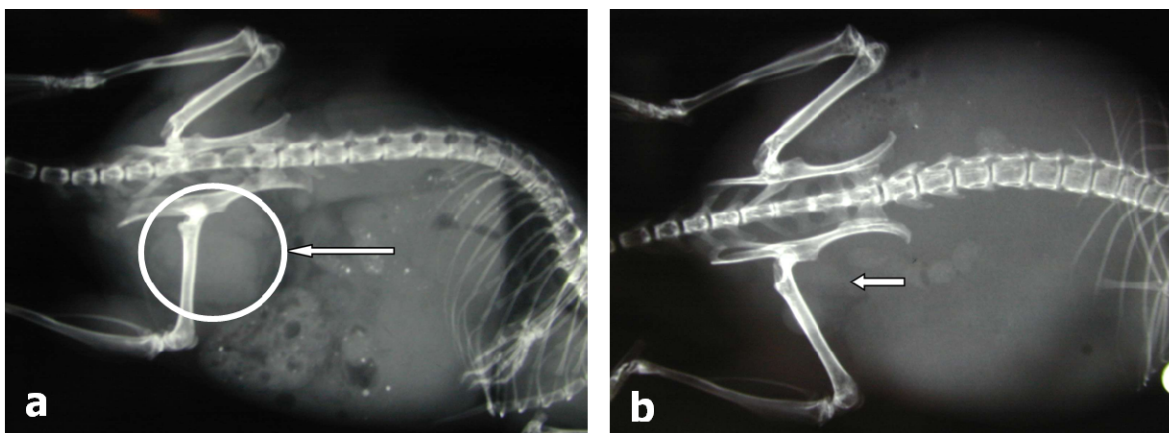
Figure 3-14. X-rays of mice after 7 days.
Mouse inoculated with tumor and treated with empty MS scaffold (a), circle denotes tumor. Mouse with empty MS scaffold implanted (b), arrow denotes area of scaffold.

3.3.6 Tumor eradication

The effectiveness of the constructs to eradicate the tumors was determined by inoculating mice with 4T1 tumor cells and treating them with gelatin constructs. The mice that received no treatment, empty constructs, or one Dox construct developed tumors. The excised tumors were measured with calipers (Figure 3-15). The volume of the tumors from the mice treated with

2Dox constructs, dox construct, and empty constructs are shown in Figure 3-16. No tumors were observed in the mice treated with 2Dox. The body weight of the each mouse was measured through the experiment to examine the toxicity due to treatment with doxorubicin. Figure 3-17 shows the time profile of the body weight following implantation of the constructs. Over the 23 days, the body weight of the mice treated with 2Dox constructs decreased. However, the weight loss was <10% of their initial body weight, and thus considered tolerable.
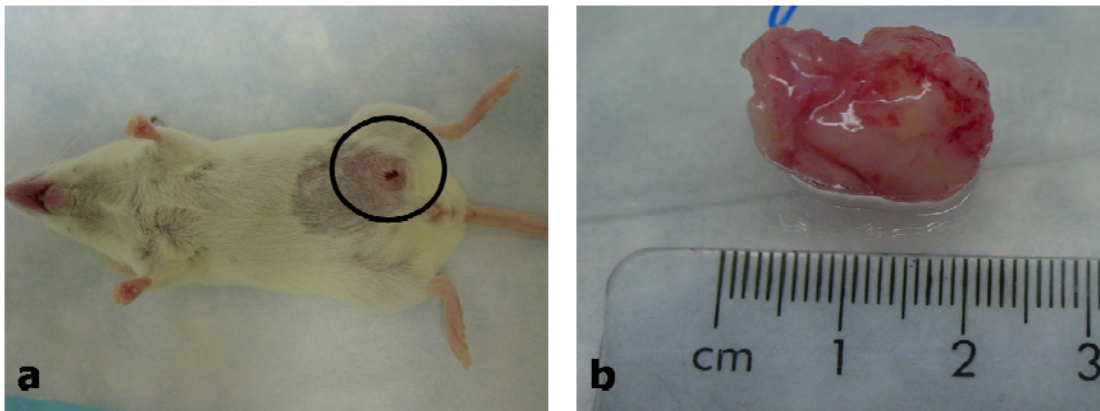
Figure 3-15. Tumor formation after 23 days *in vivo*.
Mouse with tumor treated with no scaffold (a). Excised tumor from mouse (b).
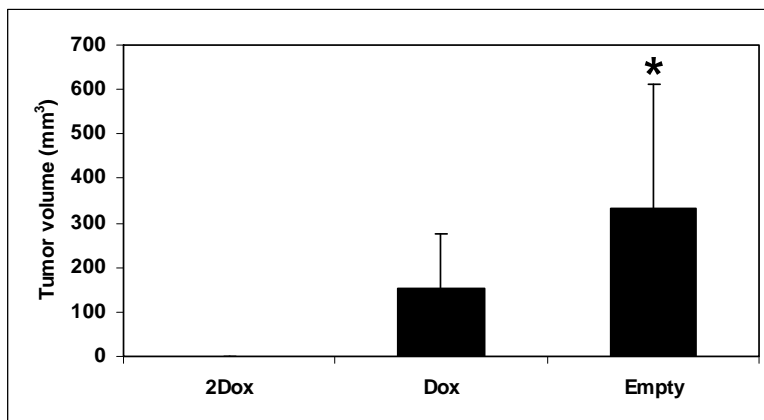
Figure 3-16. The volume of tumors excised from the mice after 23 days *in vivo*.
*p<0.05 compared to mice treated with 2Dox scaffolds. All values reported as means ± standard deviations.
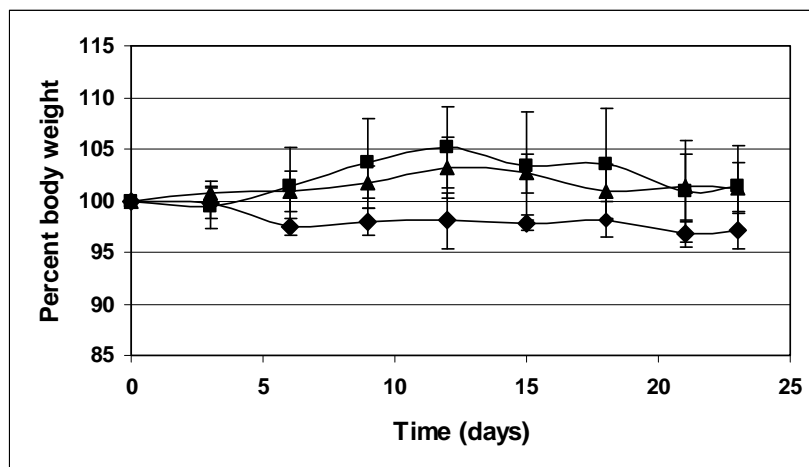
Figure 3-17. Percent body weight of mice after 23 days of treatment.
Percent body weight of mice treated with 2Dox scaffolds (-♦-), Dox scaffold (-■-), and empty scaffold (-▲-).

3.3.7 *In vivo* degradation of the scaffolds

Since the scaffolds were not grossly visible after 23 days, the degradation of the scaffolds after seven days was examined. Mice were treated with either 2Dox constructs or 2 empty constructs. After seven days, the mice were sacrificed. The tumor, construct, and surrounding area were fixed in 10% buffered formalin and embedded in paraffin. The slides were stained with H&E and Masson's Trichrome. After seven days, the scaffolds were present, as seen by gross observation (Figure 3-18). Staining with Masson's Trichrome demonstrated the presence of gelatin (Figure 3-19). Masson's Trichrome stains collagen blue, so the remaining gelatin will stain blue.
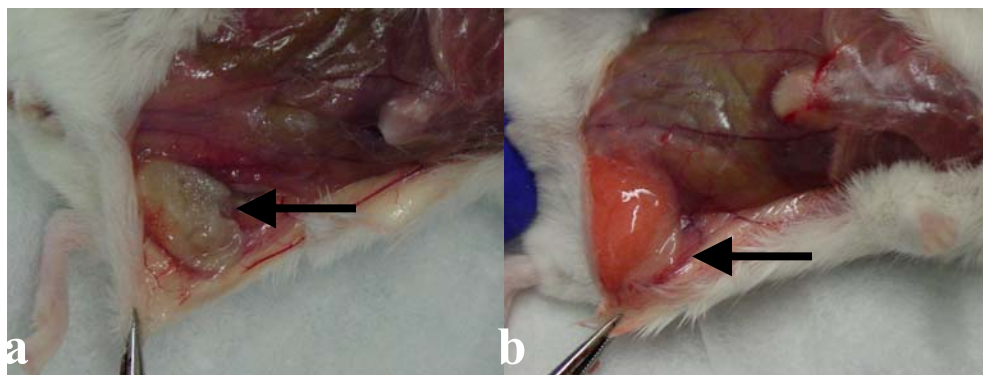
Figure 3-18. Scaffolds present after 7 days *in vivo*.
Empty MS/scaffold (a), and 2Dox scaffolds (b), arrows point to scaffolds.
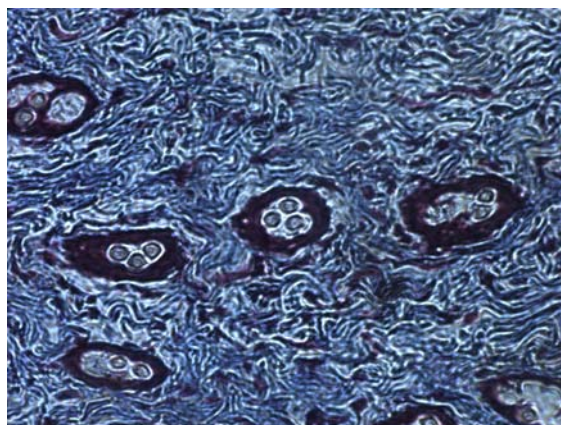
Figure 3-19. Masson's Trichrome staining of scaffold after 7 days *in vivo*.

3.3.8 Optimization of the delivery system

The degradation time of the gelatin scaffolds increased with an increasing glutaraldehyde concentration. Table 3-II shows the degradation time of each scaffold *in vitro*. As gelatin and glutaraldehyde concentrations were increased, the degradation time also increased.

Table 3-II. Degradation of gelatin scaffolds *in vitro*.

Gelatin (w/v %)	Glutaraldehyde Concentration (mmol)	Degradation time (days)
3%	0.01	5
3%	0.02	15
3%	0.04	>200
3%	0.08	>200
5%	0.01	1
5%	0.02	11
5%	0.04	>200

By encapsulating doxorubicin in its solid form instead of its liquid form, the encapsulation efficiency increased. The encapsulation efficiency of solid doxorubicin was 14.51 ± 8.90% compared to 1.03 ± 0.65% (liquid doxorubicin). As the encapsulation efficiency was increased, so was the loading capacity; the loading capacity was 3.85 ± 2.36µg Dox per mg of microspheres compared to 0.66 ± 0.41µg per mg of microspheres. However, the release of doxorubicin was much lower and could not be detected utilizing the current method. The encapsulation efficiency and release kinetics could possibly be optimized by altering other parameters in the microsphere preparation method. As discussed in the introduction (Chapter 1), many parameters affect the release and encapsulation efficiency of polymer microspheres.

3.4   DISCUSSION

In our study, we have demonstrated a controlled release of Dox by encapsulation in PLGA microspheres that were incorporated into a gelatin construct. The choice of PLGA for the microspheres is based on the widely reported use of FDA-approved PLGA for drug delivery.

The encapsulation of Dox into polymer microspheres has been demonstrated.[202, 210, 243] For example, Lin et al. reported a 60-70% total release on Day 1 from single-wall microparticles.[243] Recently, Tan et al. fabricated double-walled microspheres containing Dox in an attempt to further control the drug release.[244] They reported an initial release of 0.89-12.89% depending upon the ratio of PLLA to PLGA within the first 6 hours.   In our study at Day 1, the microspheres alone released $10.8\% \pm 6.0\%$ of the total Dox released and the Dox released from the gelatin constructs was $7.5\% \pm 0.5\%$.   Furthermore, the release of Dox was significantly delayed during days 5-16 when the PLGA microspheres were incorporated into the gelatin.

In addition to the utilization of PLGA for the microspheres, we chose gelatin as our scaffold material. Crosslinked gelatin has been used as a delivery system of chemotherapeutic drugs. Fan et al. studied the *in vitro* release of Dox from glutaraldehyde crosslinked gelatin for local delivery.[208] They reported that the non-crosslinked implants were insufficient due to poor mechanical strength and a quick release of the drug. However, glutaraldehyde crosslinked implants resulted in a more controlled release. By crosslinking the gelatin, the resistance of the scaffold material for diffusion of the drug was increased. Muvaffak et al. examined the effect of glutaraldehyde concentration on the release of the cytotoxic drug, colchicines, from gelatin microspheres.[245] As the amount of glutaraldehyde was increased, a slower release profile of the drug occurred.   In our study, we crosslinked gelatin with glutaraldehyde not only to sufficiently tailor the release of the Dox, but to also maintain the scaffold strength and thus maintain the shape or contour of the breast. It is possible that Dox may become crosslinked in the presence of glutaraldehyde, as stated by Fan et al.[208] To avoid this potential reaction, we incorporated the Dox-loaded PLGA microspheres into the gelatin that had already reacted with

glutaraldehyde for at least 5 minutes. Remaining residual glutaraldehyde was reacted with glycine, prior to the release of Dox from the microspheres. Due to our fabrication process, it appears as though very little, if any, Dox was crosslinked due to glutaraldehyde. We propose that glutaraldehyde would only be able to react with Dox released into the gelatin solution during the fabrication process. As such, the Dox released from the microspheres during the *in vitro* release studies was not inhibited by crosslinking due to residual glutaraldehyde. Our results are also consistent with those of Konishi et al.[228] They prepared gelatin hydrogels that were crosslinked with glutaraldehyde, freeze-dried, and then added a solution containing doxorubicin and cisplatin.[228] They did not report an observed interaction between the Dox and the gelatin sponge that was already crosslinked with glutaraldehyde. Furthermore, they did not observe a delayed release; approximately 60-80% and 8-20% of Dox and cisplatin, respectively, were released within 6 hours.

Research in the area of microsphere-incorporated scaffolds has focused on both the inclusion of native[21, 246-248] and synthetic[18, 76, 249-253] polymeric microspheres within scaffolds. For example, gelatin microspheres incorporated within gelatin scaffolds has been studied by Ulubayram et al.[246] Holland et al. examined gelatin microspheres encapsulating TGF-β1 in oligo(poly(ethylene glycol) fumarate) (OPF) hydrogels.[20, 21] Their study resulted in a more controlled release when the microspheres were incorporated in the OPF gel. Although microspheres containing drugs, proteins, or growth factors have been incorporated post-fabrication,[254] the inclusion of polymer microspheres during fabrication has been less studied. Zhang et al. assessed the release from hydroxyl-functionalized glycerol poly(ε-caprolactone) in poly(n-isopropylacrylamide) (PNIPAAm) hydrogels.[249] They also reported a more controlled release from the microspheres incorporated into PNIPAAm. Elisseeff et al. reported the

controlled release of IGF-I and TGF-1 from PLGA microspheres incorporated in PEO-based hydrogels.[18] Our lab has reported the incorporation of PLGA microspheres within PLGA scaffolds,[250, 251] fibrin scaffolds,[252] and more recently PEG-based hydrogels.[253] To the best of our knowledge we are the first to incorporate PLGA microspheres within gelatin scaffolds. A study by Liu et al. following our publication incorporated paclitaxel-PLGA microspheres in gelatin scaffolds.[255] The release was not different from the microspheres in the gelatin sponges compared to the microspheres alone. However, this is most likely due to the non-crosslinked gelatin as they state crosslinking the gelatin may further limit the release.

In the present work, we demonstrated the ability to induce cell death by doxorubicin delivered from the gelatin constructs *in vitro*. Lin et al explored the cytotoxicity of PLGA microparticles with glioma cells *in vitro*. They demonstrated a higher toxicity from the microparticles compared to free Dox.[243] In our results, induction of cell death was statistically significant in both the Dox microspheres and the Dox gelatin *in vitro* when compared to no treatment, gelatin, and empty microsphere-gelatin treatments (p<0.001). Our results demonstrated a dose-dependent response of the tumor cells to doxorubicin. Liu et al. demonstrated a similar response of hepatoma cells from 0.3μg/mL to 2.5μg/mL of released doxorubicin from human serum albumin microspheres.[256]

The *in vitro* characteristics of the scaffold suggest potential clinical utility for the treatment of patients having not only breast cancer but a variety of other malignancies where failure of surgical therapy alone mandates the need for additional therapy (multimodality treatment). We have tested the *in vivo* properties of the device and the device is capable of tumor eradication, biocompatible, and radiotransparent. The scaffolds were implanted into mice at the time of inoculation of a mammary tumor. This model adequately represents the clinical

scenario in which the scaffold would be implanted at the time of lumpectomy. Any remaining cancer cells after lumpectomy should be killed by the localized release of Dox from the construct, while the defect is filled by the gelatin scaffold. After the Dox is completely released, normal tissue is hypothesized to infiltrate the gelatin scaffold and form healthy tissue. In this study we examined whether a high dose of released Dox at the site would eradicate tumors.

Emerich et al. examined the effects of the placement of delivery systems.[201]. Their results show that placement around the perimeter of the tumor was better than an intra-tumor injection. As such, in this study, we placed the gelatin construct right next to the inoculation site. The dose of doxorubicin that would be used to treat these mice based on weight is 0.4μg, in this study the mice were treated with a cumulative release of 24 μg over the total 23 days. Local toxicity surrounding the scaffold was not seen in any of the mice. The mice received no treatment, empty scaffolds, Dox scaffold, or 2Dox scaffolds. The volume of the tumors from the mice treated with 2Dox scaffolds indicated complete eradication of the tumors. Conversely, tumors formed in the mice that received no treatment, empty scaffold, or Dox scaffold. The body weight of each mouse was measured through the experiment to examine the toxicity due to treatment with such a large dose of doxorubicin, and while the weight of mice treated with 2Dox scaffolds decreased, it was considered tolerable.

The degradation of gelatin scaffolds has been readily examined. Non-crosslinked gelatin sponges were placed in rats in the peritoneal cavity and had partially degraded at 3 days and almost complete degradation occurred at 7 days.[255] Ulubayram et al. examined the *in vitro* degradation and cytotoxicity of gelatin scaffolds crosslinked with glutaraldehyde.[239] Gelatin scaffolds crosslinked at a glutaraldehyde of 0.25mmol and 0.5mmol degraded 24 days and 28 days respectively *in vitro*. The scaffolds of 0.25mmol glutaraldehyde were nontoxic whereas the

scaffolds with 0.5mmol glutaraldehyde were moderately cytotoxic. In this study we utilized gelatin scaffolds that were crosslinked with a concentration of 0.2mmol glutaraldehyde. We did not see toxicity of the 4T1 tumor cells from the gelatin scaffolds. The degradation of the scaffolds *in vivo* usually occurs more quickly than *in vitro*. Thus as Ulubayram saw degradation at 24 days *in vitro*, we would expect to see degradation at 23 days *in vivo*.

We successfully eradicated tumor cells *in vitro* and *in vivo* with the Dox scaffold. However, further studies involving long term *in vivo* use to assess tissue ingrowth, a gelatin scaffold that degrades more slowly is necessary. As well, if the encapsulation efficiency of doxorubicin can be increased, a smaller amount of microspheres could be embedded within the scaffolds. As such, different concentrations of glutaraldehyde were used to crosslink different concentrations of gelatin, and the degradation time *in vitro* was observed. We can prepare gelatin scaffolds that did not degrade as quickly. Doxorubicin in its solid form was encapsulated in PLGA microspheres and the encapsulation efficiency compared to encapsulation of doxorubicin-HCL. The encapsulation efficiency was increased; however, the release could not be determined from the microspheres.

The observation that 80-90% of local recurrences that occur after surgery and radiation occur in the tumor resection bed suggest that the problem is a very local one and questions the need for whole breast irradiation.[257] The second relevant observation is that systemic administration of chemotherapy reduces the rate of local recurrence. [258, 259] These two observations together suggest the testable hypothesis that an implantable chemotherapy delivery system can reduce the local recurrence rate associated with surgery alone. Although direct administration of an anticancer agent into tumors of the breast is not routinely performed clinically this approach is used to treat other malignancies especially tumors of cutaneous origin

again suggesting clinical potential.[260] Clearly much additional preclinical study is necessary and this in turn would need to be followed by the design and completion of appropriate randomized clinical trials before this modality could challenge the current standard of care. Nonetheless there exists an unmet need to improve the current therapy for not only breast cancer but other malignancies as well.

3.5   CONCLUSIONS

In this study we aimed to develop a novel delivery system to locally deliver a chemotherapeutic agent as well as maintain the contour of the breast following a lumpectomy. We have prepared a controlled delivery system of doxorubicin to maintain local levels of the drug. The release was controlled by the incorporation of PLGA microspheres into gelatin constructs. The released doxorubicin from both the microspheres alone and microspheres incorporated into gelatin demonstrated a cytotoxic effect on 4T1 tumor cells *in vitro*. Implantation of 2Dox scaffolds resulted in tumor eradication *in vivo*. A dose 60 times the currently recommended dose was given to the mice; however, no adverse reactions were observed due to treatment with the Dox scaffolds, the body weight of the mice was not drastically effected nor was local toxicity observed.

3.6   FUTURE DIRECTIONS

We successfully achieved our aim of developing a novel delivery system to locally deliver chemotherapy and fill in the defect following a lumpectomy. Future studies must be performed to further develop and optimize this system. We encapsulated doxorubicin-HCL in PLGA microspheres; doxorubicin is also available in powder form. Encapsulation of the powder form resulted in a higher encapsulation efficiency. Similar studies as mentioned above should be performed to determine the efficacy of these microspheres to be utilized in this system.

We utilized gelatin as the scaffold in which to incorporate the microspheres. In this study we examined a low crosslinked gelatin scaffold. However after 23 days *in vivo*, we could not detect the scaffolds by gross observation. Our aim was to have a scaffold that would slowly degrade and allow tissue ingrowth. Therefore, a scaffold that degrades more slowly would be optimal.   We have examined the degradation *in vitro* of gelatin scaffolds of various glutaraldehyde and gelatin concentrations. As such the scaffold of 3% gelatin and 0.4 ml of 1.0% glutaraldehyde (0.04mmol) is recommended for further examination.   An injectable hydrogel that would gel *in situ* to fill any size and shape defect should also be examined. We are currently developing a novel PEG hydrogel that may be utilized for this application (See Chapter 5).

Furthermore, Konishi et al. demonstrated an increased effect by releasing both doxorubicin and cisplatin.[228] We have done some experiments to encapsulate cisplatin in PLGA microspheres (See Appendix B). In our delivery system, we could easily incorporate cisplatin-loaded PLGA microspheres in the gelatin scaffold in addition to the doxorubicin-loaded PLGA microspheres.

Finally, additional control groups could further demonstrate the efficacy of the delivery system. Systemic delivery of dox could be given as a control for tumor ablation as well as systemic toxicity. The systemic levels of dox should be measured to ensure a local delivery from the gelatin scaffold.

4.0 THE CONTROLLED RELEASE OF TGF-B1 FROM PEG-GENIPIN BIODEGRADABLE HYDROGELS FOR CARTILAGE REPAIR

4.1 INTRODUCTION

The need for tissue-engineered cartilage is of immense clinical significance. Traumatic and degenerative lesions of articular cartilage are leading causes of disability.[261] The poor intrinsic healing potential of articular cartilage is well described.[262] Untreated cartilage injuries are thought to progress to degenerative arthritis in the majority of patients.[263] It is estimated that over 40 million Americans currently suffer from osteoarthritis.[264] Tissue engineering methods to improve cartilage repair and regeneration will therefore have high clinical impact. There are two general approaches to tissue engineering of articular cartilage. The first approach is that of *ex vivo* tissue regeneration in which functional cartilage is created in the laboratory. Strategies used in this approach include encapsulation of repair cells into scaffolds for culture within sophisticated bioreactors delivering growth factors, nutrients, and mechanical forces. The second approach to cartilage regeneration focuses on enhancing intrinsic repair processes. As such, the emphasis is on augmenting and modulating the *in vivo* response to injury through the addition of scaffolds, cells, and growth factors.

We have incorporated PLGA microspheres in a naturally derived hydrogel (Chapter 3); however, the goal of this chapter is to examine the release from PLGA microspheres within a

novel synthetic hydrogel, PEG-genipin. We have prepared a delivery system to enhance cartilage repair. Transforming growth factor–beta1 (TGF-β1) was encapsulated in PLGA microspheres. The microspheres were incorporated into synthetic hydrogels, PEG-genipin. The release kinetics from the microspheres and hydrogels were determined. The bioactivity of the released TGF-β1 was also evaluated. The burst release of TGF-β1 was decreased by incorporating the microspheres in the hydrogels. The amount of TGF-β1 released can be tailored by the concentration of the crosslinker, genipin, and the amount of microspheres incorporated into the scaffolds.

4.1.1   Cartilage

Cartilage is a complex tissue that provides shape and support. Three types of cartilage are present in the body: hyaline, elastic, and fibrocartilage. The cartilage-resident cells, chondrocytes, secrete an avascular extracellular matrix. The extracellular matrix consists of type II collagen that provides strength and proteoglycans, which are hydrophilic.[265] Thus, cartilage is biphasic with a solid matrix consisting of a dense collagen network and a gel composed of proteoglycans.[266] Articular cartilage is hyaline cartilage that covers the joint surface where one bone meets another which enables a joint to move easily by reducing friction.[267]

Chondrocytes grown in monolayer dedifferentiate into fibroblast-like cells;[266, 268] however, a three-dimensional environment allows chondrocytes to maintain their phenotype and redifferentiate.[266] Fresh chondrocytes have a round polygonal morphology. Once they have de-differentiated, chondrocytes have a fibroblast morphology.[268] Thus for cartilage tissue engineering, the environment provided is important to maintain healthy cells and tissue.

4.1.2   Therapies for cartilage repair

Traumatic and degenerative lesions of articular cartilage are leading causes of disability. Since cartilage is avascular, repair is insufficient. Current treatments for cartilage repair are limited. Arthroplasty, replacement of the joint with an artificial prosthesis, is one treatment option for severe osteoarthritis.   An osteochondral autograft is another option. In this procedure, a small graft is removed from an area that does not bear a lot of weight and is transplanted to the damaged area.   Carticel® is the only marketed FDA approved autologous cell therapy. Carticel® utilizes autologous chondrocytes by taking a biopsy and expanding the cells *de novo*, which are then implanted. Another option is to stimulate the marrow by drilling a hole through to the bone marrow. This procedure attempts to stimulate the body to repair itself by having repair cells (possibly adult stem cells) from within the blood or bone marrow fill in the defect. Recently, tissue engineering with autologous adult stem cells has become a reality for use as a therapy. Wakitani et al. demonstrated the use of autologous bone marrow mesenchymal stem cells (BMSCs) to heal articular cartilage defects in humans.[269] BMSCs were encapsulated in collagen gels, the results showed the defects were filled with fibrocartilage and clinical symptoms had drastically improved.[270]   The potential for BMSCs to differentiate into chondrocytes and repair cartilage defects has been well studied[41, 271-274] and chondrogenesis of BMSCs from osteoarthritic patients has also been demonstrated *in vitro*.[275]

4.1.3 Transforming growth factor-β1 (TGF- β1)

Transforming growth factor-beta1 (TGF-β1) is a 25 kDa protein from the TGF-β super family. TGF-β1 acts as a growth inhibitor for epithelial, endothelial and hematopoietic cell lineages; however TGF-β1 is stimulatory for cells of mesenchymal origin.[265] TGF-β1 increases chondrocyte,[276] osteoblast precursor cell,[277] and BMSC[278] proliferation. TGF-β1 is chemotactic, inducing mesenchymal stem cell recruitment.[279, 280]

TGF-β1 is an isoform of TGF-β that plays an important role in the growth and differentiation of articular cartilage. TGF-β is very abundant in articular cartilage and TGF-β1 is the predominant isoform.[281] TGF-β1 has the potential to improve cartilage repair by promoting chondrogenic differentiation.[282-288] TGF-β1 promotes chondrogenic differentiation in chondroblasts,[282, 283, 285] and in mesenchymal cells such as bone marrow stromal cells, perichondrium and periosteum.[284, 286-289] TGF-β1 has been shown to induce chondrogenesis,[280, 290] increase collagen type II expression,[276, 280, 291] and GAG content.[291, 292] TGF-β1 also induces bone formation.[277, 278, 280, 293, 294] A repeated administration of TGF-β1 has a superior effect to single application in wound healing and sustained release of TGF-β1 induced chondrogenesis of human bone marrow stromal cells.[295, 296] In this study we have chosen to examine the sustained release of TGF-β1 from PLGA microspheres.

Sustained TGF-β1 administration is readily accomplished *in vitro* but poses difficult challenges when translated to the *in vivo* environment. Many investigators have examined the controlled delivery of TGF-β1, as seen in Table 4-I. TGF-β1 has been encapsulated in PLGA microspheres,[294, 297] PLGA microspheres within hydrogels,[18, 20] chitosan microspheres in collagen/chitosan/glycosaminoglycan scaffolds,[291] and gelatin microspheres in PEG-fumarate

hydrogels.[21, 22] In this study, we encapsulated TGF-β1 in PLGA microspheres, which were then encapsulated in PEG hydrogels.

Table 4-I. TGF-β1 Delivery Systems.

Polymer Microspheres[278, 294, 297]	PLA [298, 299]
Sodium alginate microspheres[300]	Coral Particles[301]
Chitosan microspheres[276, 277, 291]	Liposomes[302]
Gelatin microspheres in OPF[20-22, 247]	Fibrin glue[280]
PLGA Microspheres in PEO hydrogels[18]	PLGA[293]
Oligo(poly(ethylene glycol) fumarate (OPF)[21, 22]	$CaSO_4$[293]
Gelatin/Gelatin Microspheres[54, 290, 303]	Dextran Hydrogels[304]
Ethylene acetate copolymers[305]	Poly(ether-ester)[292]
Hydroxyapatite[306]	

4.1.4   Scaffolds for cartilage tissue engineering

Cartilage-like tissue has been grown in numerous scaffolds, including synthetic and native. Collagen is the most extensively studied natural scaffold for cartilage tissue engineering. [274, 307-311] Other natural scaffolds investigated include hyaluronic acid,[309, 312-314] gelatin scaffolds,[273] fibrin glue,[101, 102, 315] chitosan,[316-318] and alginate.[311, 314, 319] Synthetic polymers can be more versatile and modified to obtain desired properties. Synthetic polymers such as PCL,[280, 320] PGA,[275, 321, 322] PEG hydrogels,[323-326] PEG/PCL hydrogel,[327] polyurethanes,[328], poly(propylene fumarate) (PPF),[309] and oligo(poly(ethylene glycol) fumarate) (OPF) [20-22] have been studied as scaffolds for cartilage. We are utilizing PEG-based hydrogels as our scaffold material. While synthetic hydrogels are commonly nondegradable, biodegradable PEG hydrogels can be obtained via copolymerization with degradable polymers such as PLA, PGA and PPF. [16, 21, 329] An objective of this thesis is to examine the potential of genipin, a naturally derived molecule, as a crosslinking agent for synthetic, biocompatible polymers. Our laboratory has examined the synthesis of biodegradable PEG hydrogels using genipin, a non-toxic crosslinking agent.[25] Genipin is a readily

91

obtainable, naturally-derived compound found in the gardenia fruit and has been utilized as a crosslinking agent for primary amines. Genipin has been used to crosslink functional amine groups present in natural tissues and native polymers with very minimal cytotoxic effects as compared to studies performed with the crosslinking agent glutaraldehyde. [330-332] Genipin is further discussed in Chapter 5. We have also demonstrated the ability to tailor *in vivo* dissolution of the PEG-genipin hydrogels in osteochondral defects (Appendix C).

4.1.5 Incorporation of microspheres in scaffolds

A number of researchers have studied the combination of microspheres and scaffolds for controlled drug delivery, including our own laboratory.[20, 21, 333, 334] For example, the use of crosslinked polymers can provide highly reproducible delivery of growth factors. Holland et al. [20] reported the controlled release of TGF-β1 from crosslinked gelatin microspheres incorporated in PEG-fumarate hydrogels. They reported that composites encapsulating less crosslinked microparticles exhibited 100% release after only 18 days and were completely degraded by day 24 in collagenase-containing phosphate-buffered saline. Hydrogels encapsulating higher crosslinked gelatin microparticles did not exhibit 100% release or polymer loss until day 28. Their studies confirm that TGF-β1 release and biomaterial degradation can be controlled by altering parameters of *in situ* crosslinkable hydrogels such as PEG[20]. In this study, we have incorporated TGF-β1-loaded PLGA microspheres in PEG-genipin hydrogels with different crosslinking densities to further control the release of TGF-β1.

4.2   METHODS

4.2.1   Preparation of poly(ethylene glycol) (PEG)-genipin scaffolds

PEG-genipin hydrogels were prepared by crosslinking poly(ethylene glycol) diamine (PEG diamine) with genipin (Figure 4-1). A 10% (w/v) aqueous PEG-diamine solution was prepared by dissolving PEG-diamine in filtered Nanopure water. An 88 mM genipin aqueous solution was added to the 10% PEG aqueous solution, yielding a final concentration of 17.6 mM ("PEG-genipin low") or 35.2 mM ("PEG-genipin high") genipin. The solution reacted overnight in sealed vials at room temperature. Once the solutions became dark blue, the crosslinked solutions were poured into a Teflon® mold. After 24 hours, samples were removed and sterilized using UV light.
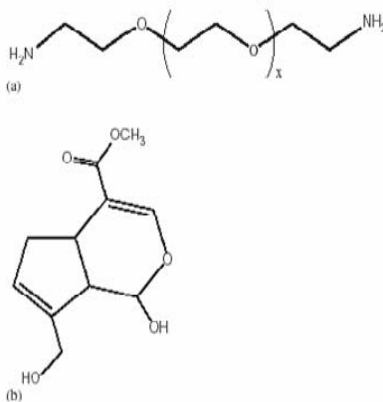
Figure 4-1. Structure of PEG-diamine (a) and genipin (b).[335]

4.2.2   TGF-β1 encapsulation and characterization

TGF-β1 was encapsulated into PLGA microspheres using a double emulsion technique, using a protocol previously described.[297] Briefly, 250mg PLGA (50:50, Sigma Aldrich) was

dissolved in 2 mL of MC. Next, 100 µL of a 10 µg/mL solution of TGF-β1 was added to 1 mL of a 1% PVA solution, and the solutions were combined. The entire mixture was emulsified on a vortexer for 1 min. The solution was re-emulsified in 50 mL of 0.1% aqueous PVA solution, resulting in a double emulsion. Next, 100 mL of a 2% aqueous isopropanol solution was added to the second emulsion and stirred for 2 hours. The microspheres were collected by centrifugation, lyophilized to dryness, and stored at -20°C. The microspheres were examined morphologically by SEM.

4.2.3   Incorporation of TGF-β1 microspheres in PEG-genipin scaffolds

PLGA microspheres were weighed and then added to the hydrogel solution in the Teflon mold during the final hours of gelation. Microsphere incorporated hydrogels were characterized using SEM. The mass of incorporated microspheres was equivalent for both the high genipin concentration and low genipin concentration.

4.2.4   *In vitro* release

The *in vitro* release of TGF-β1 from the delivery system was analyzed for the three groups. Analysis of the release kinetics from the TGF-β1 loaded microspheres, TGF-β1 loaded microspheres incorporated in "PEG-genipin high" hydrogels, and TGF-β1 loaded microspheres incorporated in "PEG-genipin low" hydrogels was conducted using a commercially available Enzyme Linked Immunosorbent Assay (ELISA) kit. To determine the release from the microspheres, 10mg of microspheres were placed in a microcentrifuge tube containing 1 mL of PBS, pH = 7.4. The release of TGF-β1 from the microspheres in the PEG-genipin scaffolds was

also determined. The scaffolds were placed in 0.5 mL of PBS in a microcentrifuge tube. All samples were maintained at 37°C up to 21 days (n=5). At each time point (days 1, 3, 7, 10, 14, 17, and 21), the tubes were centrifuged and the supernatant collected for analysis. The samples were refreshed with new PBS and then vortexed for 5 seconds. Percent cumulative release was determined by normalizing the cumulative release of TGF-β1 at each time point with the total cumulative release of TGF-β1 over the course of 21 days.

The degradation of the PLGA microspheres was analyzed under the same conditions as the release studies described above. After 14 and 21 days, the microspheres were collected for analysis. The microspheres were then examined by SEM.

4.2.5   Bioactivity of released TGF-β1

Activity of TGF-β1 released from PLGA microspheres was measured using the well-established mink lung cell growth inhibition bioassay.[292, 336, 337] TGF-β1 loaded PLGA microspheres (10mg), empty PLGA microspheres (10mg), TGF-β1-loaded microspheres in PEG-genipin (high and low), and empty microspheres in PEG-genipin (high and low) were placed in 250 µL MEM media and kept at 37°C. At each time point (Day 1, 3, 7, 10, 14, 17, and 21) the samples were centrifuged and the supernatant collected. The samples were refreshed with 250 µL MEM and vortexed. Mink lung cells (ATCC, CCL-64) were seeded into 96-well plates at 5×10^3 cells per well in MEM with 10% FBS. After cell attachment, microsphere elutes from various groups were added to the wells in triplicate and the cultures were incubated for 48 hours. Each assay plate contained control wells with known amounts of TGF-β1, ranging from 1 ng/mL to 0.04ng/mL. Following the incubation period, the media was removed and cells were rinsed with PBS and the assay plates were frozen at -70°C. DNA content of the cells was determined

by adding lysing buffer containing 0.1 mM potassium phosphate, pH 7.8, 0.2% Triton x-100, 1mM dithiothreitol and a 400-fold dilution of PicoGreen dsDNA dye. Fluorescence was read on a SpectraFluor plate reader (Tecan) and TGF-β1 bioactivity was determined by comparing the DNA/PicoGreen fluorescence in each assay well with that of cells treated with TGF-β1 standards on each assay plate.

4.2.6 Statistical analysis

The results are expressed as means ± standard deviations. Unpaired, two-tailed t-tests were performed at each time point. The threshold for statistical significance was set at $p<0.05$.

4.3   RESULTS

4.3.1 TGF-β1 microsphere and PEG-genipin scaffold characterization

The TGF-β1 loaded PLGA microspheres were prepared using a double emulsion technique and then examined using SEM. The average microsphere size was 86.64 ± 76.88 microns (Figure 4-3). The microspheres were spherical and exhibited a smooth surface morphology (Figure 4-2 a-b). Significant morphological changes occurred during the 21 days. The surface of the microspheres became rougher and the shape became less spherical. Micropores became more evident after 14 days (Figure 4-2 c-d). At day 21, the microspheres began to demonstrate a loss of preservation of their spherical structure (Figure 4-2 e-f).
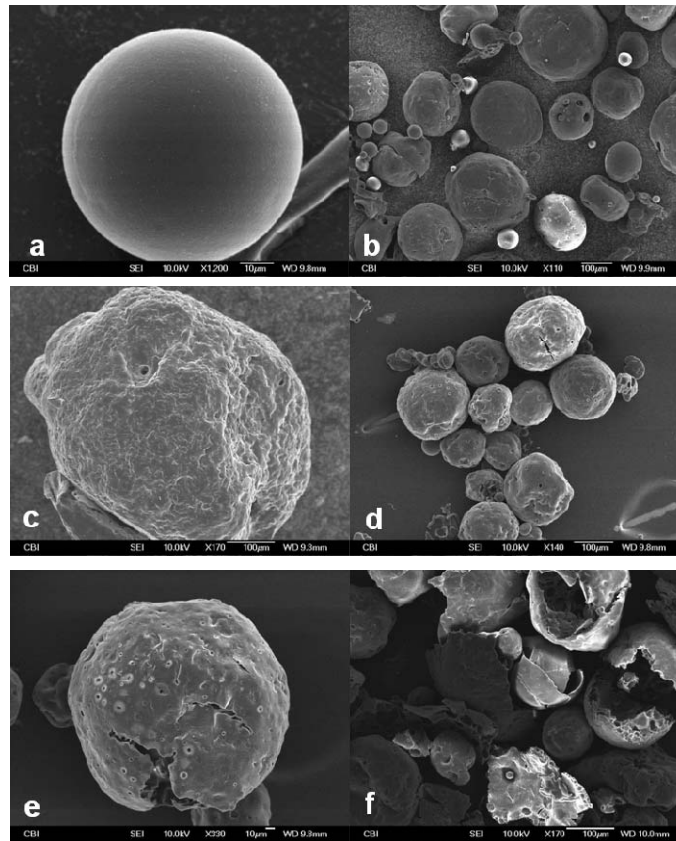
Figure 4-2. SEM of TGF-β1 PLGA microspheres.
TGF-β1-loaded microspheres at Day 0 at high magnification(a) and low magnification(b); after 14 days at high magnification(c) and low magnification(d); and after 21 days at high magnification(e) and low magnification(f).[335]
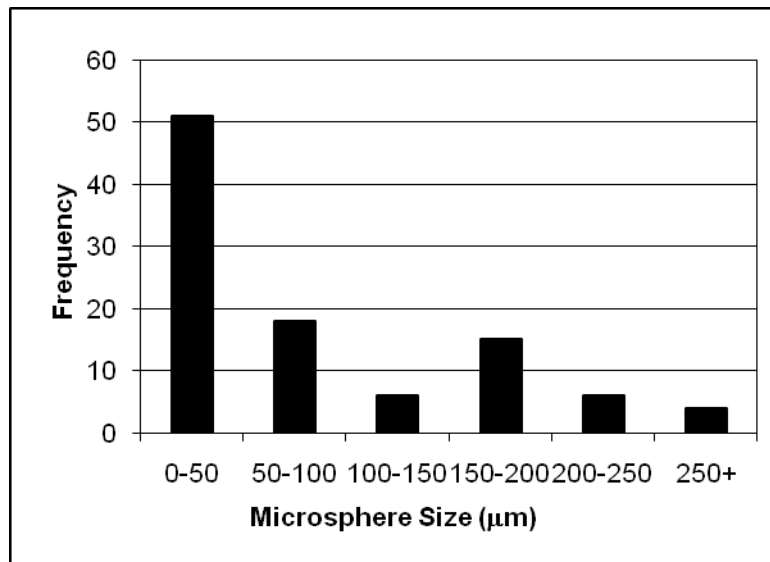
Figure 4-3. Diameter distribution of TGF-β1 microspheres.[335]

97

The microspheres were added to the hydrogel at both concentrations of genipin, 17.6 mM and 35.2 mM. Figure 4-4 depicts the scanning electron micrographs of the microspheres embedded in the PEG-genipin gels.
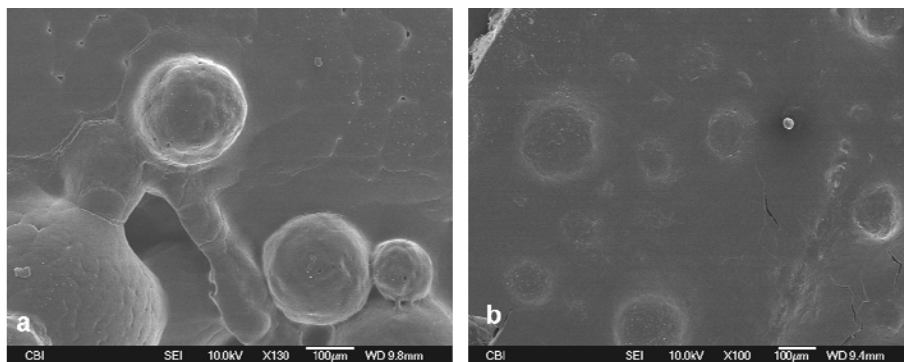
Figure 4-4. **SEM of TGF-β1 loaded microspheres in PEG-genipin hydrogels.**
Microspheres in PEG-genipin low(a) and PEG-genipin high (b).[335]

4.3.2 Release kinetics from microspheres and scaffolds

The *in vitro* release of TGF-β1 from the PLGA microspheres, the TGF-β1-loaded PLGA microspheres in PEG-genipin high, and the microspheres in PEG-genipin low into PBS (pH=7.4) was determined using an ELISA kit. The releasate was analyzed at 1, 3, 7, 10, 14, 17, and 21 days. The release of TGF-β1 was affected by incorporation into the scaffold as well as the genipin concentration of the hydrogel (Figure 4-5). Within 1 day, the microspheres demonstrated a high burst release (69.01 ± 29.25%). The burst release was delayed in both of the hydrogels incorporating the microspheres. The PEG-genipin high scaffold exhibited a burst release on day 3. The majority of the TGF-β1 was released by day 14. The PEG-genipin low scaffolds did not exhibit a large burst, at day 17, 72.7 ± 11.7% of the total released TGF-β1 was released. Statistical analysis of the cumulative release provides further evidence that the release is affected by the incorporation into PEG-genipin. The percent cumulative release of TGF-β1

from the microspheres was statistically higher than the release from the PEG-genipin low scaffolds with TGF-β1-loaded microspheres at every time point. Comparing the TGF-β1 loaded microspheres to the PEG-genipin high scaffolds with TGF-β1 loaded microspheres, the percent cumulative release was only statistically higher at day 1. The PEG-genipin high scaffold exhibited a statistically higher cumulative release of TGF-β1 than the PEG-genipin low scaffolds at days 7 and 10. This evidence demonstrates that incorporating the microspheres into PEG-genipin scaffolds delays the burst effect commonly seen in the release of growth factors from microspheres alone.
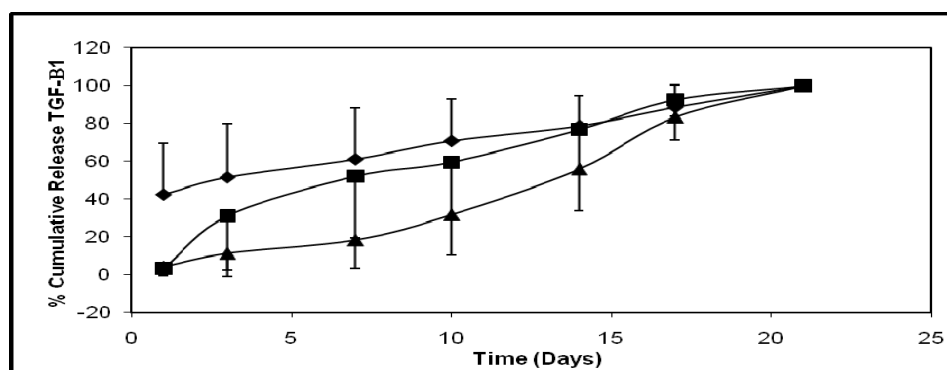
Figure 4-5. Percent cumulative release of TGF-β1.
Release from TGF-β1-loaded microspheres (-♦-), TGF-β1-loaded microspheres in PEG-genipin high(-■-), and TGF-β1 loaded microspheres in PEG-genipin low(-▲-).[335]

4.3.3 Bioactivity of released TGF-β1

The mink lung cell growth inhibition assay was used to assess the bioactivity of the released TGF-β1. Table 1 depicts the percent of cell growth inhibition of the mink lung cells when exposed to the releasate media from the microspheres when compared to normal growth media. Cell growth was significantly inhibited up to 14 days after release *in vitro*. We also examined the releasate from the low and high PEG-genipin scaffolds, and cell growth was also

initially inhibited (Figure 4-6), indicating that the delivery system fabrication process does not affect the bioactivity of TGF-β1.
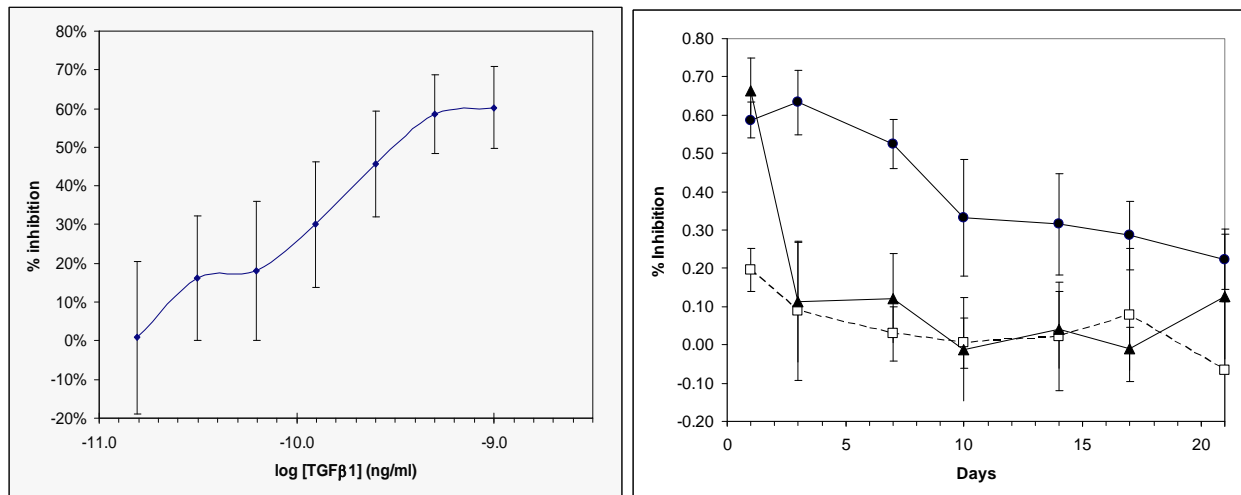
Figure 4-6. Bioactivity of released TGF-β1.
Percent mink lung inhibition from TGF-β1 loaded microspheres (-●-), TGF-β1 loaded microspheres in PEG-genipin high (-▲-), and TGF-β1-loaded microspheres in PEG-genipin low (-□-). Standard curve for TGF-β1 inhibition.

4.4 DISCUSSION

We examined PEG-genipin hydrogels as growth factor delivery vehicles for tissue engineering applications. We encapsulated TGF-β1 PLGA microspheres, and subsequently incorporated the microspheres into biodegradable PEG-genipin hydrogels. We have determined the release kinetics and bioactivity of TGF-β1 from the microspheres, and the microsphere-loaded hydrogels. The implications of such a controlled release system for understanding the effects of growth factors such as TGF-β1 on cartilage repair *in vivo* is of immense clinical significance.

In this study, we have demonstrated a significant difference in the release kinetics of TGF-β1 from our delivery systems. As expected, TGF-β1-loaded PLGA microspheres demonstrated a high burst release, whereas the hydrogels containing the microspheres demonstrated a delayed burst release. Interestingly, the PEG-genipin low hydrogel showed a longer delay in the release when compared to PEG-genipin high (Figure 4-5). This may be due to the faster dissolution of the lower genipin concentration hydrogel, resulting in hydrated PEG chains in the gel. We have previously shown that PEG-genipin hydrogels undergo dissolution in an aqueous environment, and the PEG-genipin chains are released into the solution.[25] Each leasate solution was blue; however, the PEG-genipin low solution was darker blue, and remained blue for a longer period of time as compared to PEG-genipin high. We hypothesize that the delay in the release of TGF-β1 from PEG-genipin low may be due to hydrated PEG chains in the hydrogel blocking the release of the large TGF-β1 molecule. This hypothesis is supported by results of a study conducted by Bajpai et al. who reported the release of insulin from hydrogels composed of PVA, PEG, and crosslinked polyacrylimide.[338] In that study, an increase in PEG content led to an initial increase in the release of insulin. However, at high levels of PEG, a decrease in release occurred. This decrease due to the number of hydrated PEG chains became so large that the release of insulin from inside the network was inhibited. Holland et al. examined the release from gelatin microspheres within OPF hydrogels. They saw similar results to our study, in which the release in looser gels was less than that from higher crosslinked gels.[20] They claim this may be due to the presence of uncrosslinked entangled polymer chains. We also saw a reduced release in the lower crosslinked hydrogels, which may be due to uncrosslinked PEG chains.

In this study the release of TGF-β1 was further controlled by incorporating the microspheres in either of the hydrogels. Ganguly et al. saw similar results, in which the release of dexamethasone was further sustained by incorporating ethylcellulose microspheres within chitosan gels.[137] Holland et al. also examined the release of TGF-β1 from microspheres within a hydrogel. By incorporating gelatin microspheres within OPF hydrogels, the burst was reduced. More specifically, the release of TGF-β1 was affected by diffusion through the OPF hydrogel.[20] Some investigators have incorporated microspheres within hydrogels, but only examined the release from the microspheres alone. Lee et al. examined a collagen/chitosan/glycosaminoglycan scaffold incorporating TGF-β1-loaded chitosan microspheres. The release kinetics *in vitro* were assessed from the chitosan microspheres alone; however, they state by incorporating the microspheres within the scaffold further controlled release was obtained.[291] Similarly Elisseef et al. incorporated microspheres in hydrogels and only examined the release kinetics from the microspheres alone.[18]

We also examined the bioactivity of the released TGF-β1 by assessing the inhibition of proliferation of mink lung epithelial cells. TGF-β1 is known to be a strong inhibitor of epithelial cell growth. For example, Parker et al. determined the bioactivity of released TGF-β3 from microtextured silicone and poly-L-lactic acid.[337] They reported that the released growth factor partially maintained its bioactivity, with 30–50% of the released growth factor active. In our study, we evaluated inhibition of cell growth by exposing mink lung cells to media from the *in vitro* release studies. Figure 4-6 demonstrates the inhibition of cell growth up to 21 days after exposure to TGF-β1 released from the PLGA microspheres, and the TGF-β1-loaded microspheres incorporated within PEG-genipin high and PEG-genipin low scaffolds. Cell growth inhibition was observed when the cells were exposed to media from the microsphere and

hydrogel delivery systems, with a significant decrease in inhibition observed at day 1 between the two hydrogel scaffolds (p<0.01). At day 1, growth inhibition was 59% for the PEG-genipin high scaffold, but only 20% for the PEG genipin low scaffold. By day 3, the difference in cell inhibition between the two hydrogels was no longer significant. We observed a decrease in the activity of TGF-β1 from the microspheres and from PEG-genipin hydrogels after 7 days, then a slight increase in activity after 10 days, which corresponds to the TGF-β1 release profile obtained from our ELISA data (Figure 4-5).. The initial loss of TGF-β1 activity may be attributed to damage to the growth factor by repeated freezing or thawing. This explanation was previously proposed by Parker et al.[337] Another possible explanation is that the growth factor lost its functionality by autolysis, as proposed by Nicoll et al.[339] While the loss of bioactivity over time will be addressed in future studies, we are optimistic that our fabrication protocol does not affect the bioactivity of TGF-β1.

4.5   CONCLUSIONS

Biodegradable PEG-based hydrogels containing TGF-β1-loaded PLGA microspheres were developed with potential utility in cartilage tissue engineering. The controlled release of TGF-β1 from microspheres embedded in the hydrogels is further controlled when compared to delivery from microspheres alone, resulting in a delayed burst release. ELISA results indicated a continued release of TGF-β1 up to 21 days from the PEG-genipin hydrogels. Mink lung cell growth inhibition results indicated bioactivity decreased after 7 days, but remained fairly constant throughout the study. The release of TGF-β1 was more controlled from PEG-genipin low hydrogels as compared to PEG-genipin high hydrogels. Finally, the scaffold permits

containment and conformation of the spheres to the defect shape, which is highly useful for *in situ* chondrogenesis.

4.6   FUTURE DIRECTIONS

We successfully developed a system to locally deliver TGF-β1 for cartilage tissue regeneration. However, more research must be done to further establish this delivery system for cartilage repair. The efficiency of this delivery system to induce chondrogenesis of bone marrow stem cells should be investigated. This can be demonstrated *in vitro* with the use of Transwell inserts. Another step can then be taken by encapsulating cells within the polymer. The current PEG-genipin system is not adequate for cell encapsulation, but utilizing a 4-arm or 8-arm amino terminated PEG may be more sufficient (See Chapter 5).   The use of this delivery system must be investigated *in vivo*. We examined the use of PEG-genipin scaffolds alone in osteochondral defects of rats (Appendix C). However, this animal model has a small defect (diameter = 1.5mm). Incorporating an adequate amount of microspheres to release a sufficient amount of TGF-β1 would be impossible. This could be overcome by utilizing a larger animal model and thus a larger defect. Large animals such as dogs, goats, and horses more closely resemble the human model, leading to a better study.[340]   Another possibility would be to increase the encapsulation efficiency of the PLGA microspheres. While this area has been widely studied, the results are contradicting. The encapsulation efficiency is dependent upon many factors including nature of the polymer, concentration of polymer, surfactant utilized, solvent removal rate, ratio of lactic acid and glycolic acid, and temperature (See Chapter 1).[341, 342]

5.0   MODIFICATIONS OF PEG-GENIPIN TO INCREASE GELATION RATE

5.1   INTRODUCTION

Hydrogels can be utilized as delivery systems, cell carriers, and scaffolds for tissue engineering. Injectable hydrogels allow easy and homogenous drug or cell distribution within any size or shape defect. Our goal was to modify the PEG-genipin hydrogels previously described in Chapter 4. The PEG-genipin hydrogels utilized in Chapter 4 were fromed over two days. We aimed to develop a hydrogel that will gel *in situ* utilizing PEG and genipin, by decreasing the gelation time of the current hydrogel. An injectable hydrogel could be utilized to encapsulate both cells and microspheres for tissue engineering. We examined the modification of the PEG diamine-genipin hydrogels. First we examined the structure of genipin and further characterized the PEG diamine-genipin hydrogels. The gelation time was decreased by exposure of the PEG-genipin solution to air and by exposure of the genipin solution to oxygen. We then examined the effects of the structure of PEG on the gelation rate. Multi-branched PEG was examined for this study. We examined diamine PEG (previously used in Chapter 4), 4-arm PEG, a molecule with 4 PEG chains attached at a central point, and 8-arm PEG, a molecule with 8 PEG chains attached to a central molecule. By utilizing amino-terminated multi-branched PEG, the number of amine groups for the genipin to react with would increase. The gelation time was decreased by utilizing a 4-arm PEG compared to a 2-arm or 8-arm PEG. The results lead to a

further understanding of the PEG-genipin hydrogels and modifications of parameters to decrease the gelation time.

5.1.1 Genipin

As previously mentioned, genipin reacts with primary amine groups. Genipin is isolated from the fruits of *Genipa americana* and *Gardenia jasminoides Ellis*.[343] *Genipa Americana* is found in tropical America, from Mexico to Argentina and the Caribbean. *Gardenia jasminoides* is located in the Far East. Both fruits have been utilized as diuretics, anti-inflammatory medication, and to treat jaundice and hepatic diseases.[343] The fruit of *Genipa americana* has a white flesh that turns to yellow to bluish-purple then to jet-black upon exposure to air.[344] This colorimetric change is similar to what is observed with the reaction of genipin and PEG-diamine (Figure 5-1). Eight iridoid glucosides have been extracted from the fruit including, genipin, geniposidic acid, and geniposide.[344]
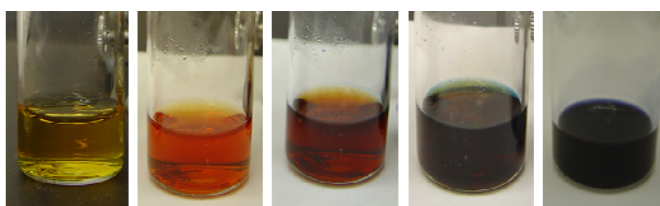
Figure 5-1. Colorimetric changes of PEG-genipin.

The use of genipin as a crosslinker is advantageous over glutaraldehyde, a commonly used crosslinker. Genipin is less cytotoxic[331, 332, 345] and genotoxic than glutaraldehyde.[331] Implantation of genipin crosslinked scaffolds has shown that they are biocompatible.[346] Materials resulted in minimal foreign body reaction[347] and less inflammation occurred in gelatin-genipin scaffolds than gelatin crosslinked with

glutaraldehyde.[348]   Genipin has been observed to have anti-inflammatory effects.[349]   To further confirm its biocompatibility, genipin crosslinked materials have been used to encapsulate cells.[347]   Similarly, cells adhere to materials crosslinked with genipin better than materials crosslinked with glutaraldehyde.[345, 350]   Due to these advantages a variety of materials crosslinked with genipin have been studied (Table 5-I).

Table 5-I. Genipin crosslinked materials.

Chitosan [235, 330, 343, 345, 347, 351-354]	Collagen [355, 356]
Albumin [343, 357]	PEG-diamine [25, 335, 358]
Gelatin [343, 346, 348, 354, 359-362]	Cartilage [363]
Pericardia [332, 350, 364, 365]	

The reaction of genipin with primary amines has been well studied. Genipin was found to only react with primary amine groups.[332] Park et al. examined the reaction of methylamine and genipin.[366] They proposed the mechanism of the reaction seen in Figure 5-2. Genipin has been observed reacting in one of two schemes (Figure 5-3).[343] Chen et al. demonstrated that genipin reacted with two chitosan molecules, thus having two functional sites.[353] However, the dimerization of genipin has also been observed.[354, 367]   The dimerization and polymerization of genipin was further confirmed when Butler et al. observed the polymerization of genipin during reaction with BSA in water.[343] The polymerization of genipin was also observed by Mi et al.[351] This study demonstrated the formation of dimers, trimers, tetramer bridges, and polymerization of genipin.
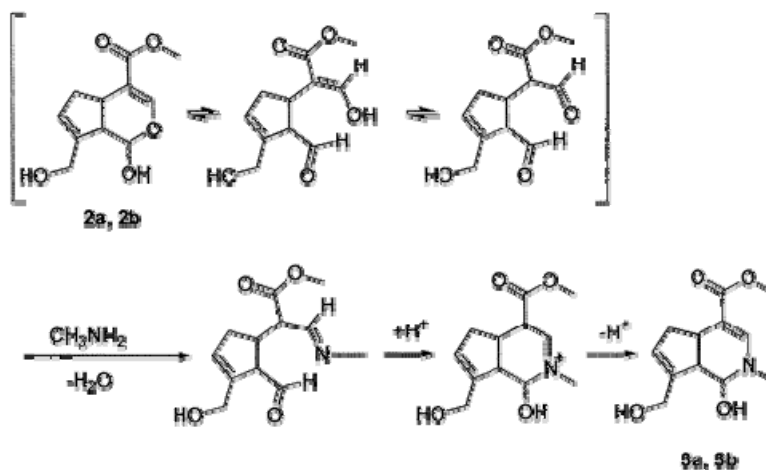
Figure 5-2. Reaction of genipin with methylamine.[366]
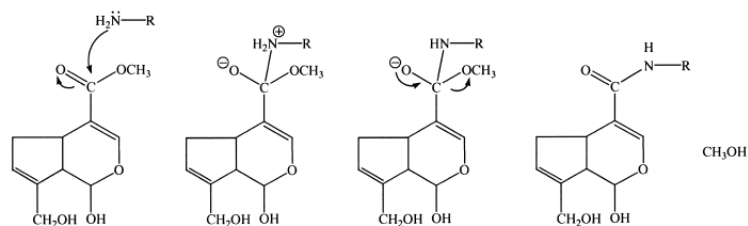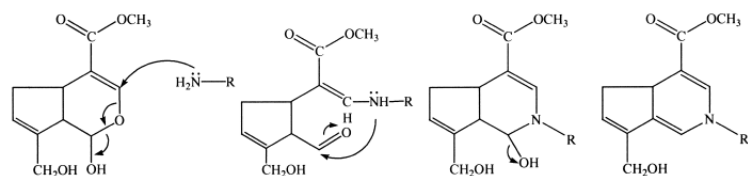
Figure 5-3. Reaction schemes of genipin with primary amine groups.[343]

Additional parameters affecting the reaction times of genipin with materials have been investigated. The main observation is that the genipin reaction occurs faster at the interface with air.[343, 344, 347] Reactions in water occurred quicker than in deuterium oxide, thus demonstrating that the reaction may require acid catalysis.[343] The reaction occurs quickest at a temperature of 37°C.[347, 352] In this study we examined some of these parameters to increase

108

the gelation rate. Specifically we examined temperature, exposure to air, exposure to oxygen, and PEG structure.

5.1.2   4-arm and 8-arm PEG

Recently, multi-branched PEG polymers have gained interest.[368-370]   The multi-branched PEGs have been used as cell scaffolds,[326] *in situ* forming hydrogels,[371, 372] adhesive medical applications,[373] and as delivery vehicles.[372, 374-378]   Examination of diamine, trisamine, and 4-arm amine PEG polymers effects on ECV 304 cells (human umbilical vein endothelial cells) demonstrated that the polymers were not cytotoxic up to a concentration of 4mg/mL.[378]

In this study, we examined the use of amine terminated 4-arm and 8-arm PEG (Figure 5-4).   By increasing the number of functional amine groups genipin can react with, we hypothesized the gelation time will decrease.
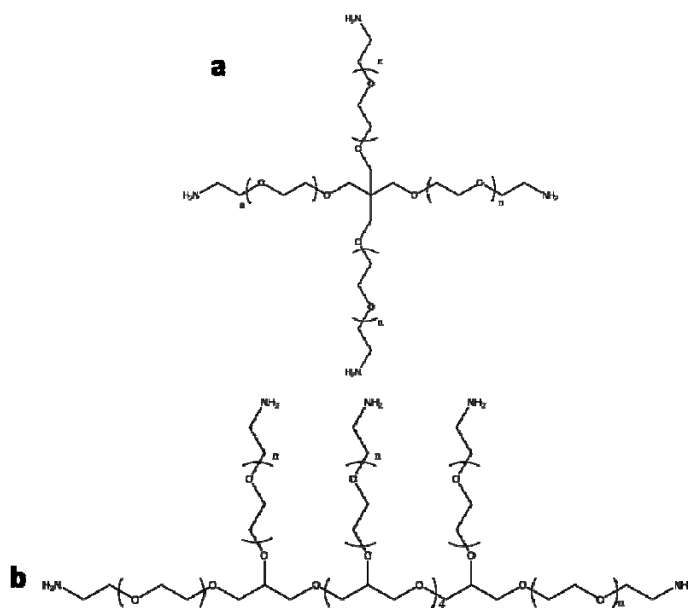
Figure 5-4. Structure of 4-arm aminated PEG (a) and 8-arm aminated PEG (b).

5.2   METHODS

5.2.1   Genipin characterization

Pure genipin was characterized as a solid. Genipin was characterized utilizing Fourier Transform infrared spectroscopy (FT-IR) and ^{1}H Nuclear Magnetic Resonance (NMR). FT-IR was performed on genipin dissolved in chloroform (in the Department of Chemistry at the University of Pittsburgh). For NMR analysis, genipin was dissolved in deuterated water (D_2O). The solution was then analyzed utilizing 300MHz spectrometer (in the NMR facility in the Department of Chemistry at the University of Pittsburgh).

5.2.2   PEG diamine-genipin characterization

We examined the PEG diamine-genipin hydrogels utilizing SEM. Hydrogels were swelled in water, frozen, and freeze-dried. The hydrogels were then gold coated using a Cressington 108 Auto (Cressington, Watford UK). Hydrogels were viewed using a JSM-6330F scanning electron microscope (JEOL, Peabody, MA) operated at 10 kV accelerating. The porosity of the PEG-genipin scaffolds was determined from the SEM images utilizing Image J Software (NIH, USA).

5.2.3 Cell adhesion to PEG diamine-genipin hydrogels

Cell adhesion to the PEG diamine hydrogels was assessed using two different cell types. Human adipose derived stem cells (ASCs) were plated at a density of 20,000 cells per well in ASC medium on PEG-genipin hydrogels, control wells (polystyrene tissue culture treated wells), and poly(caprolactone) (PCL) disks. After 5 hours, viable cells were measured using the MTS assay (Cell Titer96 Proliferation Assay, Promega Corp, Madison, WI). The attachment of bone marrow-derived mesenchymal cells (BMSCs) was also determined. BMSCs at a concentration of 10,000 cells/mL were plated on PEG-genipin hydrogels and PCL disks. After 5 hours, viable cells were determined utilizing the MTS assay.

5.2.4 Modifications to decrease gelation time

Since an *in situ* gelling hydrogel is desired, we examined possible ways to increase the gelation rate (decrease gelation time) of the PEG-diamine genipin hydrogels. Other investigators and ourselves have observed that exposure of genipin to air enhanced the reactions with amines.[343, 344, 347] PEG-genipin, yielding a final concentration of 35.2mM genipin was prepared. The solution was exposed to air to decrease the gelation time. The solution was allowed to react in a closed system (sealed vial), an open system (vial open to environment), or an open system exposed to air, by bubbling air through the solution (exposed). The PEG-genipin solutions were monitored for gelation. Gelation was initialized when the solutions became blue. Modifying the genipin solution before reaction with the PEG solution was also analyzed. The genipin solution was modified by exposure to oxygen. The genipin solution (88mM) was exposed to oxygen for 0, 10, or 30 minutes (Figure 5-5). The modified genipin solutions were

then added to PEG solutions, yielding a final concentration of 44mM. The PEG-genipin solutions were monitored for initialization of gelation.
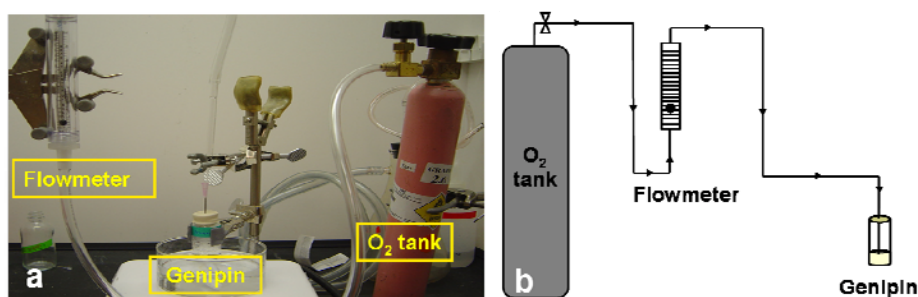
Figure 5-5. Setup for oxygenation of genipin (a), schematic of setup (b).

5.2.5   Multi-arm PEG-genipin synthesis

PEG 4-arm and PEG 8-arm (Jenkem Technology, Beijing, China) 10% (w/v) solutions were prepared. The PEG solutions were then crosslinked with 88mM genipin solutions for final concentrations of 8mM, 12mM, 15mM, 17.6mM, 25mM, and 35.2mM. The gelation times were recorded. Gelation was monitored at 25$^\text{o}$C and 37$^\text{o}$C of 4-arm PEG-genipin.

5.2.6   Multi-arm PEG-genipin hydrogel characterization

The PEG-genipin hydrogels (4-arm 35.2mM and 17.6mM, 8-arm 35.2mM and 17.6mM, and 2-arm 35.2mM) were characterized after gelation. The dissolution times were monitored. PEG-genipin hydrogel disks were punched out using a 6mm dermal biopsy punch. The disk initial weight, diameter, and height were measured. The disks were placed in 1mL PBS in microcentrifuge tubes. At each time point (1 day, 1 week, 3 weeks, 6 weeks, and 12 weeks) the wet weight, diameter, and height of the hydrogels were measured. The hydrogels were removed from the PB and then freeze-dried. The dry weight was measured and then the hydrogels were

analyzed using SEM.   The water uptake and diameter change were calculated utilizing the following equations:

$$\text{Water uptake} = 100\% \times \left(\frac{m_{twet} - m_{tdry}}{m_{tdry}} \right) \quad \textbf{Equation 5-1}$$

$$\text{Diameter change} = 100\% \times \left(\frac{d_t - d_0}{d_0} \right) \quad \textbf{Equation 5-2}$$

Where m_{twet} is the wet weight of the scaffold at time t and m_{tdry} is the dry weight of the scaffold at time t.   For the diameter change, d_t is the diameter at time t and d_o is the diameter at time 0.

5.2.7   Statistical analysis

Student's t-tests were performed when comparing two groups or two time points.   A statistical difference was determined by $p < 0.05$.

5.3   RESULTS

5.3.1   Genipin characterization

Genipin was characterized utilizing FT-IR.   The spectrum is shown in Figure 5-6.   The position and intensity of the peaks are listed in Table 5-II.   The peaks at 3400.16cm^{-1} and 3270.39cm^{-1} represent alcohol groups.   The peak at 1106.11cm^{-1} is the C-O-C stretch and 1626.10cm^{-1} the C=C stretch.   The peak at 1686.30cm^{-1} indicates the ester peak.
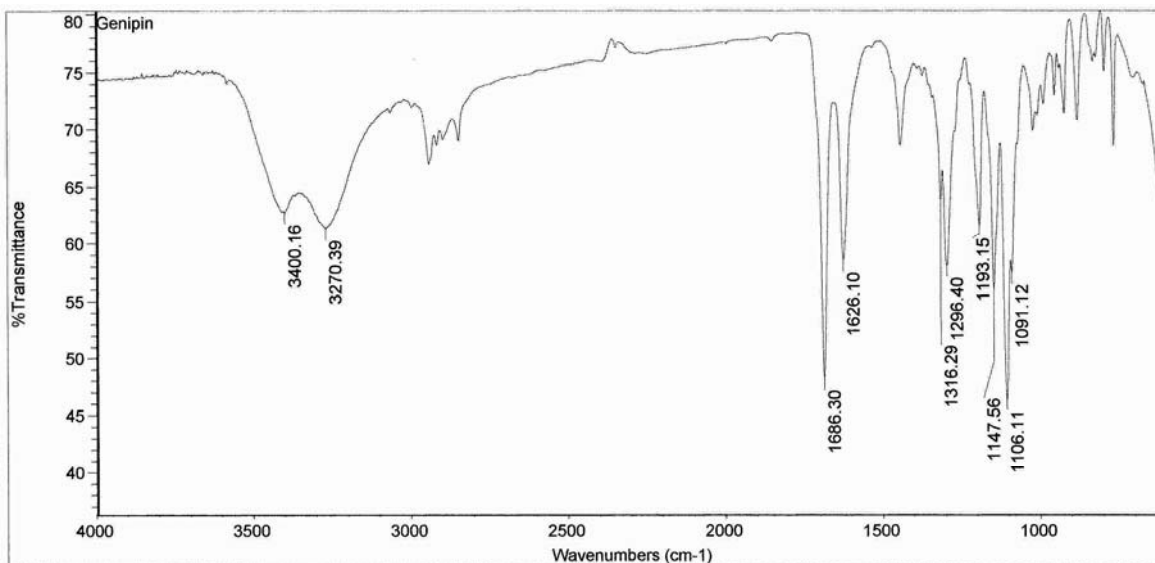
Figure 5-6. IR spectra of genipin.

Genipin was also characterized utilizing ^{1}H NMR. The resulting spectrum is shown in Figure 5-7. The chemical structure of genipin and corresponding positions are shown in Figure 5-8.
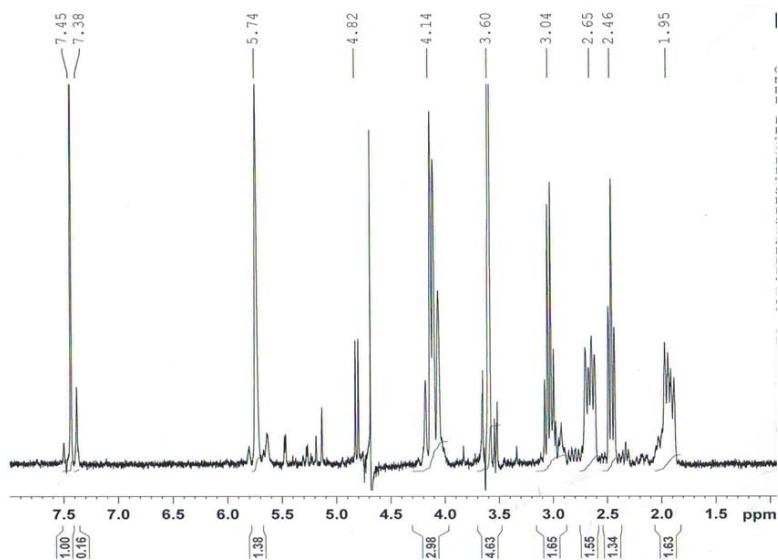
Figure 5-7. NMR spectra of genipin.
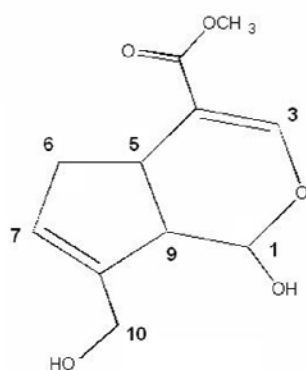
Position	¹H
1	4.82
3	7.38
5	3.04
6a	2.46
6b	1.95
7	5.74
9	2.65
10	4.14
OCH₃	3.6

Figure 5-8. ¹H NMR data of genipin.

5.3.2   PEG diamine-genipin characterization

PEG-diamine genipin scaffolds were swelled in water, frozen, and freeze-dried. The SEM images of the scaffolds demonstrate a porous scaffold (Figure 5-9). The PEG-genipin scaffolds had an average porosity of $43.67 \pm 10.36\%$ (n=5).
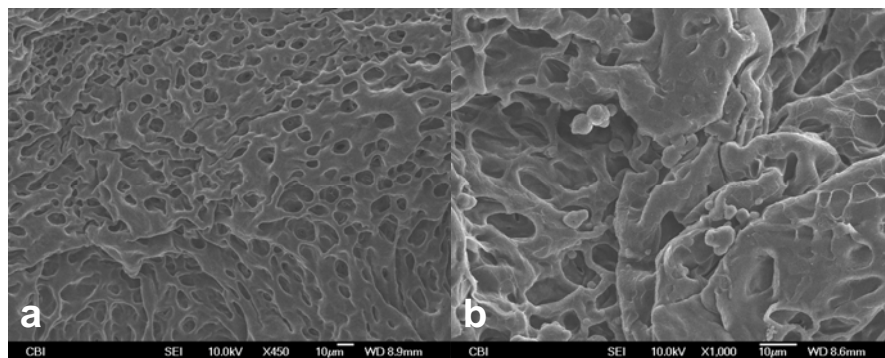
Figure 5-9. SEM of PEG diamine-genipin (a) and under higher magnification (b).

5.3.3 Cell adhesion on PEG diamine-genipin hydrogels

Previously the adhesion of smooth muscle cells to PEG-genipin gels was characterized.[25] No significant difference was seen between adhesion to the PEG-genipin hydrogels and the control wells (TCP). We observed similar results with the adhesion of human ASCs and BMSCs. There was no significant difference between the adhesion of ASCs on PEG-genipin scaffolds and the tissue-culture treated wells (Figure 5-10). However a significant difference was seen compared to PCL disks, with increased adhesion on the PEG-genipin disks. The adhesion of BMSCs resulted in a significant increase in cell adhesion on PEG-genipin scaffolds compared to the PCL disks (Figure 5-10).
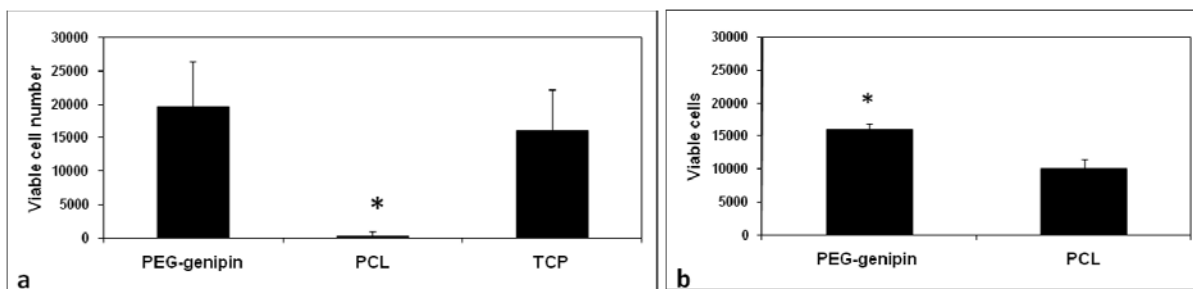
Figure 5-10. Adipose derived stem cell adhesion (a) and bone marrow stem cell adhesion (b).
*p<0.05 compared to PEG-genipin and TCP (a). *p<0.05 compared to PCL.

5.3.4 Decrease of gelation time

Exposure of the PEG diamine-genipin hydrogels to air and oxygen decreased the gelation times. During the reaction of the PEG diamine and genipin solutions, the solution will change colors, beginning as a clear solution and ending in a blue solution. The initialization of gelation was determined when the solution became dark blue. Exposure of the PEG-genipin solution to air decreased the gelation time (Figure 5-11).
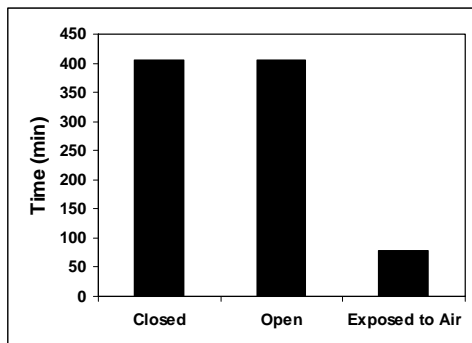
Figure 5-11. Time for initialization of gelation of PEG-genipin exposed to air.

A clinically applicable *in situ* gelling hydrogel is desired. As we observed a decrease in gelation times by exposure to air, we hypothesized that the oxygen in air was increasing the gelation rate. We wanted to decrease the gelation time by modifying the genipin solution. Therefore, we exposed the genipin solution to oxygen and then reacted the exposed genipin with PEG solutions. The gelation times of PEG-genipin hydrogels was reduced when the genipin solution was exposed to oxygen (Table 5-II). As exposure to oxygen was increased, the gelation time decreased.

Table 5-II. Initialization of gelation of PEG-genipin after oxygen exposure.

Time of treatment with Oxygen (min)	Time for solution to become blue (hr:min)
0	4:22
10	2:22
30	1:37

5.3.5   Gelation of multi-arm PEG-genipin

The gelation rate of multi-arm PEG-genipin hydrogels was monitored. Increasing the concentration of genipin decreased the gelation time. The gelation rate of the 4-arm hydrogels was quicker than the 8-arm hydrogels (Table 5-III). For both the 4-arm and 8-arm PEG, the 8mM concentration of genipin never gelled, the solution became blue, but a gel was not formed.

117

Thus, all subsequent studies were performed on the 4-arm hydrogels only. Increasing the temperature from 25°C to 37°C, led to a decrease in gelation times (Figure 5-12).

Table 5-III. Gelation times of 4-arm and 8-arm PEG at 25°C.

Genipin Concentration (mmol)	4-arm gelation time (hours)	8-arm gelation time (hours)
12	>8	>8
15	6.53 ± 0.21	>8
17.6	5.50 ± 0.87	>8
25	3.59 ± 0.58	17 ± 8.23
35.2	2.92 ± 0.63	6.52 ± 1.93
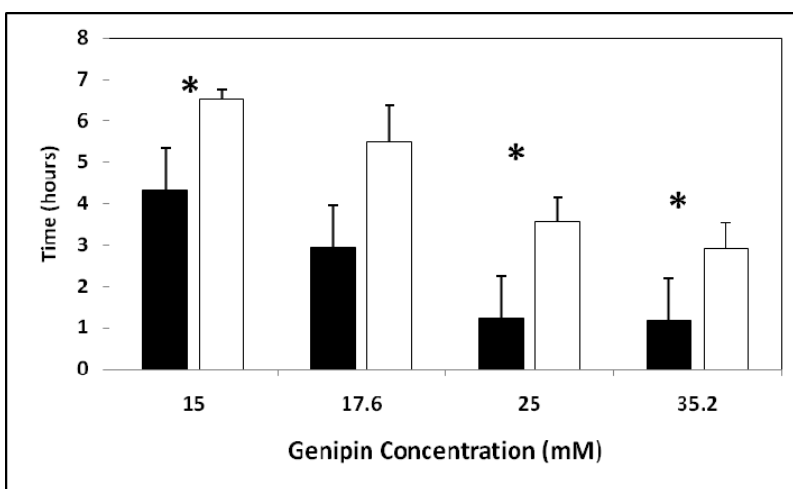
Figure 5-12. Gelation times of 4-arm PEG at 37°C (■) and 25°C(□). All values reported as means ± standard deviations (n=3). *p<0.05.

5.3.6   Characterization of multi-arm PEG-genipin hydrogels

The dissolution of the scaffolds was determined by examination at various times. At time point 1 week, the 8-arm 17.6mM scaffolds were not able to be weighed because they had begun dissolution. At this point, the scaffolds were a viscous liquid, and not a gel. At 12 weeks, the 8-arm 17.6mM scaffolds were the only scaffold samples to have degraded.

The water uptake of the hydrogels was calculated utilizing equation 5-1. The water uptake was dependent on the structure of the PEG (Table 5-IV). The water uptake within the 4-

arm PEG on the first day was significantly higher than the 2-arm or 8-arm PEG. At one week and 12 weeks, the water uptake was higher in the 4-arm PEG than 8-arm PEG hydrogels. For weeks 3 and 6, both the 2-arm and 4-arm PEG hydrogels demonstrated a significant increase in water uptake compared to the 8-arm PEG hydrogels.

Table 5-IV. Water uptake of hydrogels.

Water uptake	1 day	1 week	3 weeks	6 weeks	12 weeks
2-arm 35.2mM	686.78 ± 70.98	809.97 ± 61.66	839.84 ± 88.36*	885.30 ± 100.58*	841.16 ± 143.47
4-arm 35.2mM	1808.94 ± 174.11**	1094.43 ± 137.63*	851.57 ± 10.56*	875.89 ± 106.46*	993.20 ± 83.21*
8-arm 35.2mM	710.41 ± 234.81	710.41 ± 58.52	605.14 ± 23.78	607.95 ± 67.81	607.70 ± 69.42

**p < 0.05 compared to 2-arm and 8-arm PEG.
*p< 0.05 compared to 8-arm PEG.

The water uptake was also dependent upon the genipin concentration. A lower genipin concentration (17.6mM) resulted in an increased water uptake at all times point past one day (Table 5-V). Since the 17.6mM hydrogels are less crosslinked, the water uptake should be higher.

Table 5-V. Effects of genipin concentration on water uptake.

Water uptake	1 day	1 week	3 week	6 weeks	12 weeks
4-arm 35.2mM	1808.94 ± 174.11	1094.43 ± 137.63*	851.57 ± 10.56*	875.89 ± 106.46*	993.20 ± 83.21*
4-arm 17.6mM	1715.63 ± 420.69	1877.08 ± 174.47	1742.62 ± 79.33	1971.74 ± 347.56	1987.42 ± 51.02

*p<0.05 between 35.2mM and 17.6mM genipin concentration

The swelling ratio of the hydrogels was examined. The diameter change was calculated by equation 5-2. No significant differences were observed between the 8-arm and 4-arm 35.2mM hydrogels(Figure 5-13). The diameter change of the 4-arm 17.6mM and 2-arm 35.2mM could not be compared to the 35.2mM 4-arm and 8-arm because the scaffolds were partially dehydrated and thus swelled in one direction (diameter) instead of all directions (Figure 5-14).
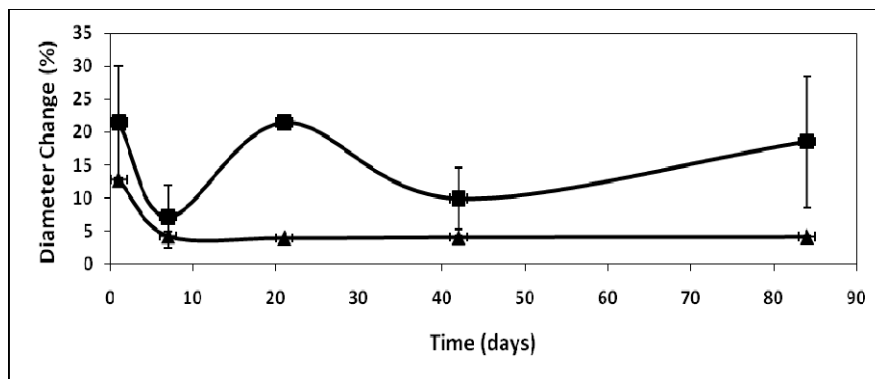
Figure 5-13. Diameter change of PEG-genipin hydrogels.
Diameter change of 35.2mM 4-arm PEG hydrogel (-■-) and 35.2mM 8-arm PEG hydrogel (-▲-). All values reported as means ± standard deviations (n=3).
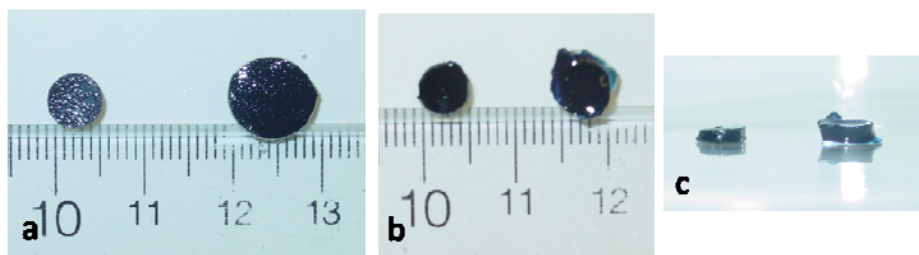
Figure 5-14. Swelling of PEG-genipin scaffolds.
2-arm 35.2mM hydrogel before and after immersion in water (a). 4-arm 35.2mM hydrogel before and after immersion in water (b) and (c).

5.4   DISCUSSION

An injectable hydrogel is clinically desired as the system could result in minimally invasive surgeries. Hydrogels that gel *in situ* could fill a defect of any size or shape. The hydrogel can be utilized for cell delivery, as well as growth factor or drug delivery. In this chapter we examined methods to modify PEG-genipin hydrogels to decrease the gelation time, thus increasing the gelation rate.

120

The structure of pure genipin was first examined by ^{1}H NMR and FT-IR. Utilizing these methods we gained a further understanding of the crosslinking mechanism of genipin with aminated PEG. Of particular interest was the fact that hydrogels were formed with the reaction of genipin with PEG diamine. For this to occur, genipin must have three functional groups or react with itself to form three functional groups to react with PEG diamine. A similar observation was seen by Lee et al. Their study examined the gelation of 4-arm PEG amine, linear 2-arm PEG diamine, and methoxy-PEG-amine with 3,4-dihydroxyphenylalanine (DOPA).[373] All of the formulations formed gels except for the methoxy-PEG-amine, thus the authors state that DOPA must react with itself to combine at least three residues to form a gel with the bis-amine PEG. The dimerization of genipin has been observed by many groups.[343, 351, 354, 367, 379] Also of importance, the polymerization of genipin was observed by Mi et al. and Butler et al., demonstrating that genipin can form trimers and tetramer bridges to react with multiple amine groups.[343, 351]

We observed that the reaction of PEG diamine was quicker at the interface of the gel and the air. This has also been noted by others.[343, 344, 347] We were able to decrease gelation time by exposing the PEG-genipin solution to air. We then examined the modification of genipin by exposure to oxygen, and the gelation time was decreased. The reaction of genipin with amine groups and the formation of dimers and polymerization has been observed to be oxygen radical-induced.[343, 345, 351, 367] This may explain why the exposure to oxygen decreased gelation time.

Our hypothesis was that the 8-arm PEG would react quicker with the genipin than the 4-arm PEG, resulting in a faster gelation rate. However, the opposite was observed. There are two possible explanations for this phenomenon. First, by examining the reaction of genipin with

different molecules, Mi et al. observed that the reaction with gelatin was slower than chitosan, as chitosan has more available reaction sites (i.e., amino functionalities).[354] However, when Butler et al. examined the gelation of genipin with chitosan, BSA, and gelatin, their study demonstrated that the structure of the molecule reacting with genipin was more important than the number of primary amines.[343] In our study, the gelation rate was quicker with 4-arm PEG than the 8-arm PEG. This is most likely due to the structure of the 8-arm PEG. This leads to the examination of 8-arm PEG. Similar to our study, Lee et al. observed that the gelation of 4-arm PEG amine and DOPA was quicker than the linear bis-amine PEG and DOPA.[373] We also reported a decrease in gelation time of the 4-arm PEG compared to the 8-arm PEG and 2-arm PEG with genipin. Lin et al. examined the properties of copolymers of PEG and poly(N-isopropylacrylamide) (PNIPAAM). As the number of arms increased from one to two to four, the strength and deformability increased; however, the mechanical properties decreased when 8-arm structures were examined.[380] They explain this phenomenon due to intramolecular aggregation which prevented crosslinking of the chains. In another study, Dai et al. analyzed the interaction between sodium dodecyl sulfate (SDS) and different PEG structures. The structures of two, three, four, and eight arm PEG were examined. They examined the saturation concentration of all of the PEG structures and saw similar values for the two, three, and four arm PEG, but a much lower value for the 8-arm PEG. They also explain this phenomenon on the structure. The 8-arm PEG has a more compact structure and thus gives rise to a smaller binding capacity. In our study, we observed a much slower reaction with the 8-arm PEG than the 4-arm PEG. We also believe this to be due to the structure of PEG and the ability of genipin to react with the amine groups.

5.5   CONCLUSIONS

We examined the modification of experimental parameters of PEG-genipin reaction in an attempt to decrease gelation time. We characterized the PEG diamine-genipin hydrogels. Adult stem cells adhere to the hydrogels, thus they may provide an alternative to current cell scaffolds. However, an *in situ* gelling hydrogel is clinically desired and may have immense impacts in the area of tissue engineering. We have examined the use of natural and synthetic scaffolds (gelatin and PEG-genipin), neither of which is an injectable hydrogel. Therefore, we analyzed methods to reduce the gelation time of the current PEG-genipin scaffolds. We demonstrated a decrease in gelation time by exposure of PEG-genipin solution to air, as well as a decrease due to exposure of genipin to oxygen. We then examined the use of multi-branched PEG. A decrease in gelation time was observed in both the 4-arm and 8-arm PEG compared to the linear (2-arm) PEG. However, the gelation time was most reduced by use of the 4-arm PEG. The gelation occurred more quickly by increasing the temperature from 25$^{\text{o}}$C to 37$^{\text{o}}$C. Important, initial steps to decrease the gelation time were demonstrated in this study.

5.6   FUTURE DIRECTIONS

We have demonstrated methods to decrease the gelation time of PEG-genipin scaffolds. We examined the use of 4-arm and 8-arm PEG.   Our results revealed that the structure of PEG was an important factor in gelation time. By examining other PEG structures, such as 3-arm and 6-arm PEG, these can be further explored. We also demonstrated a decrease in gelation time of the PEG diamine-genipin by exposing the genipin to oxygen. A similar experiment may

be performed with the multi-branched PEG. A further understanding of the genipin modification occurring during exposure to air and oxygen is required as well as the reaction with aminated PEG. Finally, solid state NMR could be performed on the scaffolds to further analyze this reaction.

6.0   OVERALL CONCLUSIONS

Delivery systems have been investigated to control the delivery of proteins or drugs. Delivery systems can provide protection of the drug, maintain desired levels of the drug, prolong the release, localize delivery, and decrease adverse side effects. The overall goal of this thesis was to examine PLGA microspheres as delivery systems in tissue engineering applications. We have created novel delivery systems for each of the applications.

The study presented in Chapter 2 demonstrated the use of PLGA microspheres as an injectable delivery system to create and maintain the desired microenvironment *in vivo*. We demonstrated that FGF-2 released from PLGA microspheres could induce ASC proliferation and increase survival *in vitro*. The results of a 14 day *in vitro* study in the absence of serum confirmed that delivery of FGF-2 from microspheres was superior to a repeated bolus of free FGF-2. Based on these findings, we examined the effects of FGF-2 microspheres on ASC survival *in vivo*. Although no difference was observed on cell survival after two weeks, a difference was observed in the angiogenesis of the surrounding area. The number of blood vessels present was significantly increased in the mice treated with FGF-2 microspheres. Angiogenesis provides nutrients and waste removal, and thus is an important factor in cell and tissue survival *in vivo*. After two weeks, no adipogenesis was seen in any of the groups.

Since we did not observe mature adipocytes derived from our injected ASCs, we investigated the delivery of adipogenic factors to induce differentiation. Insulin and

dexamethasone were encapsulated in PLGA microspheres. The adipogenesis of ASCs was induced by replacing dex and insulin in media with the corresponding PLGA microspheres. Adipogenesis was confirmed by oil red O staining and expression of PPAR-γ.

The results of this study have implications for new clinical therapies in soft tissue reconstruction. An injectable engineered soft tissue replacement can be used to reconstruct a defect. The success of this replacement would depend on successful vascularization and differentiation of the stem cells. Including FGF-2 microspheres with the cells and scaffold mixture would not only enhance survival of the implanted cells, but could decrease the time required for successful vascularization and accelerate the treatment process. These injections could be followed by dex and insulin microspheres to enhance adipogenesis of the cells.

Chapter 3 presents a study in which a novel delivery system to locally deliver a chemotherapeutic agent as well as maintain the contour of the breast following a lumpectomy was developed. In this chapter we examined a delivery system in which PLGA microspheres were embedded within a gelatin scaffold. The gelatin scaffold was utilized to further control the release of the chemotherapeutic agent as well as provide structure to the defect. The delivery system was utilized to maintain local levels of the drug that have adverse side effects when delivered systemically. The release was further controlled by the incorporation of PLGA microspheres into gelatin constructs. The efficacy of released doxorubicin from the microspheres and the gelatin scaffolds to kill tumor cells was demonstrated *in vitro*.

The delivery system we developed was successful *in vitro*, thus *in vivo* studies were subsequently performed. The animal model utilized simulated a lumpectomy; at the time of inoculation of tumor in the mammary fat pad, the mice were treated with gelatin scaffolds. Implantation of the 2Dox scaffold resulted in tumor eradication. No adverse reactions were

observed in the mice due to treatment with the 2Dox scaffolds even though a large dose of dox was delivered.

The results of Chapter 3 demonstrate a potential alternative adjuvant treatment for breast cancer patients following a lumpectomy. A scaffold that promotes tissue ingrowth and temporarily maintains breast contour can be utilized as the delivery system. Dox-loaded PLGA microspheres embedded within the scaffold locally release Dox to kill any remaining tumor cells. An implantable chemotherapy delivery system can possibly reduce the local recurrence rate following surgery. An unmet need to improve the current therapy for not only breast cancer but other malignancies as well exists. We have developed a novel delivery system by embedding synthetic polymer microspheres within a natural hydrogel at the time of fabrication that may lead to improvement of these current therapies.

The next study presented in Chapter 4 described the development of a delivery system incorporating PLGA microspheres within in a novel synthetic hydrogel. Biodegradable PEG-based hydrogels containing TGF-β1-loaded PLGA microspheres were developed with potential utility in cartilage tissue engineering. The release of TGF-β1 was further controlled when the microspheres were incorporated in the hydrogel compared to microspheres alone. The results indicate that the release can be further modified by changing the genipin concentration of the PEG-genipin hydrogels. The bioactivity of the released TGF-β1 was confirmed utilizing a mink lung inhibition assay.

The development of this delivery system permits a scaffold to be placed in the cartilage defect and containment of the microspheres within the hydrogel. The concentration of released TGF-β1 can be determined by the amount of microspheres and genipin concentration of the

hydrogels. This is important because use of this delivery system *in vivo* can be utilized to determine the effects of released TGF-β1 in cartilage repair.

The final study presented in Chapter 5 focused on developing a hydrogel that could gel *in situ*. The clinical applications of this are of immense importance. Defects in soft tissue or cartilage tissue are not of uniform shape, thus a hydrogel that can fill in any size and shape defect is highly desired. We demonstrated that the gelation time of PEG-genipin scaffolds can be reduced by modification of the parameters involved. Exposure of the PEG-genipin solution to air and the genipin solution to oxygen before the reaction occurred decreased the gelation time. The PEG structure also affected the gelation time. The 4-arm PEG gelled most rapidly compared to 2-arm and 8-arm PEG. Finally, the reaction occurred quicker at 37°C compared to 25°C. These steps demonstrated modification of the parameters can decrease the gelation time.   These results also reveal insights into the reaction between genipin and PEG, gaining a further understanding of the mechanism.

APPENDIX A

ADIPOSE DERIVED STEM CELL PLASTICITY

The plascity of ASCs has been examined by many investigators. As mentioned in Chapter 2, the plasticity of ASCs into all three lineages has been demonstrated. The following tables outline the differentiation of ASCs and their references cited. These tables correspond to Figure 2-1.

Appendix Table I. ASC differentiation into endodermal lineage

In Vitro	*In Vivo*
Hepatocytes [381, 382]	Hepatocytes [382]
Epithelial Cells [383]	
Pancreatic Islets [384]	

Appendix Table II. ASC differentiation into mesenchymal lineage.

In Vitro	*In Vivo*
Adipocytes [1, 2]	Adipocytes [184, 385]
Endothelial Cells [3, 4]	Endothelial Cells [3, 4]
Muscle Cells [1, 2, 386]	Muscle Cells [387]
Osteoblasts [1, 2, 107]	Osteoblasts [388, 389]
Chondrocytes [1, 2, 93, 390]	Chondrocytes [42, 101, 389, 390]
Bone Marrow Cells [391]	Bone Marrow Cells [391]
Cardiomyocytes [392-394]	Cardiomyocytes [395-397]
Smooth Muscle Cells	

Appendix Table III. ASC differentiation into ectodermal lineage.

In Vitro	*In Vivo*
Neuronal [2, 398-400]	Neuronal [401]

APPENDIX B

CISPLATIN ENCAPSULATION

B.1   INTRODUCTION

We have demonstrated the release of doxorubicin from PLGA microspheres. Other chemotherapeutic agents can be encapsulated in a similar manner to be embedded within the gelatin scaffolds. Cisplatin is a platinum based chemotherapeutic drug (App Figure 1). As previously mentioned, chemotherapeutics have adverse side reactions that may be overcome by local controlled delivery. Cisplatin has been delivered from PEG hydrogels,[402] polymer microspheres,[403-408] PLA,[409] and gelatin.[228]
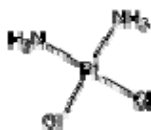
Appendix figure 1. Structure of cisplatin

B.2   METHODS

Cisplatin was encapsulated in PLGA (75:25) microspheres utilizing a modified protocol.[406] Briefly, 500mg PLGA was dissolved in methylene chloride. Cisplatin (15mL of 1mg/mL cisplatin) was added to the dissolved polymer. This emulsion was then added to the aqueous phase (0.15 w/v% PVA and 0.05 w/v% methyl cellulose in distilled water) which was saturated with 30mg of cisplatin. The mixture was then stirred for 4 hours at 500rpm. The microspheres were collected by centrifugation, washed with DI water, frozen, and lyophilized. The microspheres were examined morphologically by SEM. The images were also used to determine the diameter distribution of the microspheres.

Cisplatin microspheres were placed in microcentrifuge tubes with 1mL of PBS and incubated at 37°C. At various time points the tubes were centrifuged, the supernatant removed, and analyzed for released cisplatin. The tubes were refreshed with PBS. The released cisplatin was measured by reacting with sodium diethyldithiocarbamate (NaDDTC) solution (1mol NaDDTC to 10mol cisplatin) with the samples. The pH was adjusted to 8.0 and the samples were stirred for 24 hours. The precipitate was vacuum-dried and then dissolved in 1mL MC. The absorbance of the resulting solution was measured on a spectrophotometer at 347nm.

B.3   RESULTS AND DISCUSSION

Cisplatin was encapsulated in PLGA microspheres. The microspheres exhibited a round smooth morphology (Appendix Figure 2). The average diameter of the microspheres was 115.5μm, with the diameter distribution as seen in Appendix Figure 3.
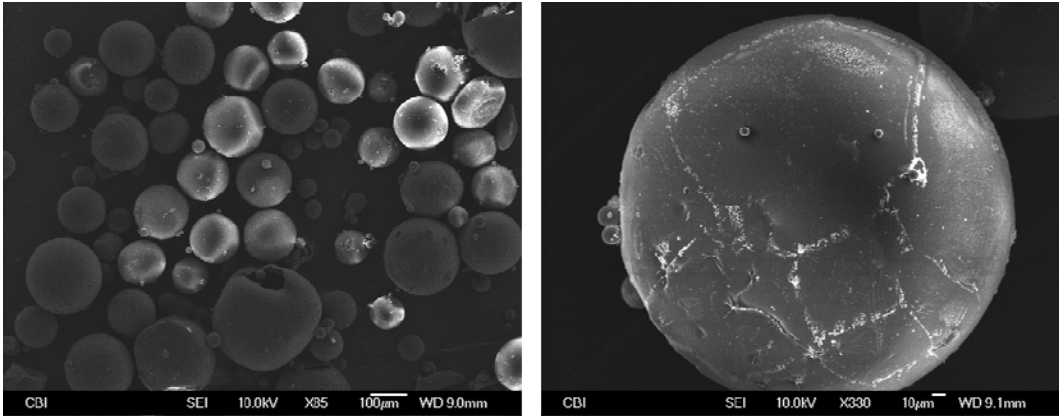
Appendix figure 2. SEM of cisplatin-loaded PLGA microspheres.
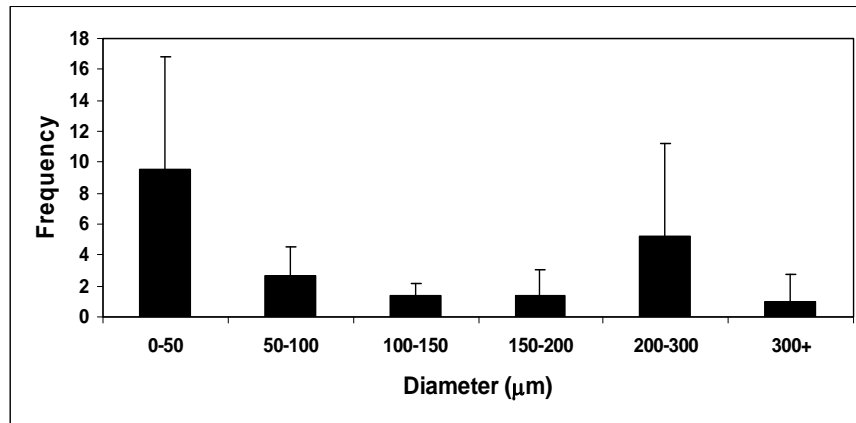
Appendix figure 3. Diameter distribution of cisplatin-loaded microspheres.

The method to analyze the released cisplatin had its limitations. Thus the release could only be detected up to day 17 (App Figure 4). Since this method is not sensitive enough to determine low amounts, caution should be taken to rely on these results. Another method should be utilized to determine the release. Reliable results utilizing atomic absorption spectrophotometry, which detects platinum, have been observed.[228, 410, 411] This could be a possible method to detect the release cisplatin. Another method is measuring the cisplatin utilizing colorimetric oPDA method as described in articles from Gemeinhart's lab.[402, 403]
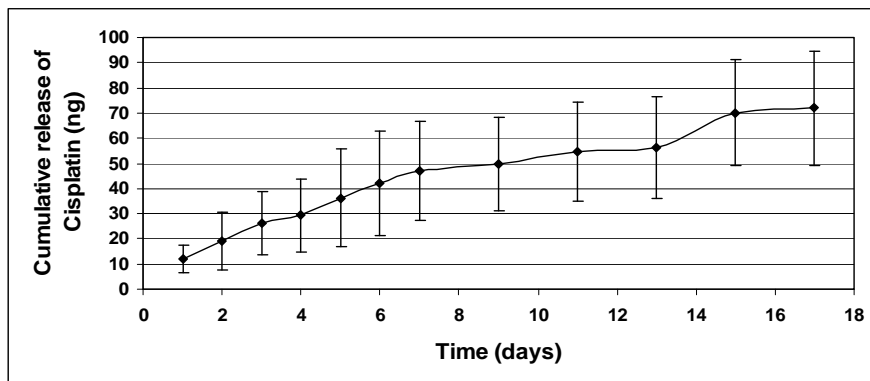
Appendix figure 4. Cumulative release of cisplatin.
All results reported as means ± standard deviations. (n=3)

We encapsulated cisplatin in PLGA microspheres. We were unable to successfully determine the release kinetics. However, other methods to detect released cisplatin have been suggested. Once the release kinetics have been determined, cell studies similar to those in Chapter 3 should be performed to assess the effectiveness to kill tumor cells. Then the efficacy of the gelatin scaffolds loaded with both doxorubicin and cisplatin microspheres to ablate tumors *in vitro* and *in vivo* should be assessed.

IN VIVO DISSOLUTION OF PEG-GENIPIN HYDROGELS WITHIN OSTEOCHONDRAL DEFECTS

C.1   INTRODUCTION

PEG hydrogels show promise as scaffolds for growth factor delivery to enhance cartilage repair.   We have demonstrated that we can control the release of TGF-β1 from PLGA microspheres by incorporating microspheres in PEG-genipin hydrogels and further alter these kinetics by changing the crosslinker concentration (Chapter 4).   However, the *in vivo* behavior and dissolution of PEG-genipin hydrogels within the osteochondral defect was unknown. Therefore, we conducted the *in vivo* study described below.

C.2   METHODS

PEG-genipin hydrogels were prepared as described previously (Section 4.2.1).   PEG solutions were crosslinked with genipin to yield final concentrations of 8mM, 17.6mM, and

35.2mM genipin. Once the solutions turned blue, the solutions were pipeted into Teflon molds with a diameter of 1mm and 1mm in height (Figure C1).

1mm

1mm
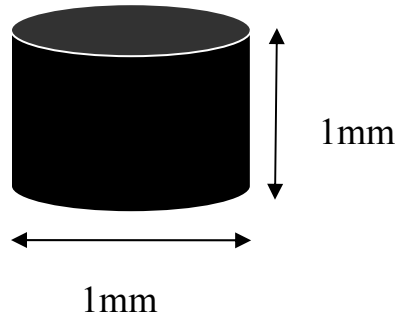
Appendix figure 5. Diagram of PEG-genipin plug.

Twenty-four male Sprague-Dawley (Harlan Laboratories, 12 weeks old) rats were anesthetized with 50 mg/kg of Nembutal (Abbott Laboratories, North Chicago, IL, USA). Lateral parapatelar incisions were performed. The patella was dislocated to the medial sides and the trochlea was exposed. A defect of 1.5 mm^2 was created bilaterally in the trochlea by drilling. The rats were divided into three different groups. In the first group, the defect of the right knee was filled with the 8mM polymer and the defect of the left knee was filled with 35.2 mM (n=8). In the second group, the right knee defect was filled by 8mM polymer and the left knee filled with 17.6 mM (n=8). The third group was 17.6 mM polymer in the defect of the right knee and 35.2 mM in the defect of the left knee (n=8). It is important to note that the PEG-genipin polymer was 1mm in diameter and the trochlear defect was 1.5 mm in diameter. Upon contact of the hydrogel with blood or saline solution, the polymer swelled and fully filled the trochlear defect (Appendix Figure 6). This is an important characteristic of this hydrogel that facilitates the surgical procedure during the implantation of the polymer in the osteochondral defect. The rats were sacrificed after 5 weeks and the distal femurs were harvested and fixed.

Appendix figure 6. PEG-genipin in osteochondral defect initially.

C.3   RESULTS AND DISCUSSION

The dissolution of PEG-genipin scaffolds was inversely related to genipin concentration. The lowest concentration (8mM) had a faster dissolution rate with most of the polymer fully dissolved (10 out of 16), the remaining knees showed a slight presence of the polymer (6 out of 10). Intermediate dissolution was observed in the 17.6mM group compared to the other two groups. All of the polymers in the 17.6mM group had partially dissolved. However, none of the knees presented total dissolution of the polymer. The highest concentration (35.2mM) offered the slowest dissolution at 5 weeks (Appendix Figure 7).
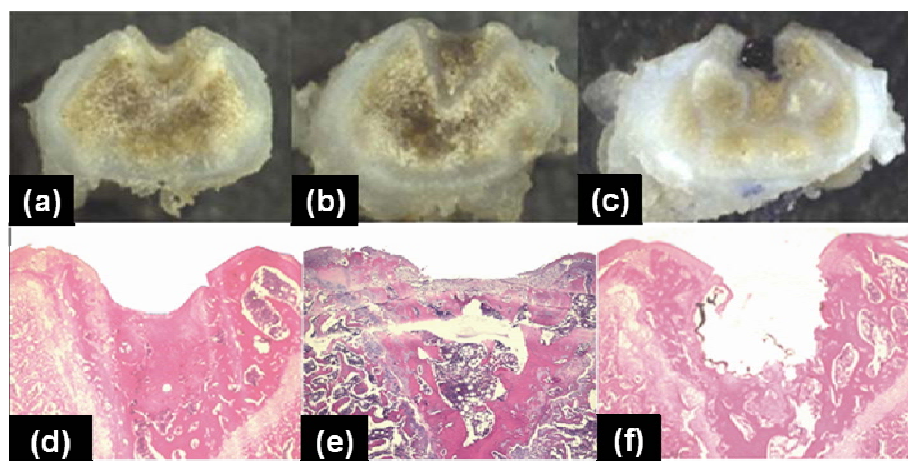
Appendix figure 7. Gross observation and histology of the knees.
Gross observation of the knee with 8mM PEG-genipin (a), 17.6mM PEG-genipin (b), and 35.2mM PEG-genipin (c). Histology of the knee with 8mM PEG-genipin degraded and almost fully filled (d), 17.6mM PEG-genipin showing partial dissolution and partial repair (e), and 35.2mM PEG-genipin still present with no filling of the defect (f).

The 8mM and 17.6mM PEG-genipin groups demonstrated repair of the osteochondral defect in the trochlea. However, the 35.2mM group did not show cartilage repair due to the lack of complete dissolution of the scaffold. All 48 knees were compatible with PEG-genipin. No inflammatory reaction was seen, no synovitis was observed during the harvesting, and all the animals were able to walk properly in the first post-operative day.

The 8mM group, with a faster dissolution rate, achieved a larger area of the defect filled with repair tissue. The 17.6mM group presented either areas filled with the repair tissue or areas with the residual polymer. The 35.2mM group presented a small area of dissolved polymer, with the dissolution occurring in the outermost part of the polymer. The 17.6mM provided superior extracellular matrix and a larger number of chondrocyte-like cells. These results demonstrate that the histological cartilage repair is also genipin concentration-dependent.

In conclusion, this is the first study to show PEG-genipin as a concentration-dependent polymer *in vivo*, also its viability for intra-articular use for osteochondral defect therapy. Further studies are needed in order to enhance cartilage quality utilizing the PEG-genipin hydrogel.

Nonetheless, PEG-genipin shows to be a promising polymer to be used in cartilage tissue engineering. An optimal polymer would be an injectable polymer that would gel *in situ*. As mentioned in Chapter 5, we are working towards this goal.

BIBLIOGRAPHY

1.   Zuk, P.A., et al., *Multilineage cells from human adipose tissue: implications for cell-based therapies.* Tissue Engineering, 2001. **7**(2): p. 211-228.

2.   Zuk, P.A., et al., *Human adipose tissue is a source of multipotent stem cells.* Mol Biol Cell, 2002. **13**(12): p. 4279-4295.

3.   Miranville, A., et al., *Improvement of postnatal neovascularization by human adipose tissue-derived stem cells.* Circulation, 2004. **110**(3): p. 349-355.

4.   Planat-Benard, V., et al., *Plasticity of human adipose lineage cells toward endothelial cells: physiological and therapeutic perspectives.* Circulation, 2004. **109**(5): p. 656-663.

5.   Sinha, V.R. and A. Trehan, *Biodegradable microspheres for protein delivery.* J Control Release, 2003. **90**: p. 261-280.

6.   *Handbook of pharmaceutical controlled release technology*, ed. D.L. Wise. 2000, New York: Marcel Dekker.

7.   Drury, J.L. and D.J. Mooney, *Hydrogels for tissue engineering: scaffold design variables and applications.* Biomaterials, 2003. **2003**(24).

8.   Korbelar, P., J. Vacik, and I. Dylevasky, *Experimental implantation of hydrogel into the bone.* J Biomed Mater Res, 1998. **22**(9): p. 751-762.

9.   Winn, S.R., H. Uludag, and J.O. Hollinger, *Sustained release emphasizing recombinant human bone morphogenetic protein-2.* Adv Drug Deliv Rev, 1998. **31**: p. 303-318.

10.   Shin, H., et al., *In vivo bone and soft tissue response to injectable, biodegradable oligo(poly(ethylene glycol) fumarate) hydrogels.* Biomaterials, 2003. **24**(19): p. 3201-3211.

11.   Al Ruhaimi, K.A., *Bone graft substitutes: a comparative qualitative histologic review of current osteoconductive grafting materials.* Int J Oral Maxillofac Implants, 2001. **16**(1): p. 105-114.

12.	Bryant, S.J. and K.S. Anseth, *The effects of scaffold thickness on tissue engineered cartilage in photocrosslinked poly(ethylene oxide) hydrogels.* Biomaterials, 2001. **22**(6): p. 619-626.

13.	Bryant, S.J. and K.S. Anseth, *Controlling the spatial distribution of ECM components in degradable PEG hydrogels for tissue engineering cartilage.* J Biomed Mater Res A, 2003. **64**(1): p. 70-79.

14.	Elisseeff, J., et al., *Photoencapsulation of chondrocytes in poly(ethylene oxide)-based semi-interpenetrating networks.* J Biomed Mater Res, 2000. **51**(2): p. 164-171.

15.	Sawhney, A.S., C.P. Pathak, and J.A. Hubbell, *Bioerodible hydrogels based on photopolymerized poly(ethylene glycol)-co-poly(a hydroxy acid) diacrylate macromers.* Macromolecules, 1993. **26**: p. 581-587.

16.	Behravesh, E., V.I. Sikavitsas, and A.G. Mikos, *Quantification of ligand surface concentration of bulk-modified biomimetic hydrogels.* Biomaterials, 2003. **24**: p. 4365-4374.

17.	van de Wetering, P., et al., *Poly(ethylene glycol) hydrogels formed by conjugate addition with controllable swelling, degradation, and release of pharmaceutically active proteins.* J Control Release, 2005. **102**(3): p. 619-627.

18.	Elisseeff, J., et al., *Controlled-release of IGF-I and TGF-beta1 in a photopolymerizing hydrogel for cartilage tissue engineering.* J Orthop Res, 2001. **19**(6): p. 1098-1104.

19.	Bhattarai, N., et al., *PEG-grafted chitosan as an injectable thermosensitive hydrogel for sustained protein release.* J Control Release, 2005. **103**: p. 609-624.

20.	Holland, T.A., Y. Tabata, and A.G. Mikos, *In vitro release of transforming growth factor-beta 1 from gelatin microparticles encapsulated in biodegradable, injectable oligo(poly(ethylene glycol) fumarate) hydrogels.* J Control Release, 2003. **91**(3): p. 299-313.

21.	Holland, T.A., et al., *Transforming growth factor-beta 1 release from oligo(poly(ethylene glycol) fumarate) hydrogels in conditions that model the cartilage wound healing environment.* J Control Release, 2004. **94**(1): p. 101-114.

22.	Holland, T.A., Y. Tabata, and A.G. Mikos, *Dual growth factor delivery from degradable oligo(poly(ethylene glycol) fumarate) hydrogel scaffolds for cartilage tissue engineering.* J Control Release, 2005. **101**(1-3): p. 111-125.

23.	Watanabe, J., et al., *Fibroblast adhesion and proliferation on poly(ethylene glycol) hydrogels crosslinked by hydrolyzable polytaxane.* Biomaterials, 2002. **23**: p. 4041-4048.

24. Lee, W.K., et al., *Novel poly(ethylene glycol) scaffolds crosslinked by hydrolyzable polyrotaxane for cartilage tissue engineering.* J Biomed Mater Res, 2003. **67A**: p. 1087-1092.

25. Moffat, K.L. and K.G. Marra, *Biodegradable poly(ethylene glycol) hydrogels crosslinked with genipin for tissue engineering applications.* J Biomed Mater Res B Appl Biomater, 2004. **71**(1): p. 181-187.

26. Huang, M.-H., et al., *Degradation and cell culture studies on block copolymers prepared by ring opening polymerization of caprolactone in the presence of poly(ethylene glycol).* J Biomed Mater Res, 2004. **69A**: p. 417-427.

27. Yeh, J., et al., *Micromolding of shape-controlled, harvestable cell-laden hydrogels.* Biomaterials, 2006. **27**: p. 5391-5398.

28. Martens, P.J., J. Bryant, and K.S. Anseth, *Tailoring the Degradation of Hydrogels Formed from Multivinyl Poly(ethylene glycol) and Poly(vinyl alcohol) Macromers for Cartilage Tissue Engineering.* Biomacromolecules, 2003. **4**: p. 283-292.

29. Ghaderi, R., C. Sturesson, and J. Carlfors, *Effect of preparative parameters on the characteristics of poly(D,L-lactide-co-glycolide) microspheres made by the double emulsion method.* Int J Pharm, 1996. **141**: p. 205-216.

30. Mehta, R.C., B.C. Thanoo, and P.P. DeLuca, *Peptide containing microspheres from low molecular weight and hydrophilic poly(D,L-lactide-co-glycolide).* J Control Release, 1996. **41**: p. 249-257.

31. Freytag, T., et al., *Improvement of the encapsulation efficiency of oligonucleotide-containing biodegradable microspheres.* J Control Release, 2000. **69**: p. 197-207.

32. Yang, Y.Y., T.-S. Chung, and N. Ping Ng, *Morphology, drug distribution, and in vitro release profiles of biodegradable polymeric microspheres containing protein fabricated by double-emulsion solvent extraction/evaporation method.* Biomaterials, 2001. **22**: p. 231-241.

33. Kohane, D.S., *Microparticles and nanoparticles for drug delivery.* Biotech Bioeng, 2007. **96**(2): p. 203-209.

34. Zhang, X.Z., P. Jo Lewis, and C.C. Chu, *Fabrication and characterization of a smart drug delivery system: Microsphere in hydrogel.* Biomaterials, 2005. **16**: p. 3299-3309.

35. Leach, J.B. and C.E. Schmidt, *Characterization of protein release from photocrosslinkable hyaluronic acid-polyethylene glycol hydrogel tissue engineering scaffolds.* Biomaterials, 2005. **26**: p. 125-135.

36.   Ersek, R.A., *Transplantation of purified autologous fat: a 3-year follow-up is disappointing.* Plast Reconstr Surg, 1991. **87**(2): p. 219-297.

37.   Weissman, I.L., D.J. Anderson, and F. Gage, *Stem and progenitor cells: origins, phenotypes, lineage commitments, and transdifferentiations.* Annu Rev Cell Dev Biol, 2001. **17**: p. 387-403.

38.   Bianco, P. and P.G. Robey, *Stem cells in tissue engineering.* Nature, 2001. **414**(6859): p. 118-121.

39.   Bianco, P., et al., *Bone marrow stromal stem cells: nature, biology, and potential applications.* Stem Cells, 2001. **19**(3): p. 180-192.

40.   Wakitani, S., T. Saito, and A.I. Caplan, *Myogenic cells derived from rat bone marrow mesenchymal stem cells exposed to 5-azacytidine.* Muscle Nerve, 1995. **18**(12): p. 1417-1426.

41.   Pittenger, M.F., et al., *Multilineage potential of adult human mesenchymal stem cells.* Science, 1999. **284**(5411): p. 143-147.

42.   Nathan, S., et al., *Cell-based therapy in the repair of osteochondral defects: a novel use for adipose tissue.* Tissue Engineering, 2003. **9**(4): p. 733-744.

43.   Hemmrich, K., et al., *Implantation of preadipocyte-loaded hyaluronic acid-based scaffolds into nude mice to evaluate potential for soft tissue engineering.* Biomaterials, 2005. **26**: p. 7025-7037.

44.   Rehman, J., et al., *Secretion of angiogenic and antiapoptotic factors by human adipose stromal cells.* Circulation, 2004. **109**: p. 1292-1298.

45.   Niemela, S.-M., et al., *Fat Tissue: Views on Reconstruction and Exploitation.* J Craniofac Surg, 2007. **18**(2): p. 325-335.

46.   Otto, T.C. and M.D. Lane, *Adipose Development: From Stem cell to Adipocyte.* Crit Rev Biochem Mol Biol, 2005. **40**(4): p. 229-242.

47.   Gregoire, F.M., C.M. Smas, and H.S. Sul, *Understanding adipocyte differentiation.* Physiol Rev, 198. **78**(3): p. 783-809.

48.   Ibelgaufts, H., *Cytokines and Cells Online Pathfinder Encyclopedia.* 2004.

49.   Jeon, O., et al., *Control of basic fibroblast growth factor release from fibrin gel with heparin and concentrations of fibrinogen and thrombin.* J Control Release, 2005. **105**(3): p. 249-259.

50. Sakiyama-Elbert, S.E. and J.A. Hubbell, *Development of fibrin derivatives for controlled release of heparin-binding growth factors.* J Control Release, 2000. **65**(3): p. 389-402.

51. Wong, C., et al., *Fibrin-based biomaterials to deliver human growth factors.* Thromb Haemost, 2003. **89**(3): p. 573-582.

52. Hatano, T., et al., *Acceleration of aneurysm healing by controlled release of basic fibroblast growth factor with use of polyethylene terephthalate fiber coils coated with gelatin hydrogel.* Neurosurgery, 2003. **53**(2): p. 393-400.

53. Hong, L., et al., *Enhanced formation of fibrosis in a rabbit aneurysm by gelatin hydrogel incorporating basic fibroblast growth factor.* Neurosurgery, 2001. **49**(4): p. 954-960.

54. Yamamoto, M., Y. Ikada, and Y. Tabata, *Controlled release of growth factors based on biodegradation of gelatin hydrogel.* J Biomater Sci Polym Ed., 2001. **12**(1): p. 77-88.

55. Tabata, Y. and Y. Ikada, *Vascularization effect of basic fibroblast growth factor released from gelatin hydrogels with different biodegradabilities.* Biomaterials, 1999. **20**(22): p. 2169-2175.

56. Nakajima, H., et al., *Therapeutic angiogenesis by the controlled release of basic fibroblast growth factor for ischemic limb and heart injury: toward safety and minimal invasiveness.* J Artif Organs, 2004. **7**(2): p. 58-61.

57. Cote, M.F., et al., *Denatured collagen as support for a FGF-2 delivery system: physicochemical characterizations and in vitro release kinetics and bioactivity.* Biomaterials, 2004. **25**(17): p. 3761-3772.

58. Masuda, T., M. Furue, and T. Matsuda, *Photocured, Styrenated Gelatin-Based Microspheres for de Novo Adipogenesis through Corelease of Basic Fibroblast Growth Factor, Insulin, and Insulin-Like Growth Factor.* Tissue Engineering, 2004. **10**(3/4): p. 523-535.

59. Zamora, P.O., et al., *Local delivery of basic fibroblast growth factor (bFGF) using adsorbed silyl-heparin, benzyl-bis(dimethylsilylmethyl)oxycarbamoyl-heparin.* Bioconjug Chem, 2002. **13**(5): p. 920-926.

60. Midy, V., et al., *Basic fibroblast growth factor adsorption and release properties of calcium phosphate.* J. Biomed Mater Res, 1998. **41**(3): p. 405-411.

61. Liu, L.S., et al., *Hyaluronate-heparin conjugate gels for the delivery of basic fibroblast growth factor (FGF-2).* J. Biomed Mater Res, 2002. **62**(1): p. 1280135.

62. Kimura, Y., et al., *Time course of de novo adipogenesis in matrigel by gelatin microspheres incorporating basic fibrobast growth factor.* Tissue Engineering, 2002. **8**(4): p. 603-613.

63. Tabata, Y., et al., *De Novo Formation of Adipose Tissue by Controlled Release of Basic Fibroblast Growth Factor.* Tissue Engineering, 2000. **6**(3): p. 279-289.

64. Iwakura, A., et al., *Intramyocardial sustained delivery of basic fibroblast growth factor improves angiogenesis and ventricular function in a rat infarct model.* Heart Vessels, 2003. **18**(2): p. 93-99.

65. Kimura, Y., et al., *Adipose tissue engineering based on human preadipocytes combined with gelatin microspheres containing basic fibroblast growth factor.* Biomaterials, 2003. **24**: p. 2513-2521.

66. Sakakibara, Y., et al., *Toward surgical angiogenesis using slow-released basic fibroblast growth factor.* Euro J of Cardio-thoracic Surg, 2003. **24**: p. 105-112.

67. Cai, S., et al., *Injectable glycosaminoglycan hydrogels for controlled release of human basic fibroblast growth factor.* Biomaterials, 2005. **26**(30): p. 6054-6067.

68. Yuksel, E., et al., *De novo adipose tissue generation through long-term, local delivery of insulin and insulin-like growth factor-1 by PLGA/PEG microspheres in an in vivo rat model: A novel concept and capability.* Plast Reconstr Surg, 2000. **105**: p. 1721-1729.

69. Thula, T.T., et al., *Effects of EGF and bFGF on irradiated parotid glands.* Ann Biomed Eng, 2005. **33**(5): p. 685-695.

70. Marra, K.G., et al., *FGF-2 Enhances Vascularization for Adipose Tissue Engineering.* Plast Reconstr Surg, 2007. **In press**.

71. Ozeki, M. and Y. Tabata, *In vivo promoted growth of mice hair follicles by the controlled release of growth factors.* Biomaterials, 2003. **24**(13): p. 2387-2394.

72. Laham, R.J., et al., *Local perivascular delivery of basic fibroblast growth factor in patients undergoing coronary bypass surgery: results of a phase I randomized, double-blind, placebo-controlled trial.* Circulation, 1999. **100**(18): p. 1865-1871.

73. Fujita, M., et al., *Vascularization in vivo caused by the controlled release of fibroblast growth factor-2 from an injectable chitosan/non-anticoagulant heparin hydrogel.* Biomaterials, 2004. **25**(4): p. 699-706.

74. Fujita, M., et al., *Efficacy of photocrosslinkable chitosan hydrogel containing fibroblast growth factor-2 in a rabbit model of chronic myocardial infarction.* J. Surg Res, 2005. **126**(1): p. 27-33.

75. Ishihara, M., et al., *Controlled release of fibroblast growth factors and heparin from photocrosslinked chitosan hydrogels and subsequent effect on in vivo vascularization.* J Biomed Mater Res A, 2003. **64**(3): p. 551-559.

76. Perets, A., et al., *Enhancing the vascularization of three-dimensional porous alginate scaffolds by incorporating controlled release of basic fibroblast growth factor microspheres.* J Biomed Mater Res A, 2003. **65**: p. 489-497.

77. Dogan, A.K., M. Gumusderelioglu, and E. Aksoz, *Controlled release of EGF and bFGF from dextran hydrogels in vitro and in vivo.* j bIOMED Mater Res B Appli Biomater, 2005. **74**(1): p. 504-510.

78. Hiraoka, Y., et al., *In Situ Regeneration of Adipose Tissue in Rat Fat Pad by Combining a Collagen Scaffold with Gelatin Microspheres Containing Basic Fibroblast Growth Factor.* Tissue Engineering, 2006. **12**(6): p. 1475-1487.

79. Vashi, A.V., et al., *Adipose Tissue Engineering Based on the Controlled Release of Fibroblast Growth Factor-2 in a Collagen Matrix.* Tissue Engineering, 2006. **12**(11): p. 3035-3043.

80. Pike, D.B., et al., *Heparin-regulated release of growth factors in vitro and angiogenic response in vivo to implanted hyaluronan hydrogels containing VEGF and bFGF.* Biomaterials, 2006. **27**: p. 5242-5251.

81. Yamaguchi, N. and K.L. Kiick, *Polysaccharide-Poly(ethylene glycol) Star Copolymer as a Scaffold for the Production of Bioactive Hydrogels.* Biomacromolecules, 2005. **6**: p. 1921-1930.

82. Lazarous, D.F., et al., *Effects of chronic systemic administration of basic fibroblast growth factor on collateral development in the canine heart.* Circulation, 1995. **91**(1): p. 145-153.

83. Whalen, G.F., Y. Shing, and J. Folkman, *The fate of intravenously administered bFGF and the effect of heparin.* Growth Factors, 1989. **1**(2): p. 157-164.

84. Edelman, E.R., M.A. Nugent, and M.J. Karnovsky, *Perivascular and intravenous administration of basic fibroblast growth factor: vascular and solid organ deposition.* Proc Natl Acad Sci, 1993. **90**(4): p. 1513-1517.

85. Dinbergs, I.D., L. Brown, and E.R. Edelman, *Cellular response to transforming growth factor-beta1 and basic fibroblast growth factor depends on release kinetics and extracellular matrix interactions.* J of Biol Chem, 1996. **271**(47): p. 29822-29829.

86. Morimoto, N., et al., *In Vivo Culturing of a Bilayered Dermal Substitute with Adipo-Stromal Cells.* J. Surg Res, 2007. **Epub ahead of print**.

87. Tsutsumi, S., et al., *Retention of multilineage differentiation potential of mesenchymal cells during proliferation in response to FGF.* Biochem Biophys Res Commun, 2001. **288**(2): p. 413-419.

88. Locklin, R.M., R.O.C. Oreffo, and J.T. Triffit, *Effects of TGFB and bFGF on the differentiation of human bone marrow stromal fibroblasts.* Cell Bio Int, 1999. **23**(3): p. 185-194.

89. Neubauer, M., et al., *Adipose Tissue Engineering Based on Mesenchymal Stem Cells and Basic Fibroblast Growth Factor in Vitro.* Tissue Engineering, 2005. **11**(11/12): p. 1840-1851.

90. Solchaga, L., et al., *FGF-2 Enhances the Mitotic and Chondrogenic Potentials of Human Adult Bone Marrow-Derived Mesenchymal Stem Cells.* J Cell Physiol, 2005. **203**: p. 398-409.

91. Hankemeier, S., et al., *Modulation of Proliferation and Differentiation of Human Bone Marrow Stromal Cells by Fibroblast Growth Factor 2: Potential Implications for Tissue Engineering of Tendons and Ligaments.* Tissue Engineering, 2005. **11**(1/2): p. 41-49.

92. Neubauer, M., et al., *Basic fibroblast growth factor enhances PPARγ ligand-induced adipogenesis of mesenchymal stem cells.* FEBS Letts, 2004. **577**: p. 277-283.

93. Chiou, M., Y. Xu, and M.T. Longaker, *Mitogenic and chondrogenic effects of fibroblast growth factor-2 in adipose-derived mesenchymal cells.* Biochem and Biophys Res Comm, 2006. **343**: p. 644-652.

94. Inoue, S., et al., *Effect of culture substrate and fibroblast growth factor addition on the proliferation and differentiation of human adipo-stromal cells.* J Biomater Sci Polym Ed., 2005. **16**(1): p. 57-77.

95. Quarto, N. and M.T. Longaker, *FGF-2 Inhibits Osteogenesis in Mouse Adipose Tissue-Derived Stromal Cells and Sustains their Proliferative and Osteogenic Potential State.* Tissue Engineering, 2006. **12**(6): p. 1405-1418.

96. Broad, T.E. and R.G. Ham, *Growth and adipose differentiation of sheep preadipocyte fibroblasts in serum-free medium.* Eur J Biochem, 1983. **135**(1): p. 33-39.

97. Flynn, L., et al., *Adipose tissue engineering with naturally derived scaffolds and adipose-derived stem cells.* Biomaterials, 2007. **28**(26): p. 3834-3842.

98. Halbleib, M., et al., *Tissue engineering of white adipose tissue using hyaluronic acid-based scaffolds. I: in vitro differentiation of human adipocyte precursor cells on scaffolds.* Biomaterials, 2003. **24**(18): p. 3125-3132.

99. von Heimburg, D., et al., *Influence of different biodegradable carriers on the in vivo behavior of human adipose precursor cells.* Plast Reconstr Surg, 2001. **108**(2): p. 411-420.

100. Rubin, J.P., et al., *Collagenous microbeads as a scaffold for tissue engineering with adipose-derived stem cells.* Plast Reconstr Surg, 2007. **120**(2): p. 414-424.

101. Dragoo, J.L., et al., *Healing full-thickness cartilage defects using adipose-derived stem cells.* Tissue Engineering, 2007. **13**(7): p. 1615-1621.

102. Wei, Y., et al., *A novel injectable scaffold for cartilage tissue engineering using adipose-derived adult stem cells.* J Orthop Res, 2007. **Epub ahead of pring**.

103. Leddy, H.A., H.A. Awad, and F. Guilak, *Molecular diffusion in tissue-engineered cartilage constructs: effects of scaffold material, time, and culture conditions.* J Biomed Mater Res A, 2004. **70**(2): p. 397-406.

104. Zhang, Y.S., et al., *Cellular compatibility of type collagen I scaffold and human adipose-derived stem cells.* Nan Fang Yi Ke Da Xue Xue Bao, 2007. **27**(2): p. 223-225.

105. DiMuzio, P., et al., *Development of a tissue-engineered bypass graft seeded with stem cells.* Vascular, 2006. **14**(6): p. 338-342.

106. Hong, L., et al., *Ex vivo adipose tissue engineering by human marrow stromal cell seeded gelatin sponge.* Ann Biomed Eng, 2005. **33**(4): p. 511-517.

107. Dudas, J., et al., *The osteogenic potential of adipose-derived stem cells for the repair of rabbit calvarial defects.* Ann Plast Surg, 2006. **56**(5): p. 543-548.

108. Voytik-Harbin, S.L., et al., *Identification of extractable growth factors from small intestinal submucosa.* J. Cell Biochem, 1997. **67**(4): p. 478-491.

109. Ansaloni, L., et al., *Hernia repair with procine small-intestinal submucosa.* Hernia, 2007. **11**(4): p. 321-326.

110. Lindberg, K. and S.F. Badylak, *Porcine small intestinal submucosa (SIS): a bioscaffold supporting in vitro primary human epidermal cell differentiation and synthesis of basement membrane proteins.* Burns, 2001. **27**(3): p. 254-266.

111. Badylak, S.F., et al., *Endothelial cell adherence to small intestinal submucosa: an acellular bioscaffold.* Biomaterials, 1999. **20**(23-24): p. 2257-2263.

112. Badylak, S.F., et al., *Small Intestinal Submucosa : a substrate for in vitro cell growth* J Biomater Sci Polym Ed., 1998. **9**(8): p. 863-878.

113. Hodde, J.P., et al., *Retention of endothelial cell adherence to porcine-derived extracellular matrix after disinfection and sterilization.* Tissue Engineering 2002. **8**(2): p. 225-234.

114. Li, H., et al., *Study on the Osteogenesis ability of co-culturing bone marrow stromal cells (BMSCs) and small intestinal submucosa.* Shanghai Kou Qiang Yi Xue 2006. **15**(2): p. 167-171.

115. Zhang, K.G., B.F. Zeng, and C.Q. Zhang, *Periosteum construction in vitro by small intestinal submucosa combined with bone marrow mesenchymal stem cell.* Wai Ke Za Zhi 2005. **43**(24): p. 1594-1597.

116. Liao, B., L. Deng, and F. Wang, *Effects of bone marrow mesenchymal stem clls enriched by small intestinal submucosal films on cardiac function and compensatory circulation after myocardial infarction in goats.* Zhongguo Xiu Chong Jian Wai Ke Za Zhi, 2006. **29**(12): p. 1248-1252.

117. Chung, S.Y., et al., *Bladder reconstruction with bone marrow derived stem cells seeded on small intestinal submucosa improves morphological and molecular composition.* J Urol, 2005. **174**(1): p. 353-359.

118. Xiaohui, T., et al., *Small Intestinal Submucos improves islet survival and function in vitro culture.* Transplant Proc 2006. **38**(5): p. 1552-1558.

119. Lu, S.H., et al., *Muscle-derived stem cells seeded into acellular scaffolds develop calcium-dependent contractile activity that is modulated by nicotoni receptors.* Urology, 2003. **61**(6): p. 1285-1291.

120. Hausman, G.J., *The influence of dexamethasone and insulin on expression of CCAAT/enhancer binding protein isoforms during preadipocyte differentiation in porcine stromal-vascular cell cultures: Evidence for very early expression of C/EBPα.* J Anim Sci, 2000. **78**: p. 1227-1235.

121. Malladi, P., et al., *Functions of Vitamin D, Retinoic Acid, and Dexamethasone in Mouse Adipose-Derived Mesenchymal Cells.* Tissue Engineering, 2006. **12**(7): p. 2031-2040.

122. Tchoukalova, Y.D., et al., *Enhancing effect of troglitazone on porcine adipocyte differentiation in primary culture: a comparison with dexamethasone.* Obes Res, 2000. **8**(9): p. 664-672.

123. Schugart, E.C. and R.M. Umek, *Dexamethasone Signaling Is Required to Establish the Postmitotic State of Adipocyte Development.* Cell Growth & Diff, 1997. **8**: p. 1091-1098.

124. Gaillard, D., et al., *Control of terminal differentiation of adipose precursor cells by glucocorticoids.* J. Lipid Res, 1991. **32**: p. 569-579.

125. Hauner, H., et al., *Promoting Effect of Glucocorticoids on the Differentiation of Human Adipocyte Precursor Cells Cultured in a Chemically Defined Medium.* J Clin Invest, 1989. **84**: p. 1663-1670.

126.   Nuttelman, C.R., M.C. Tripodi, and K.S. Anset, *Dexamethasone-functionalized gels induce osteogenic differentiation of encapsulated hMSCs.* J Biomed Mater Res A, 2006. **76**: p. 183-195.

127.   Hickey, T., et al., *In vivo evaluation of a dexamethasone/PLGA microsphere system designed to suppress the inflammatory tissue response to implantable medical devices.* J Biomed Mater Res, 2002. **61**: p. 180-187.

128.   Norton, L.W., et al., *In vitro characterization of vascular endothelial growth factor and dexamethasone releasing hydrogels for implantable probe coatings.* Biomaterials, 20025. **26**: p. 3285-3297.

129.   Gomez-Gaete, C., et al., *Encapsulation of dexamethasone into biodegradable polymeric nanoparticles.* Int J Pharm, 2007. **331**: p. 153-159.

130.   Eroglu, H., et al., *The in vitro and in vivo characterization of PLGA:LPLA microsphere containing dexamethasone sodium phosphate.* J Microencapsul, 2001. **18**(5): p. 603-612.

131.   Eroglu, H., M.F. Sargon, and L. Oner, *Chitosan formulations for steroid delivery: effect of formulation variables on in vitro characteristics.* Drug Dev Ind Pharm, 2007. **33**(3): p. 265-271.

132.   Jaraswekin, S., S. Prakongpan, and R. Bodmeier, *Effect of poly(lactide-co-glycolide) molecular weight on the release of dexamethasone sodium phosphate from miroparticles.* J Microencapsul, 2007. **24**(2): p. 117-128.

133.   Zhang, Z., D.W. Grijpma, and J. Feijen, *Poly(trimethylene carbonate) and monomethoxy poly(ethylene glycol)-block-poly(trimethylene carbonate) nanoparticles for the controlled release of dexamethasone.* J Control Release, 2006. **111**(3): p. 263-270.

134.   Zignani, M., et al., *A poly(ortho ester) designed for combined ocular delivery of dexamethasone sodium phosphate and 5-fluorouracil: subconjunctival tolerance and in vitro release.* Eur J Pharm Biopharm, 2000. **50**(2): p. 251-255.

135.   Silva, G.A., et al., *Entrapment ability and release profile of corticosteroids from starch-based microparticles.* J Biomed Mater Res A, 2005. **73**(2): p. 234-243.

136.   Herrero-Vanrell, R., et al., *Self-assembled particles of an elastin-like polymer as vehicles for controlled drug release.* J Control Release, 2005. **102**(1): p. 113-122.

137.   Ganguly, S. and A.K. Dash, *A novel in situ gel for sustained drug delivery and targeting.* Int J Pharm, 2004. **276**(1-2): p. 83-92.

138.   Anglin, E.J., et al., *Engineering the Chemistry and Nanostructure of Porous Silicon Fabry-Perot Films for Loading and Release of a Steroid.* Langmuir, 2004. **20**: p. 11264-11269.

139. Chorny, M., et al., *Site-specific delivery of dexamethasone from biodegradable implants reduces formation of pericardial adhesions in rabbits.* J Biomed Mater Res A, 2006. **78**: p. 276-282.

140. Stevens, K.R., et al., *In vivo biocompatibility of gelatin-based hydrogels and interpenetrating networks.* J Biomater Sci Polym Ed., 2002. **13**(12): p. 1353-1366.

141. Wadhwa, R., C.F. Lagenaur, and X.T. Cui, *Electrochemically controlled release of dexamethasone from conducting polymer polypyrrole coated electrode.* J Control Release, 2006. **110**: p. 531-541.

142. Yoon, J.J., J.H. Kim, and P. T.G., *Dexamethasone-releasing biodegradable polymer scaffolds fabricated by a gas-foaming/salt-leaching method.* Biomaterials, 2003. **24**: p. 2323-2329.

143. Cascone, M.G., P.M. Pot, and L. Lazzeri, *Release of dexamethasone from PLGA nanoparticles entrapped into dextran/poly(vinyl alcohol) hydrogels.* J Mater Sci Mater Med, 2002. **13**(3): p. 265-269.

144. Galeska, I., et al., *Controlled release of dexamethasone from PLGA microspheres embedded within polyacid-containing PVA hydrogels.* AAPS J, 2005. **7**(1): p. E231-240.

145. Kim, J.H., et al., *Use of polyurethane with sustained release dexamethasone in delayed adjustable strabismus surgery.* Br J Ophthalmol, 2004. **88**(11): p. 1450-1454.

146. Kim, D.-H. and D.C. Martin, *Sustained release of dexamethasone from hydrophilic matrices using PLGA nanoparticles for neural drug delivery.* Biomaterials, 2006. **27**: p. 3031-3037.

147. Chen, X.-L., R.G. Dean, and G.J. Hausman, *Expression of leptin mRNA and CCAAT-enhancer binding proteins in response to insulin deprivation during preadipocyte differentiation in primary culutres of porcine stromal-vascular cells.* Domest Anim Endocrinol, 1999. **17**(4): p. 389-401.

148. Yamaguchi, Y., et al., *Insulin-loaded biodegradable PLGA microcapsules: initial burst release controlled by hydrophilic additives.* J Control Release, 2002. **81**: p. 235-249.

149. Ibrahim, M.A., et al., *Stability of insulin during the erosion of poly(lactic acid) and poly(lacti-co-glycolic acid) microspheres.* J Control Release, 2005. **106**: p. 241-252.

150. Kang, F. and J. Singh, *Preparation, In Vitro Release, In Vivo Absorbtion and Biocompatibility Studies of Insulin-loaded Microspheres in Rabbits.* AAPS PharmSciTech, 2005. **6**(3): p. E487-494.

151. Hinds, K.D., et al., *PEGylated insulin in PLGA microparticles. In vivo and in vitro analysis.* J Control Release, 2005. **104**(3): p. 447-460.

152. Aguiar, M.M.G., J.M. Rodriques, and A.S. Cunha, *Encapsulation of insulin-cyclodextrin complex in PLGA microspheres: a new approach for prolonged pulmonary insulin delivery.* J Microencapsul, 2004. **21**(5): p. 553-564.

153. Yeh, M.-K., J.-L. Chen, and C.-H. Chiang, *In vivo and in vitro characteristics for insulin-loaded PLA microparticles prepared by w/o/w solvent evaporation method with electrolytes in the continuous phaswe.* J Microencapsul, 2004. **21**(7): p. 719-728.

154. Furtado, S., et al., *Oral delivery of insulin loaded poly(fumaric-co-sebacic) anhydride microspheres.* Int J Pharm, 2007. **Epub ahead of print**.

155. Ramkissoon-Ganorkar, C., et al., *Modulating insulin-release profile from pH/thermosensitive polymeric beads through polymer molecular weight.* J Control Release, 1999. **59**(3): p. 287-298.

156. Shenoy, D.B., et al., *Potential applications of polymeric microsphere suspension as subcutaneous depot for insulin.* Drug Dev Ind Pharm, 2003. **29**(5): p. 555-563.

157. Jiang, H.L. and K.J. Zhu, *Bioadhesive fluorescent microspheres as visible carriers for local delivery of drugs. I: preparation and characterization of insulin-loaded PCEFB/PLGA microspheres.* J Microencapsul, 2002. **19**(4): p. 451-461.

158. DiRamio, J.A., et al., *Poly(ethylene glycol) Methacrylate/Dimethacrylate Hydrogels for Controlled Release of Hydrophobic Drugs.* Biotechnol Prog, 2005. **21**: p. 1281-1288.

159. Lowman, A.M., et al., *Oral delivery of insulin using pH-responsive complexation gels.* J Pharm Sci, 1999. **88**(9): p. 933-937.

160. Tuesca, A., et al., *Complexation hydrogels for oral insulin delivery: Effects of polymer dosing on in vivo efficacy.* J Pharm Sci, 2007. **Epub ahead of print**.

161. Kumar, A., S.S. Lahiri, and H. Singh, *Development of PEGDMA: MAA based hydrogel microparticles for oral insulin delivery.* Int J Pharm, 2006. **323**(1-2): p. 117-124.

162. Bugamelli, F., et al., *Controlled Insulin Release from Chitosan Microparticles.* Arch Pharm Pharm Med Chem, 1998. **331**: p. 133-138.

163. Ubaidulla, U., et al., *Development and in-vivo evaluation of insulin-loaded chitosan phthalate microspheres for oral delivery.* J Pharm Pharmacol, 2007. **59**(10): p. 1345-1351.

164.   Ubaidulla, U., et al., *Development and characterization of chitosan succinate microspheres for the improved oral bioavailability of insulin.* J Pharm Sci, 2007. **96**(11): p. 3010-3023.

165.   Varshosaz, J., H. Sadrai, and R. Alinagari, *Nasal delivery of insulin using chitosan microspheres.* J Microencapsul, 2004. **21**(7): p. 761-774.

166.   Kofuji, K., et al., *Retention and release behavior of insulin in chitosan gel beads.* J Biomater Sci Polym Ed., 2003. **14**(11): p. 1243-1253.

167.   Wu, J., et al., *A thermosensitive hydrogel based on quaternized chitosan and poly(ethylene glycol) for nasal drug delivery system.* Biomaterials, 2007. **28**(13): p. 2220-2232.

168.   Kashyap, N., et al., *Design and evaluation of biodegradable, biosensive in situ gelling system for pulsatile delivery of insulin.* Biomaterials, 2007. **28**(11): p. 2051-2060.

169.   Wang, J.C., Y. Tabata, and K. Morimoto, *Aminated gelatin microspheres as a nasal delivery system for peptide drugs: evaluation of in vitro release and in vivo insulin absorption in rats.* J Control Release, 2006. **113**(1): p. 31-37.

170.   Uchida, T., et al., *Preparation and characterization of insulin-loaded acrylic hydrogels containing absorption enhancers.* Chem Pharm Bull, 2001. **49**(10): p. 1261-1266.

171.   Surendrakumar, K., et al., *Sustained release of insulin from sodium hyaluronate based dry powder formulations after pulmonary delivery to beagle dogs.* J Control Release, 2003. **91**(3): p. 385-394.

172.   Liu, J., et al., *Controlled release of insulin from PLGA nanoparticles embedded within PVA hydrogels.* J Mater Sci Mater Med, 2007. **Epub ahead of print**.

173.   Reis, C.P., et al., *Nanoparticulate delivery system for insulin: design, characterization and in vitro/in vivo bioactivity.* Eur J Pharm Sci, 2007. **30**(5): p. 392-397.

174.   Trotta, M., et al., *Solid lipid micro-particles carrying insulin formed by solven-in-water emulsion-diffusion technique.* Int J Pharm, 2005. **288**: p. 281-288.

175.   Yuksel, E., et al., *Augmentation of adipofascial flaps using the long-term local delivery of insulin and insulin-like growth factor-1.* Plast. Reconstr Surg, 2000. **106**: p. 373-382.

176.   Clavijo-Alvarez, J.A., et al., *A novel perfluoroelastomer seeded with adipose-derived stem cells for soft-tissue repair.* Plast Reconstr Surg, 2006. **118**(5): p. 1132-42.

177.   Jones, L.J., et al., *Sensitive determination of cell number using the CYQUANT cell proliferation assay.* J Immunol Methods, 2001. **254**(1-2): p. 85-98.

178.   Lee, G.M., et al., *Characterization and efficacy of PKH26 as a probe to study the replication history of the human hematopoietic KG1a progenitor cell line.* In Vitro Cell Dev Biol Anim. , 2002. **38**(2): p. 90-96.

179.   Ford, J.W., et al., *PKH26 and 125I-PKH95: characterization and efficacy as labels for in vitro and in vivo endothelial cell localization and tracking.* J. Surg Res, 1996. **62**(1): p. 23-28.

180.   Sah, H., *A new strategy to determine the actual protein content of poly(lactide-co-glycolide) microspheres.* J Pharm Sci, 1997. **86**(11): p. 1315-1318.

181.   Marra, K.G., et al., *FGF-2 Enhances Vascularization for Adipose Tissue Engineering.* PRS.

182.   Patel, P.N., et al., *Poly(ethylene glycol) hydrogel system supports preadipocyte viability, adhesion, and proliferation.* Tissue Engineering, 2005. **11**(9-10): p. 1498-1505.

183.   Kakudo, N., A. Shimotsuma, and K. Kusumoto, *Fibroblast growth factor-2 stimulates adipogenic differentiation of human adipose-derived stem cells.* Biochem and Biophys Res Comm, 2007. **359**: p. 239-244.

184.   Choi, Y.S., S.-N. Park, and H. Suh, *Adipose tissue engineering using mesenchymal stem cells attached to injectable PLGA spheres.* Biomaterials, 2005. **26**: p. 5855-5863.

185.   Lee, J.A., et al., *Biological Alchemy: Engineering Bone and Fat From Fat-Derived Stem Cells.* Ann Plast Surg, 2003. **50**: p. 610-617.

186.   Yuksel, E., et al., *Increased free fat-graft survival with the long-term, local delivery of insulin, insulin-like growth factor-I, and basic fibroblast growth factor by PLGA/PEG microspheres.* Plast. Reconstr. Surg., 2000. **105**(5): p. 1712-1720.

187.   DeSantis, C., R. Siegel, and A. Jemal, *Breast Cancer Facts and Figures 2007-2008*, in *American Cancer Society*. 2007, American Cancer Society: Atlanta, GA. p. 1-34.

188.   Jemal, A., et al., *Cancer statistics, 2007.* CA Cancer J Clin, 2007. **57**(1): p. 43-66.

189.   Love, S.M. and K. Lindsey, *Dr. Susan Love's Breast Book.* 4th ed. 2005, Cambridge: Da Capo Press. 592.

190.   Fisher, B., et al., *Postoperative radiotherapy in the treatment of breast cancer: Results of the NSABP clinical trial.* Ann Surg, 1970. **172**: p. 711-732.

191.   Asari, F. and I. Gage, *Radiation therapy in management of breast cancer.* Curr Opin Oncol, 1999. **11**: p. 463-467.

192.   Bajaj, A., et al., *Aesthetic outcomes in patients undergoing breast conservation therapy for the treatment of localized breast cancer.* Plast Reconstr Surg, 2004. **114**: p. 1442-1449.

193.   Matory, W.J., et al., *Aesthetic results following partial mastectomy and radiation therapy.* Plast Reconstr Surg, 1990. **85**: p. 739-746.

194.   Olivotto, I., et al., *Late cosmetic outcome after conservative surgery and radiotherapy: Analysis of causes of cosmetic failure.* Int J Radiat Oncol Biol Phys, 1989. **17**: p. 747-753.

195.   Grisotti, A., *Immediate reconstruction after partial mastectomy.* Operative Techniques in Plastic and Reconstructive Surgery, 1994. **1**: p. 1-12.

196.   Slavin, S., S. Love, and N. Sadowsky, *Reconstruction of the radiated partial mastectomy defect with autogenous tissues.* Plast Reconstr Surg, 1992. **90**: p. 854-865.

197.   Saltzman, W.M. and L.K. Fung, *Polymeric implants for cancer chemotherapy.* Adv Drug Deliv Rev, 1997. **26**(2-3): p. 209-230.

198.   Sharifi, R. and M. Soloway, *Clinical study of leuprolide depot formulation in the treatment of advanced prostate cancer. The Leuprolide Study Group.* J Urol, 1990. **143**: p. 68-71.

199.   Doughty, J.C., et al., *Intra-arterial adminstration of adriamycin-loaded albumin microspheres for locally advanced breast cancer.* Postgrad Med J., 1995. **71**(831): p. 47-49.

200.   Ibrahim, N.K., et al., *Multicenter phase II trial of ABI-007, an albumin-bound paclitaxel, in women with metastatic breast cancer.* J Clin Oncol., 2005. **23**(25): p. 6019-6026.

201.   Emerich, D.F., et al., *Sustained release chemotherapeutic microspheres provide superior efficacy over systemic therapy and local bolus infusions.* Pharm Res, 2002. **19**: p. 1052-1060.

202.   Ike, O., et al., *Biodegration and antitumour effect of adriamycin-containing poly(L-lactic acid) micropheres.* Biomaterials, 1991. **12**: p. 757-762.

203.   Di Marco, A., *Mechanism of action and mechanism of resistance to antineoplastic agents that bind to DNA.* Antibiot Chemother, 1978. **23**: p. 216-227.

204.   Sinha, B.K. and J.L. Gregory, *Role of one-electron and two electron reduction products of adriamycin and daunomycin in deoxyribonucleic acid binding.* Biochem Pharmacol, 1981. **30**: p. 2626-2629.

205. Swain, S.M., F.S. Whaley, and M.S. Ewer, *Congestive heart failure in patients treated with doxorubicin: A retrospective analysis of three trials.* Cancer, 2003. **87**: p. 2869-2879.

206. Morandi, P., et al., *Cardiac toxicity of high-dose chemotherapy.* Bone Marrow Transplant, 2005. **35**: p. 323-334.

207. Berry, G.J. and M. Jorden, *Pathology of Radiation and Anthracycline Cardiotoxicity.* Pediatr Blood Cancer, 2005. **44**: p. 630-637.

208. Fan, H. and A.K. Dash, *Effect of cross-linking on the in vitro release kinetics of doxorubicin from gelatin implants.* Int Pharm, 2001. **213**: p. 103-116.

209. Lin, R., L.S. Ng, and C.-H. Wang, *In vitro study of anticancer drugdoxorubicin in PGLA-based microparticles.* Biomaterials, 2005. **26**: p. 4476-4485.

210. Mallery, S.R., et al., *Controlled-release of doxorubicin from poly(lactide-co-glycolide) microspheres significantly enhances cytotoxicity against cultured AIDS-related Kaposi's sarcoma cells.* Anticancer Res, 2000. **20**: p. 2817-2826.

211. Tan, E.C., R. Lin, and C.-H. Wang, *Fabrication of double-walled microspheres for the sustained-release of doxorubicin.* J Colloid Interface Sci, 2005. **291**: p. 135-143.

212. Vail , D.M., et al., *Pegylated liposomal doxorubicin: Proof of principle using preclinical animal models and pharmacokinetic studies.* Semin Oncol, 2004. **31**: p. 16-35.

213. Charrois, G.J.R. and A.T. M., *Drug release rate influences the pharmacokinetics, biodistribution, therapeutic activity, and toxicity of pegylated liposomal doxorubicin formulations in murine breast cancer.* Biochimica et Biophysica Acta, 2004. **1663**: p. 167-177.

214. Katsaros , D., et al., *Clinical and pharmacokinetic phase II study of pegylated liposomal doxorubicin and vinorelbine in heavily pretreated recurrent ovarian carcinoma.* Ann Oncol, 2005. **16**: p. 300-306.

215. Gabizon, A.A., et al., *Cardiac safety of pegylated liposomal doxorubicin (Doxil/Caelyx) demonstrated by endomyocardial biopsy in patients with advanced malignancies.* Cancer Invest, 2994. **22**: p. 663-669.

216. Lu, W.L., et al., *A pegylated liposomal platform: Pharmacokinetics, pharmacodynamics, and toxicity in mice using doxorubicin as a model drug.* J Pharmacol Sci, 2004. **95**: p. 381-389.

217. Chiu, G.N., et al., *Encapsulation of doxorubicin into thermosensitive liposomes via complexation with the transition metal manganese.* J Control Release, 2005. **104**: p. 271-288.

218.   Abraham, S.A., et al., *The liposomal formulation of doxorubicin.* Methods Enzymol, 2005. **391**: p. 71-74.

219.   Wang, J.C., et al., *Pharmacokinetics of intravenously administered stealth liposomal doxorubicin modulated with verapamil in rats.* J Pharm Biopharm, 2006. **62**: p. 44-51.

220.   Yoo, H.S., et al., *In vitro and in vivo anti-tumor activities of nanoparticles based on doxorubicin-PLGA conjugates.* J Control Release, 2000. **68**: p. 419-431.

221.   Cheung, R.Y., A.M. Rauth, and X.Y. Wu, *In vivo efficacy and toxicity of intratumorally delivered mitomycin C and its combination with doxorubicin using microsphere formulations.* Anti-Cancer Drugs, 2005. **16**: p. 423-433.

222.   Orienti, I., et al., *Modified doxorubicin for improved encapsulation in PVA polymeric micelles.* Drug Deliv, 2005. **12**(1): p. 15-20.

223.   Mitra, S., et al., *Tumour targeted delivery of encapsulated dextran-doxorubicin conjugate using chitosan nanoparticles as carrier.* J Control Release, 2001. **74**(1-3): p. 317-323.

224.   Kovar, M., et al., *HPMA copolymer-bound doxorubicin targeted to tumor-specific antigen of BCL1 mouse B cell leukemia.* J Control Release, 2003. **92**(3): p. 315-330.

225.   Rihova, B., et al., *Doxorubicin bound to a HPMA copolymer carrier through hydrazone bond is effective also in a cancer cell line with a limited content of lysosomes.* J Control Release, 2001. **74**(1-3): p. 225-232.

226.   Burton, M.A., et al., *In vitro and in vivo responses of doxorubicin ion exchange microspheres to hyperthermia.* Int J Hyperthermia, 1992. **8**(4): p. 485-494.

227.   Chen, Y., et al., *Evaluation of ion-exchange microspheres as carriers for the anticancer drug doxorubicin: in-vitro studies.* J Pharm Pharmacol, 1992. **44**(3): p. 211-215.

228.   Konishi, M., et al., *In vivo anti-tumor effect of dual release of cisplatin and adriamycin from biodegradable gelatin hydrogel.* J Control Release, 2005. **103**: p. 7-19.

229.   Gupta, P.K., C.T. Hung, and F.C. Lan, *Application of regression analysis in the evaluation of tumor response following the administration of adriamycin either as a solution or via albumin microspheres to the rat.* J Pharm Sci, 1990. **79**(7): p. 634-637.

230.   Prokopowicz, M., J. Lukasiak, and A. Przyjazny, *Utilization of a sol-gel method for encapsulation of doxorubicin.* J Biomater Sci Polym Ed., 2004. **15**(3): p. 343-356.

231.   Barraud, L., et al., *Increase of doxorubicin sensitivity by doxorubicin-loading into nanoparticles for hepatocellular carcinoma cells in vitro and in vivo.* J Hepatol, 2005. **42**(5): p. 736-743.

232.   Laurand, A., et al., *Quantification of the expression of multidrug resistance-related genes in human tumour cell lines grown with free doxorubicin or doxorubicin encapsulated in polyisohexylcyanoacrylate nanospheres.* Anticancer Res, 2004. **24**(6): p. 3781-3788.

233.   Teder, H. and C.J. Johansson, *The effect of different dosages of degradable starch microspheres (Spherex) on the distribution of doxorubicin regionally administered to the rat.* Anticancer Res, 1993. **13**(6A): p. 2161-2164.

234.   Papagiannaros, A., et al., *Doxorubicin-PAMAM dendrimer complex attached to liposomes: Cytotoxic studies against human cancer cell lines.* Int J Pharm, 2005. **302**: p. 29-38.

235.   Liu, D.-Z., et al., *Synthesis, characterization, and drug delivery behaviors of new PCP polymeric micelles.* Carbohydrate Polymers, 2007. **68**(3): p. 544-554.

236.   Liu, Z., et al., *Delivery of an anticancer drug and a chemosensitizer to murine breast sarcoma by intratumoral injection of sulfopropyl dextran microspheres.* J Pharm Pharmacol, 2003. **55**: p. 1063-1073.

237.   Kang, H.W., Y. Tabata, and Y. Ikada, *Fabrication of porous gelatin scaffolds for tissue engineering.* Biomaterials, 1999. **20**: p. 1339-1344.

238.   Mao, J.S., et al., *Structure and properites of bilayer chitosan-gelatin scaffolds.* Biomaterials, 2003. **24**: p. 1067-1074.

239.   Ulubayram, K., et al., *Cytotoxicity evaluation of gelatin sponges prepared with different cross-linking agents.* J Biomater Sci Polym Ed., 2002. **13**: p. 1203-1219.

240.   Ulubayram, K., et al., *Cytotoxicity evaluation of gelatin sponges prepared with different cross-linking agents.* J. Biomater. Sci. Polym. Ed., 2002. **13**: p. 1203-1219.

241.   Hyung Park, J., et al., *Self-assembled nanoparticles based on glycol chitosan bearing hydrophobic moieties as carriers for doxorubicin: in vivo biodistribution and anti-tumor activity.* Biomaterials, 2006. **27**(1): p. 119-26.

242.   DeFail, A.J., et al., *Controlled release of bioactive doxorubicin from microspheres embedded within gelatin scaffolds.* J Biomed Mater Res A, 2006. **79**(4): p. 954-962.

243.   Lin, R., Ng, L.S., Wang, C.-H., *In vitro study of anticancer drug doxorubicin in PGLA-based microparticles.* Biomaterials, 2005. **26**: p. 4476-4485.

244.   Tan, E.C., Lin, R., Wang, C.-H., *Fabrication of double-walled microspheres for the sustained-release of doxorubicin.* Journal of Colloid and Interface Surface, 2005.

245. Muvaffak, A., I. Gurhan, and N. Hasirci, *Prolonged cytotoxic effect of colchicine released from biodegradable microspheres.* J Biomed Mater Res B Appl Biomater, 2004. **71**: p. 295-304.

246. Ulubayram, K., I. Eroglu, and N. Hasirci, *Gelatin microspheres and sponges for delivery of macromolecules.* J Biomater Appl, 2002. **16**(3): p. 227-241.

247. Park, H., et al., *Delivery of TGF-beta1 and chondrocytes via injectable, biodegradable hydrogels for cartilage tissue engineering applications.* Biomaterials, 2005. **26**(34): p. 7095-7103.

248. Swatschek, D., et al., *Microparticles derived from marine sponge collagen (SCMPs): preparation, characterization and suitability for dermal delivery of all-trans retinol.* Eur J Pharm Biopharm, 2002. **54**(2): p. 125-133.

249. Zhang, X.Z., Jo Lewis, P., Chu, C.C., *Fabrication and characterization of a smart drug delivery system: microsphere in hydrogel.* Biomaterials, 2005. **16**: p. 3299-3309.

250. Meese, T.M., Hu, Y., Nowak, R.W., Marra, K.G., *Surface studies of coated polymer microspheres and protein release from tissue-engineered scaffolds.* J Biomater Sci, Polym, Ed, 2002. **13**: p. 141-151.

251. Hu, Y., Hollinger, J.O., and Marra, K.G., *Controlled release from coated polymer microparticles embedded in tissue-engineered scaffolds.* J. Drug Targeting, 2001. **9**(6): p. 431-438.

252. Royce, S.M., M. Askari, and K.G. Marra, *Effects of fibrin gels on the release of FGF-1 from PLGA microspheres.* J Biomater Sci Polym Ed., 2004. **15**: p. 1327-1336.

253. DeFail, A.J., Chu, C.R., Izzo, N., Marra, K.G., *Controlled release of bioactive TGF-β1 from microspheres embedded within biodegradable hydrogels.* Biomaterials, 2005.

254. Mooney, D.J., et al., *Localized delivery of epidermal growth factor improves the survival of transplanted hepatocytes.* Biotech Bioeng, 1996. **50**: p. 422-429.

255. Liu, J., et al., *A novel trans-lymphatic drug delivery system: implantable gelatin sponge impregnated with PLGA-paclitaxel microspheres.* Biomaterials, 2007. **28**(21): p. 3236-3244.

256. Liu XB, C.M., Gong Y, Zhang ZR, Wei DP, Wang X, Li G, *Preliminary study on preparation and pharmaceutic features of adrimycin-loaded human serum albumin microspheres.* Sichuan Da Xue Xue Bao Yi Xue Ban., 2004. **35**(1): p. 107-9.

257. Sarin, R., *Partial-breast treatment for early breast cancer: emergence of a new paradigm.* Nat Clin Pract Oncol, 2005. **2**(1): p. 40-47.

258. Fisher B, F.E., Redmond C., *Ten-year results from the National Surgical Adjuvant Breast and Bowel Project (NSABP) clinical trial evaluating the use of L-phenylalanine mustard (L-PAM) in the management of primary breast cancer.* J Clin Oncol., 1986. **4**(6): p. 929-941.

259. Fisher B, D.J., Mamounas EP, Costantino JP, Wickerham DL, Redmond C, Wolmark N, Dimitrov NV, Bowman DM, Glass AG, Atkins JN, Abramson N, Sutherland CM, Aron BS, Margolese RG., *Sequential methotrexate and fluorouracil for the treatment of node-negative breast cancer patients with estrogen receptor-negative tumors: eight-year results from National Surgical Adjuvant Breast and Bowel Project (NSABP) B-13 and first report of findings from NSABP B-19 comparing methotrexate and fluorouracil with conventional cyclophosphamide, methotrexate, and fluorouracil.* J Clin Oncol., 1996. **14**(7): p. 1982-1992.

260. Toschi E, S.C., Monini P, Barillari G, Bacigalupo I, Palladino C, Baccarini S, Carlei D, Grosso G, Sirianni MC, Ensoli B., *Treatment of Kaposi's sarcoma--an update.* Anticancer Drugs, 2002. **13**(10): p. 977-987.

261. Cooper, C., et al., *Risk factors for the incidence and progression of radiographic knee osteoarthritis.* Arthritis Rheum, 2000. **43**(5): p. 995-1000.

262. Akeson WH, B.W., Chu C, Giurea A, *Differences in mesenchymal tissue repair.* Clin Orthop Relat Res, 2001. **391**(supp): p. 124-41.

263. Messner, K.W.M., *The long-term prognosis for severe damage to weight bearing cartilage in the knee: a 14-year clinical and radiographic follow-up in 28 young athletes.* Acta Orthop Scand, 1996. **67**(2): p. 165-8.

264. Lawrence R, H.C., Arnett F, Deyo R, Felson D, Giannini E, et al, *Estimates of the prevalence of arthritis and selected musculoskeletal disorders in the United States.* Arthritis Rheum, 1998. **41**(5): p. 778-99.

265. Blair, H.C., *Differentiation of the Skeleton.* 2002: p. 1-15.

266. Randolph, M.A., K. Anseth, and M.J. Yaremchuk, *Tissue engineering of cartilage.* Clin Plastic Surg, 2003. **20**: p. 519-537.

267. Saladin, K.S. and D. Van Wynsberghe, *Anatomy and Physiology: The Unity of Form and Function.* 2nd Edition ed. 2001, New York: McGraw-Hill.

268. Schnabel, M., et al., *Dedifferentiation-associated changes in morphology and gene expression in primary human articular chondrocytes in cell culture.* Osteoarthritis and Cartilage, 2002. **10**: p. 62-70.

269.   Wakitani, S., et al., *Autologous Bone Marrow Stromal Cell Transplantation for Repair of Full-Thickness Articular Cartilage Defects in Human Patellae: Two Case Reports.* Cell Transplatation, 2004. **13**: p. 595-600.

270.   Wakitani, S., et al., *Autologous Bone Marrow Stromal Cell Transplantation for Repair of Full-Thickness Articular Cartilage Defects in Human Patellae: Two Case Reports.* Cell Transplatation, 2003. **13**: p. 595-600.

271.   Chen, J., et al., *In vivo chondrogenesis of adult bone-marrow-derived autologous mesenchymal stem cells.* Cell Tissue Res, 2005. **310**(3): p. 429-438.

272.   Zhou, G., et al., *Repair of Porcine Articular Osteochondral Defects in Non-Weightbearing Areas with Autologous Bone Marrow Stromal Cells.* Tissue Engineering, 2006. **12**(11): p. 3209-3221.

273.   Liu, Y., X.Z. Shu, and G.D. Prestwich, *Osteochondroal Defect Repair with Autologous Bone Marrow-Derived Mesenchymal Stem Cells in an Injectable, In Situ, Cross-linked Synthetic Extracellular Matrix.* Tissue Engineering, 2006. **12**(12): p. 3405-3416.

274.   Noth, U., et al., *Chondrogenic differentiation of human mesenchymal stem cells in collagen type I hydrogels.* J Biomed Mater Res A, 2007. **Epub ahead of print**.

275.   Kafienah, W., et al., *Three-Dimensional Cartilage Tissue Engineering Using Adult Stem Cells From Osteoarthritis Patients.* Arthritis Rheum, 2007. **56**(1): p. 177-187.

276.   Cai, D.Z., et al., *Biodegradable chitosan scaffolds containing microspheres as carriers for controlled transforming growth factor-beta1 delivery for cartilage tissue engineering.* Chin Med J (Engl), 2007. **120**(3): p. 197-203.

277.   Lee, J.-Y., et al., *Enhanced bone formation by transforming growth factor-B1-releasing collagen/chitosan microgranules.* J Biomed Mater Res, 2006. **76A**: p. 530-539.

278.   Peter, S.J., et al., *Effects of transforming growth factor beta1 released from biodegradable polymer microparticles on marrow stromal osteoblasts cultured on poly(propylene fumarate) substrates.* J Biomed Mater Res, 2000. **50**(3): p. 452-462.

279.   Hunziker, E.B. and L.C. Rosenberg, *Repair of Partial-Thickness Defects in Articular Cartilage: Cell Recruitment from the Synovial Membrane.* J Bone Joint Surg Am, 1996. **78**(5): p. 721-733.

280.   Huang, Q., et al., *In Vivo Mesenchymal Cell Recruitment by a Scaffold Loaded with Transforming Growth Factor B1 and the Potential for in Situ Chondrogenesis.* Tissue Engineering, 2002. **8**(3): p. 469-482.

281.   Morales, T.I., et al., *Transforming growth factor-beta in calf articular cartilage organ cultures: synthesis and distribution.* Arch Biochem Biophys, 1991. **288**(2): p. 397-405.

282.   Fukumura, K., et al., *Immunolocalization of transforming growth factor-betas and type I and type II receptors in rat articular cartilage.* Anticancer Res, 1998. **18**(6A): p. 4189-4193.

283.   Hayes, A.J., et al., *The development of articular cartilage: evidence for an appositional growth mechanism.* Anat Embryol (Berl), 2001. **203**(6): p. 469-479.

284.   Goomer, R.S., et al., *Nonviral in vivo gene therapy for tissue engineering of articular cartilage and tendon repair.* Clin Orthop, 2000. **379**: p. S189-S200.

285.   Valcourt, U., et al., *Alternative splicing of type II procollagen pre-mRNA in chondrocytes is oppositely regulated by BMP-2 and TGF-beta1.* FEBS Letts, 2003. **545**(2-3): p. 115-119.

286.   Johnstone, B., et al., *In vitro chondrogenesis of bone marrow-derived mesenchymal progenitor cells.* . Exp Cell Res, 1998. **238**(1): p. 265-272.

287.   Joyce, M.E., et al., *Transforming growth factor-beta and the initiation of chondrogenesis and osteogenesis in the rat femur.* . J Cell Biol, 1990. **100**(6): p. 2195-2207.

288.   Mizuta, H., et al., *The spatiotemporal expression of TGF-beta1 and its receptors during periosteal chondrogenesis in vitro.* J Orthop Res, 2002. **20**(3): p. 562-574.

289.   Miura, Y., et al., *Brief exposure to high-dose transforming growth factor-beta1 enhances periosteal chondrogenesis in vitro: a preliminary report.* J Bone Joint Surg Am, 2002. **84-A**(5): p. 793-799.

290.   Fan, H., et al., *Porous gelatin-chondroitin-hyaluronate tri-copolymer scaffold containing microspheres loaded with TGF-B1 induces differentiation of mesenchymal stem cells in vivo for enhancing cartilage repair.* J Biomed Mater Res, 2006. **77A**: p. 785-794.

291.   Lee, E.H., et al., *Effects of controlled-released TGF-B1 from chitosan microspheres on chondrocytes culutred in a collagen/chitosan/glycosaminoglycan scaffold.* Biomaterials, 2004. **25**: p. 4163-4173.

292.   Sohier, J., et al., *Tailored release of TGF-B1 from porous scaffolds for cartilage tissue engineering.* Int J Pharm, 2007. **332**: p. 80-89.

293.   Gombotz, W.R., et al., *Stimulation of bone healing by transforming growth factor-beta1 released from polymeric or ceramic implants.* J of Appl Biomaterials, 2004. **5**(2): p. 141-150.

294.   Lu, L., M.J. Yaszemski, and A.G. Mikos, *TGF-beta1 release from biodegradable polymer microparticles: its effects on marrow stromal osteoblast function.* J Bone Joint Surg Br, 2001. **83A**: p. S82-91.

295.   Roberts, A.B., *Transforming growth factor-beta: activity and efficacy in animal models of wound healing.* Wound Repair Regen, 1995. **3**: p. 408-418.

296.   Kawamura, K., et al., *Sustained expression of TGF-b1 but not IGF-1 induces chondrogenic differentiation of adult human mesenchymal stem cells.* Trans Orthop Res Soc, 2004: p. 29.

297.   Lu, L., G.N. Stamatas, and A.G. Mikos, *Controlled release of transforming growth factor Bl from biodegradable polymer microsperes.* J. Biomed Mater Res, 2000. **50**: p. 440-451.

298.   Schmidmaier, G., et al., *Local application of growth factors (insulin-like growth factor-1 and transforming growth factor-beta1) from a biodegradable poly(D,L-lactide) coating of osteosynthetic implants accelerates fracture healing in rats.* Bone, 2001. **28**(4): p. 341-350.

299.   Wildemann, B., et al., *Local and controlled release of growth factors (combination of IGF-I and TGF-beta I, and BMP-2 alone) from a polylactide coating of titanium implants does not lead to ectopic bone formation in sheep muscle.* J Control Release, 2004. **95**(2): p. 249-256.

300.   Nehra, A., et al., *Transforming growth factor-beta1 (TGF-beta1) is sufficient to induce fibrosis of rabbit corpus cavernosum in vivo.* J Urol, 1999. **163**(3 Pt1): p. 910-915.

301.   Demers, C.N., et al., *Effect of experimental parameters on the in vitro release kinetics of transforming growth factor beta1 from coral particles.* J Biomed Mater Res, 2002. **59**(3): p. 403-410.

302.   Giannoni, P. and E.B. Hunziker, *Release kinetics of transforming growth factor-beta1 from fibrin clots.* Biotechnol Bioeng, 2003. **83**(1): p. 121-123.

303.   Ehrhart, N.P., et al., *Effect of transforming growth factor-beta1 on bone regeneration in critical-sized bone defects after irradiation of host tissues.* Am J Vet Res, 2005. **66**(6): p. 1039-1045.

304.   Maire, M., et al., *Retention of transforming growth factor Bl using functionalized dextran-based hydrogels.* Biomaterials, 2005. **26**: p. 1771-1780.

305.   Mikhailowski, R., et al., *Controlled release of TGF-beta1 impedes rat colon carcinogenesis in vivo.* Int J Cancer, 1998. **78**(5): p. 618-623.

306.   Gille, J., et al., *Bone substitutes as carriers for transforming growth factor-beta(1) (TGF-beta(1)).* Int Orthop, 2002. **26**(4): p. 203-206.

307. Jancar, J., et al., *Mechanical response of porous scaffolds for cartilage engineering.* Physiol Res, 2007. **Epub ahead of pring**.

308. Sanz, E., L. Penas, and J.L. Lequerica, *Formation of cartilage in vivo with immobilized autologous rabbit auricular cultured chondrocytes in collagen matrices.* Plast Reconstr Surg, 2007. **119**(6): p. 1707-1713.

309. Liao, E., et al., *Tissue-engineered cartilage constructs using composite hyaluronic acid/collagen I hydrogels and designed poly(propylene fumarate) scaffolds.* Tissue Engineering, 2007. **13**(3): p. 537-550.

310. Cortial, D., et al., *Activation by IL-1 of bovine articular chondrocytes in culture within a 3D collagen-based scaffold. An in vitro model to address the effect of compounds with therapeutic potential in osteoarthritis.* Osteoarthritis and Cartilage, 2006. **14**(7): p. 631-640.

311. Bosnakovski, D., et al., *Chondrogenic differentiation of bovine bone marrow mesenchymal stem cells (MSCs) in different hydrogels: influence of collagen type II extracellular matrix on MSC chondrogenesis.* Biotechnol Bioeng, 2006. **93**(6): p. 1152-1163.

312. Tognana, E., et al., *Hyalograft C: hyaluronan-based scaffolds in tissue-engineered cartilage.* Cells Tissues Organs, 2007. **186**(2): p. 97-103.

313. Chung, C., et al., *Effects of auricular chondrocyte expansion on neocartilage formation in photocrosslinked hyaluronic acid networks.* Tissue Engineering, 2006. **12**(9): p. 2665-2673.

314. Gerard, C., et al., *The effect of alginate, hyaluronate and hyaluronate derivatives biomaterials on synthesis of non-articular chondrocyte extracellular matrix.* J Mater Sci Mater Med, 2005. **16**(6): p. 541-551.

315. Dare, E.V., et al., *Differentiation of a fibrin gel encapsulated chondrogenic cell line.* Int J Artif Organs, 2007. **30**(7): p. 619-627.

316. Suzuki, D., et al., *Comparison of various mixtures of beta-chitin and chitosan as a scaffold for three-dimensional culture of rabbit chondrocytes.* J Mater Sci Mater Med, 2007. **Epub ahead of print**.

317. Guo, C.A., et al., *Novel gene-modified-tissue engineering of cartilage using stable transforming growth factor-beta1-transfected mesenchymal stem cells grown on chitosan scaffolds.* J Biosci Bioeng, 2007. **103**(6): p. 547-556.

318. Griffon, D.J., et al., *Chitosan scaffolds: interconnective pore size and cartilage engineering.* Acta Biomater, 2006. **2**(3): p. 313-320.

319. Melhorn, A.T., et al., *Mesenchymal stem cells maintain TGF-beta-mediated chondrogenic phenotype in alginate bead culture.* Tissue Engineering, 2006. **12**(6): p. 1393-1403.

320. Li, W.J., et al., *A three-dimensional nanofibrous scaffold for cartilage tissue engineering using human mesenchymal stem cells.* Biomaterials, 2005. **26**(6): p. 599-609.

321. Hannouche, D., et al., *Engineering of implantable cartilaginous structures from bone marrow-derived mesenchymal stem cells.* Tissue Engineering, 2007. **13**(1): p. 87-99.

322. Stewart, K., et al., *The effect of growth factor treatment on meniscal chondrocyte proliferation and differentiation on polyglycolic acid scaffolds.* Tissue Engineering, 2007. **13**(2): p. 271-280.

323. Riley, S.L., et al., *Formulation of PEG-based hydrogels affects tissue-engineered cartilage construct characteristics.* J Mater Sci Mater Med, 2001. **12**(10-12): p. 983-990.

324. Nicodemus, G.D., I. Villanueva, and S.J. Bryant, *Mechanical stimulation of TMJ condylar chondrocytes encapsulated in PEG hydrogels.* J Biomed Mater Res A, 2007. **83**(2): p. 323-331.

325. Buxton, A.N., et al., *Design and characterization of poly(ethylene glycol) photopolymerizable semi-interpenetrating networks for chondrogenesis of human mesenchymal stem cells.* Tissue Engineering, 2007. **13**(10): p. 2549-2560.

326. Park, Y.-J., et al., *Bovine primary chondrocyte culture in synthetic matrix metalloproteinase-sensitive poly(ethylene glycol)-based hydrogels as a scaffold for cartilage repair.* Tissue Engineering, 2004. **10**(3-4): p. 515-522.

327. Park, J.S., et al., *In vitro and in vivo test of PEG/PCL-based hydrogel scaffold for cell delivery application.* J Control Release, 2007. **Epub ahead of print**.

328. Grad, S., et al., *Effects of simple and complex motion patterns on gene expression of chondrocytes seeded in 3D scaffolds.* Tissue Engineering, 2006. **12**(11): p. 3171-3179.

329. Metters, A.T., K.S. Anseth, and C.N. Bowman, *Fundamental studies of biodegradable hydrogels as cartilage replacement materials.* Biomed Sci Instrum, 1999. **35**(33-38).

330. Mi, F.-L., et al., *In vitro evaluation of a chitosan membrane cross-linked with genipin.* J Biomater Sci Polym Ed., 2001. **12**(8): p. 835-850.

331. Tsai, C.C., et al., *In vitro evaluation of the genotoxicity of a naturally occurring crosslinking agent (genipin) for biologic tissue fixation.* J Biomed Mater Res, 2000. **52**(1): p. 58-65.

332. Sung, H.-W., et al., *Feasibility study of a natural crosslinking reagent for biological tissue fixation.* J Biomed Mater Res, 1998. **42**(560-567).

333. Hu, Y., J.O. Hollinger, and K.G. Marra, *Controlled release from coated polymer microparticles embedded in tissue-engineered scaffolds.* J Drug Trageting, 2001. **9**(6): p. 431-438.

334. Meese, T.M., et al., *Surface studies of coated polymer microspheres and protein release from tissue-engineered scaffolds.* J Biomater Sci Polym Ed., 2002. **13**(2): p. 141-151.

335. DeFail, A.J., et al., *Controlled release of bioactive TGF-beta 1 from microspheres embedded within biodegradable hydrogels.* Biomaterials, 2006. **27**(8): p. 1579-1585.

336. Connor, T.B., et al., *Correlation of fibrosis and transforming growth factor-beta type 2 levels in the eye.* J Clin Invest, 1989. **83**(5): p. 1661-1666.

337. Parker, J.A.T.C., et al., *Release of Bioactive Transforming Growth Factor B3 from Microtextured Polymer Surfaces in Vitro and in Vivo.* Tissue Engineering, 2002. **8**(5): p. 853-861.

338. Bajpai, A.K. and S. Bhanu, *In vitro release dynamics of insulin from a loaded hydrophilic polymeric network.* J Mater Sci Mater Med, 2004. **15**(1): p. 43-53.

339. Nicoll, S.B., A.E. Denker, and R.S. Tuan, *In vitro characterization of transforming growth factor-beta1-loaded composites of biodegradable polymer and mesenchymal cells.* Cells Mater, 1995. **5**: p. 231.

340. Reinholz, G.G., et al., *Animal models for cartilage reconstruction.* Biomaterials, 2004. **25**: p. 1511-1521.

341. Yeo, Y. and K. Park, *Control of Encapsulation Efficiency and Initial Burst in Polymeric Microparticle Systems.* Arch Pharm Res, 2004. **27**(1): p. 1-12.

342. Freibert, S. and X.X. Zhu, *Polymer microspheres for controlled drug release.* Int J Pharm, 2004. **282**(1-2): p. 1-18.

343. Butler, M.F. and Y.-F.P. Ng, P.D.A., *Mechanism and Kinetics of Crosslinking Reaction between Biopolymers Containing Primary Amine Groups and Genipin.* J Polym Sci Part A: Polym Chem, 2003. **41**: p. 3941-3953.

344. Ono, M., et al., *Iridoid Glucosides from the Fruit of Genipa americana.* Chem Pharm Bull, 2005. **53**(10): p. 1342-1344.

345. Mi, F.-L., et al., *Physicochemical, Antimicrobial, and Cytotoxic Characteristics of a Chitosan Film Cross-linked by a Naturally Occurring Cross-Linking Agent, Aglycone Geniposidic Acid.* J Agric Food Chem, 2006. **54**: p. 3290-3296.

346. Chen, Y.S., et al., *An in vivo evaluation of a biodegradable genipin-cross linked gelatin peripheral nerve guide conduit material.* Biomaterials, 2005. **26**(18): p. 3911-3918.

347. Mwale, F., et al., *Biological Evaluation of Chitosan Salts Cross-LInked to Genipin as a Cell Scaffold for Disk Tissue Engineering.* Tissue Engineering, 2005. **11**(1/2): p. 130-140.

348. Liang, H.-C., et al., *Genipin-crosslinked gelatin microspheres as a drug carrier for intramuscular administration: In vitro and in vivo studies.* J Biomed Mater Res, 2003. **65A**: p. 271-282.

349. Koo, H.-J., et al., *Antiinflammatory effects of genipin, an active principle of gardenia.* Eur J Pharm, 2004. **495**: p. 201-208.

350. Sung, H.-W., et al., *In vitro surface characterization of a biological patch fixed with a naturally occurring crosslinking agent.* Biomaterials, 2000. **21**: p. 1353-1362.

351. Mi, F.-L., S.-S. Shyu, and C.H. Pen, *Characterization of Ring-Opening Polymerization of Genipin and pH-Dependent Cross-Linking Reactions Between Chitosan and Genipin.* J Polym Sci Part A: Polym Chem, 2005. **43**: p. 1985-2000.

352. Chen, H., et al., *Reaction of chitosan with genipin and its fluorgenic attributes for potential microcapsule membrane characterization.* J Biomed Mater Res, 2005. **75A**: p. 917-927.

353. Chen, H., et al., *Genipin Cross-linked Alginate-Chitosan Microcapsules: Membrane Characterization and Optimization of Cross-Linking Reaction.* Biomacromolecules, 2006. **7**: p. 2091-2098.

354. Mi, F.-L., *Synthesis and Characterization of a Novel Chitosan-Gelatin Bioconjugate with Fluorescence Emission.* Biomacromolecules, 2005. **6**: p. 975-987.

355. Chen, M.-C., et al., *A novel drug-eluting stent spray coated with multi-layers of collagen and sirolimus.* J Control Release, 2005. **108**: p. 178-189.

356. Yang, C.H., *Evaluation of the release rate of bioactive recombinant human epidermal growth factor from crosslinking collagen sponges.* J Mater Sci Mater Med, 2007. **Epub ahead of print**.

357. Lauto, A., et al., *Albumin-genipin solder for laser tissue repair.* Lasers Surg Med, 2004. **35**(2): p. 104-145.

358. Ferretti, M., et al., *Controlled in vivo degradation of genipin crosslinked polyethylene glycol hydrogels within osteochondral defects.* Tissue Engineering, 2006. **12**(9): p. 2657-2663.

359.   Nickerson, M.T., et al., *Some physical and microstructural properties of genipin-crosslinked gelatin-malodextrin hydrogels.* Int J Biol Macromol, 2006. **38**: p. 40-44.

360.   Nickerson, M.T., et al., *Kinetic and mechanistic considerations in the gelation of genipin-crosslinked gelatin.* Int J Biol Macromol, 2006. **39**(4-5): p. 298-302.

361.   Bigi, A., et al., *Stabilization of gelatin films by crosslinking with genipin.* Biomaterials, 2002. **23**: p. 4827-4832.

362.   Liu, B.S., et al., *A novel use of genipin-fixed gelatin as extracellular matrix for peripheral nerve regeneration.* J Biomater Appl, 2004. **19**(1): p. 21-34.

363.   Englert, C., et al., *Bonding of articular cartilage using a combination of biochemical degradation and surface cross-linking.* Arthritis Res Ther, 2007. **9**(3): p. R47.

364.   Sung, H.-W., et al., *Fixation of biological tissues with a naturally occuring crosslinking agent: Fixation rate and effects of pH, temperature, and initial fixative concentration.* J Biomed Mater Res, 2000. **52**: p. 77-87.

365.   Chang, Y., et al., *In vivo evaluation of cellular and acellular bovine pericardia fixed with a naturally occurring crosslinking agent (genipin).* Biomaterials, 2002. **23**(12): p. 2447-2457.

366.   Park, J.-E., et al., *Isolation and Characterization of Water-Soluble Intermediates of Blue Pigments Transformed from Geniposide of Gardenia jasminoides.* J Agric Food Chem, 2002. **50**: p. 6511-6514.

367.   Fujikawa, S., et al., *Structure of Genipocyanin G1, A Spontaneous Reaction Product Between Genipin and Glycine.* Tetrahedron Letters, 1987. **28**(40): p. 4699-4700.

368.   Peppas, N.A., A. Argade, and S. Bhargava, *Preparation and Properties of Poly(ethylene oxide) Star Polymers.* J Appl Polym Sci, 2003. **87**: p. 322-327.

369.   Oral, E. and N.A. Peppas, *Responsive and recognitive hydrogels using star polymers.* J Biomed Mater Res A, 2004. **68**(3): p. 439-447.

370.   Heyes, C.D., et al., *Synthesis, patterning and applications of star-shaped poly(ethylene glycol) biofunctionalized surfaces.* Mol BioSyst, 2007. **3**: p. 419-430.

371.   Hiemstra, C., et al., *Rapidly in Situ Forming Biodegradable Robust Hydrogels by Combining Stereocomplexation and Photopolymerization.* J Am Chem Soc, 2007. **129**(32): p. 9918-9926.

372.   Hiemstra, C., et al., *In vitro and in vivo protein delivery from in situ forming poly(ethylene glycol)-poly(lactide) hydrogels.* J Control Release, 2007. **119**: p. 320-327.

373. Lee, B.P., J.L. Dalsin, and P.B. Messersmith, *Synthesis and Gelation of DOPA-Modified Poly(ethylene glycol) Hydrogels.* Biomacromolecules, 2002. **3**: p. 1038-1047.

374. Yang, Z., et al., *Poly(glutamic acid) poly(ethylene glycol) hydrogels prepared by photoinduced polymerization: Synthesis, characterization, and preliminary release studies of protein drugs.* J Biomed Mater Res A, 2002. **62**(1): p. 14-21.

375. Bae, K.H., Y.-M. Lee, and T.G. Park, *Oil-Encapsulating PEG-PPO-PEO/PEG Shell Cross-linked Nanocapsules for Target-Specific Delivery of Paclitaxel.* Biomacromolecules, 2007. **8**: p. 650-656.

376. Yamaguchi, N., et al., *Rheological Characterization of Polysaccharide-Poly(ethylene glycol) Star Copolymer Hydrogels.* Biomacromolecules, 2005. **6**: p. 1931-1940.

377. Wieland, J.A., T.L. Houchin-Ray, and L.D. Shea, *Non-viral vector delivery from PEG-hyaluronic acid hydrogels.* J Control Release, 2007. **120**: p. 233-241.

378. Berna, M., et al., *Novel Monodisperse PEG-Dendrons as New Tools for Targeted Drug Delivery: Synthesis, Characterization and Cellular Uptake.* Biomacromolecules, 2006. **7**: p. 146-153.

379. Frederiksen, S.M. and F.R. Stermitz, *Pyridine Monoterpene Alkaloid Formation from Iridoid Glycosides. A Novel PMTA Dimer from Geniposide.* J Nat Prod, 1996. **59**: p. 41-46.

380. Lin, H.-H. and Y.-L. Cheng, *In-Situ Thermoreversible Gelation of Block and Star Copolymers of Poly(ethylene glycol) and Poly(N-isopropylacrylamide) of Varying Architectures.* Macromolecules, 2001. **34**: p. 3710-3715.

381. Talens-Visconti, R., et al., *Human mesenchymal stem cells from adipose tissue: Differentiation into hepatic lineag.* Toxicol In Vitro, 2007. **21**(2): p. 324-329.

382. Seo, M.J., et al., *Differentiation of human adipose stromal cells into hepatic lineage in vitro and in vivo.* Biochem Biophys Res Commun, 2005. **328**(1): p. 258-264.

383. Brzoska, M., et al., *Epithelial differentiation of human adipose tissue-derived adult stem cells.* Biochem Biophys Res Commun, 2005. **330**(1): p. 142-150.

384. Timper, K., et al., *Human adipose tissue-derived mesenchymal stem cells differentiate into insulin, somatostatin, and glucagon expressing cells.* Biochem Biophys Res Commun, 2006. **341**(4): p. 1135-1140.

385. Patrick, C.W.J., et al., *Long-term implantation of preadipocyte-seeded PLGA scaffolds.* Tissue Engineering, 2002. **8**(2): p. 283-293.

386.   Lee, J.H. and D.M. Kemp, *Human adipose-derived stem cells display myogenic potential and perturbed function in hypoxic condition.* Biochem Biophys Res Commun, 2006. **341**(3): p. 882-888.

387.   Kim, M., et al., *Muscle regeneration by adipose tissue-derived adult stem cells attached to injectable PLGA spheres.* Biochem Biophys Res Commun, 2006. **348**(2): p. 386-392.

388.   Cowan, C.M., et al., *Adipose-derived adult stromal cells heal critical-size mouse calvarial defects.* Nat Biotechnol, 2004. **22**(5): p. 560-567.

389.   Dragoo, J.L., et al., *Tissue-engineered cartilage and bone using stem cells from human infrapatellar fat pads.* J Bone Joint Surg Br, 2003. **85**(5): p. 740-747.

390.   Lin, Y., et al., *Molecular and cellular characterization during chondrogenic differentiation of adipose tissue-derived stromal cells in vitro and cartilage formation in vivo.* J Cell Mol Med, 2005. **9**(4): p. 929-939.

391.   Ogawa, R., et al., *Bone marrow regeneration using adipose-derived stem cells.* J. Nippon Med Scho, 2006. **73**(1): p. 45-47.

392.   Planat-Benard, V., et al., *Spontaneous cardiomyocyte differentiation from adipose tissue stroma cells.* Circ Res, 2004. **94**(2): p. 223-229.

393.   Gaustad, K.G., et al., *Differentiation of human adipose tissue stem cells using extracts of rat cardiomyocytes.* Biochem Biophys Res Commun, 2004. **314**(2): p. 420-427.

394.   Rangappa, S., et al., *Transformation of adult mesenchymal stem cells isolated from the fatty tissue into cardiomyocytes.* Ann Thorac Surg, 2003. **75**(3): p. 775-779.

395.   Miyahara, Y., et al., *Monolayered mesenchymal stem cells repair scarred myocardium after myocardial infarction.* Nat Med, 2006. **12**(4): p. 459-465.

396.   Yamada, Y., et al., *Cardiac progenitor cells in brown adipose tissue repaired damaged myocardium.* Biochem Biophys Res Commun, 2006. **342**(2): p. 662-670.

397.   Strem, B.M., et al., *Expression of cardiomyocytic markers on adipose tissue-derived cells in a murine model of acute myocardial injury.* Cytotherapy, 2005. **7**(3): p. 282-291.

398.   Fujimura, J., et al., *Neural differentiation of adipose-derived stem cells isolated from GFP transgenic mice.* Biochem Biophys Res Commun, 2005. **333**(1): p. 116-121.

399.   Tholpady, S.S., A.J. Katz, and R.C. Ogle, *Mesenchymal stem cells from rat visceral fat exhibit multipotential differentiation in vitro.* Anat Rec A Discov Mol Cell Evol Biol, 2003. **272**(1): p. 398-402.

400. Safford, K.M., et al., *Neurogenic differentiation of murine and human adipose-derived stromal cells.* Biochem Biophys Res Commun, 2002. **294**(2): p. 371-379.

401. Kang, S.K., et al., *Autologous adipose tissue-derived stromal cells for treatment of spinal cord injury.* Stem Cells Dev, 2006. **15**(4): p. 583-594.

402. Tauro, J.R. and R.A. Gemeinhart, *Matrix Metalloprotease Triggered Delivery of Cancer Chemotherapeutics from Hydrogel Matrixes.* Bioconjug Chem, 2005. **16**: p. 1133-1139.

403. Yan, X. and R.A. Gemeinhart, *Cisplatin delivery form poly(acrylic acid-co-methyl methacrylate) microparticles.* J Control Release, 2005. **106**: p. 198-208.

404. Huo, D., et al., *Studies on the poly(lactic-co-glycolic) acid microspheres of cisplatin for lung-targeting.* Int J Pharm, 2005. **289**: p. 63-67.

405. Chandy, T., et al., *Changes in Cisplatin Delivery Due to Surface-Coated Poly(lactic acid)-Poly(ε–caprolactone) Microspheres.* J Biomater Appl, 2002. **16**: p. 275-291.

406. Garcia-Contreras, L., K. Abu-Izza, and D.R. Lu, *Biodegradable cisplatin microspheres for direct brain injection: preparation and characterization.* Pharm Dev Technol, 1997. **2**(1): p. 53-65.

407. Verrijk, R., et al., *Reduction of Systemic Exposure and Toxicity of Cisplatin by Encapsulation in Poly-lactide-co-glycolide.* Cancer Res, 1992. **52**: p. 6653-6656.

408. Fujiyama, J., et al., *Cisplatin incorporated in microspheres: development and fundamental studies for its clinical application.* J Control Release, 2003. **89**: p. 397-408.

409. Ehrhart, N.P., et al., *Effects of a controlled-release cisplatin delivery system used after resection of mammary carcinoma in mice.* Am J Vet Res, 1999. **60**(11): p. 1347-1351.

410. Kloft, C., et al., *Determination of platinum complexes in clinical samples by a rapid flameless atomic absorption spectrometry assay.* Ther Drug Monit, 1999. **21**(6): p. 631-637.

411. Bandak, S., et al., *Pharmacological studies of cisplatin encapsulated in long-circulating liposomes in mouse tumor models.* Anticancer Drugs, 1999. **10**(10): p. 911-920.